

LINEAR AND NONLINEAR ANALYSIS OF HUMAN POSTURAL SWAY

A THESIS SUBMITTED TO
THE GRADUATE SCHOOL OF NATURAL AND APPLIED SCIENCES
OF
MIDDLE EAST TECHNICAL UNIVERSITY

BY

HÜSEYİN ÇELİK

IN PARTIAL FULFILLMENT OF THE REQUIREMENTS
FOR
THE DEGREE OF MASTER OF SCIENCE
IN
ENGINEERING SCIENCES

SEPTEMBER 2008

Approval of the thesis:

LINEAR AND NONLINEAR ANALYSIS OF HUMAN POSTURAL SWAY

Submitted by **HÜSEYİN ÇELİK** in partial fulfillment of the requirements for the degree of **Master of Science in Engineering Science Department, Middle East Technical University** by,

Prof. Dr. Canan Özgen
Dean, Graduate School of **Natural and Applied Sciences**

Prof. Dr. Turgut Tokdemir
Head of Department, **Engineering Sciences**

Assist. Prof. Dr. Senih Gürses
Supervisor, **Engineering Sciences Dept., METU**

Prof. Dr. Turgut Tokdemir
Co-Supervisor, **Engineering Sciences Dept., METU**

Examining Committee Members:

Prof. Dr. Turgut Tokdemir
Engineering Sciences Dept., METU

Assist. Prof. Dr. Senih Gürses
Engineering Sciences Dept., METU

Prof. Dr. M. Kemal Özgören
Mechanical Engineering Dept., METU

Prof. Dr. Mehmet Çalışkan
Mechanical Engineering Dept., METU

Assoc. Prof. Dr. Hakan I. Tarman
Engineering Sciences Dept., METU

Date: September 05, 2008

I hereby declare that all information in this document has been obtained and presented in accordance with academic rules and ethical conduct. I also declare that, as required by these rules and conduct, I have fully cited and referenced all material and results that are not original to this work.

Name, Last Name: Hüseyin Çelik

Signature:

ABSTRACT

LINEAR AND NONLINEAR ANALYSIS OF HUMAN POSTURAL SWAY

Çelik, Hüseyin

M.S., Department of Engineering Sciences

Supervisor: Assist. Prof. Dr. Senih Gürses

Co-Supervisor: Prof. Dr. Turgut Tokdemir

September 2008, 195 pages

Human upright posture exhibits an everlasting oscillatory behavior of complex nature, called as human postural sway. Variations in the position of the Center-of-Pressure (CoP) were used to describe the human postural sway. In this study; CoP data, which has experimentally been collected from 28 different subjects (14 males and 14 females with their ages ranging from 6 to 84), who were divided into 4 groups according to their ages has been analyzed. The data collection from each of the subjects was performed in 5 successive trials, each of which has lasted for 180-seconds long. Linear analysis methods such as the variance/standard deviation, Fast Fourier Transformation, and Power Spectral Density estimates were applied to the detrended CoP signal of human postural sway. Also the Run test and Ensemble averages methods were used to search for stationarity and ergodicity of the CoP signal respectively. Furthermore, in order to reveal the nonlinear characteristics of the human postural sway, its dynamics were reconstructed in m -dimensional state space from the CoP_x signals. Then, the correlation dimension (D_2) estimates from the embedded dynamics were calculated. Additionally, the statistical and dynamical measures computed were checked against any significant changes, which may occur during aging. The results of the study suggested that human postural sway is a stationary process when 180-second long biped quiet stance data is considered. In

addition, it exhibits variable dynamical structure complex in nature (112 deterministic chaos versus 28 stochastic time series of human postural sway) for five successive trials of 28 different subjects. Moreover, we found that groups were significantly different in the correlation dimension (D_2) measure ($p \leq 0.0003$). Finally, the behavior of the experimental CoP_x signals was checked against two types of linear processes by using surrogate data method. The shuffled CoP_x signals (Surrogate I) suggested that temporal order of CoP_x is important; however, phase-randomization (Surrogate II) did not change the behavioral characteristics of the CoP_x signal.

Keywords: Human Postural Sway, Center-of-Pressure, Determinism versus Stochasticity, Stationarity and Ergodicity, Surrogate Data, Correlation Dimension, Aging

ÖZ

DURUŞ SAPMASININ DOĞRUSAL VE DOĞRUSAL OLMAYAN ANALİZ YÖNTEMLERİ İLE ARAŞTIRILMASI

Çelik, Hüseyin

Yüksek Lisans, Mühendislik Bilimleri Bölümü

Tez Yöneticisi: Yard. Doç. Dr. Senih Gürses

Yardımcı Tez Yöneticisi: Prof. Dr. Turgut Tokdemir

Eylül 2008, 195 sayfa

Ayakta sakin halde dik duran bir insanın sonu gelmeyen, karmaşık özellikler gösteren salınımlarına duruş sapması adı verilmektedir. Basma merkezi (“Center-of-Pressure”, CoP)’nin pozisyonundaki değişimler, duruş sapmasını incelemek için kullanılmaktadır. Bu çalışmada, 6 ile 84 yaş arasında değişen 28 farklı denekten (14 kadın, 14 erkek); her denekten, bir tanesi 180 saniye süren 5 farklı deneme olmak üzere, deneysel olarak CoP sinyali kaydedilmiştir. Denekler yaşlarına göre dört farklı gruba ayrılmışlardır. Varyans/standard sapma, Hızlı Fourier Dönüşümü, Güç Spektrum Yoğunluğu gibi doğrusal analiz yöntemleri, CoP zaman serilerinin ortalaması sinyalden çıkartılarak uygulanmıştır. Ayrıca, Run testi ve Topluluk Ortalaması yöntemleri sırasıyla durağanlığı ve ergodikliği araştırmak için kullanılmıştır. Bunların yanı sıra, duruş sapmasının doğrusal olmayan davranışını ortaya çıkarmak için duruş dinamiği, CoP_x sinyalinden m -boyutlu durum uzayında yeniden inşa edilmiştir. Daha sonra, korelasyon boyutu (D_2) kestirimleri, m -boyutlu durum uzayına gömülmüş dinamikten hesaplanmıştır. İlaveten, bahsi geçen ölçütlerin yaşlanma ile olası anlamlı değişimleri istatistiksel yöntemlerle araştırılmıştır. Çalışmanın sonuçları, duruş yan sapmasının, 180 saniye iki ayak üstünde sakin vaziyette yapılan gözlemlerde durağan bir süreç olduğunu ortaya koymuştur. Bunun

yanısıra, duruş yan sapması farklı kişi veya aynı kişinin farklı denemeleri için farklı dinamik yapılar (112 belirlenimci kaosa karşı 28 stokastik duruş yan sapması zaman serileri) sergilemiştir. Ayrıca, D_2 ölçütü için gruplar arasında anlamlı farklılık saptanmıştır ($p \leq 0.0003$). Son olarak, deneysel olarak elde edilmiş CoP_x sinyallerinin davranışı, iki doğrusal sürece karşı vekil veri (Surrogate data) kullanılarak sınanmıştır. Karıştırılmış CoP sinyalleri göstermiştir ki, zamansal sıra CoP sinyalleri için önemlidir; ama, fazın rasgeleleştirilmesi CoP sinyallerinin karakteristik davranışında bir farklılığa yol açmamıştır.

Anahtar Kelimeler: Duruş Yan Sapması, Basma Merkezi (“Center-of-Pressure”), Stokastikliğe karşı Belirlenimcilik, Durağanlık ve Ergodiklik, Vekil Veri, Korelasyon Boyutu, Yaşlanma

To My Family

ACKNOWLEDGEMENTS

Firstly, I want to thank my Department, Engineering Sciences as it has provided me the opportunity to study as a M.S. Student and work as a Research Assistant in the department.

I wish to offer my sincere thanks and appreciation to my supervisor Dr. Senih Gürses for his precious help, invaluable suggestions, continuous support, and guidance throughout this study.

I also want to thank my co-supervisor and Department Head, Dr. Turgut Tokdemir; former Vice Department Head, Dr. Dilek Keskin; and my colleagues Semih Erhan, Serdar Çarbaş, Cengizhan Durucan for their encouragements.

Besides, I want to thank all subjects who participated in the experiments of this study.

Last but not least thanks to my dear wife, Serap Sevimli Çelik who not only helped me in the experiments performed with the children but also always has given me support throughout the study.

TABLE OF CONTENTS

ABSTRACT.....	IV
ÖZ.....	VI
ACKNOWLEDGEMENTS.....	IX
TABLE OF CONTENTS.....	X
LIST OF TABLES.....	XIII
LIST OF FIGURES.....	XV
CHAPTERS	
1.INTRODUCTION.....	1
1.1 General Overview.....	1
1.2 Motivation of the Thesis.....	4
1.2.1 Dynamics of the Human Postural Sway: Determinism versus Stochasticity... 4	
1.2.2 Stationarity of the CoP Signals.....	8
1.2.3 Aging and Human Upright Posture.....	9
1.3 Aim and Scope of the Thesis.....	10
1.4 Outline of the Study.....	11
2.MATERIALS AND METHODS.....	12
2.1 Data Acquisition.....	12
2.1.1 The Experimental Set-up.....	12
2.1.2 Subjects and the Experimental Procedure.....	13
2.1.3 Center-of-Pressure.....	16
2.2 Analysis of the Signals.....	19
2.2.1 Linear Analysis.....	19
2.2.1.1 Time Domain Analysis.....	19
2.2.1.1.1 Mean and Variance.....	19
2.2.1.1.2 Run Test.....	20

2.2.1.1.3 Ensemble Average	22
2.2.1.2 Frequency Domain Analysis.....	25
2.2.1.2.1 Fast Fourier Transformation	25
2.2.1.2.2 Power Spectral Density Estimates	25
2.2.2 Nonlinear Analysis.....	26
2.2.2.1 Correlation Dimension.....	26
2.2.2.2 Reconstruction of Dynamics in m -dimensional Embedding State Space.....	27
2.2.6.2 Estimate of Time Delay (τ).....	28
2.2.6.3 Correlation Dimension Estimates	32
3.RESULTS	35
3.1 Results of the Linear Analysis	35
3.1.1 Results of the Time Domain Analysis	35
3.1.1.1 Variance/Standard Deviation of the Signals	35
3.1.1.1.1 Standard Deviation of the CoP _x Signals.....	35
3.1.1.1.2 Standard Deviation of the CoP _y Signals.....	36
3.1.1.2 Results of Run Test.....	40
3.1.1.3 Results of Ensemble Average Analysis	40
3.1.1.4 Sign Test of the Results of Run Test and Ergodicity Analysis.....	45
3.1.1.5 Robustness of Run Test Results.....	46
3.1.2 Results of Frequency Domain Analysis.....	51
3.1.2.1 Fast Fourier Transformation and Power Spectral Density estimates.....	51
3.2 Results of the Nonlinear Analysis.....	59
3.2.1 Results of the Time Delays (τ).....	59
3.2.2 Correlation Dimension Estimates	75
4.MODELING	110
4.1 Surrogate Data.....	110
4.1.1 Surrogate Data I.....	110
4.1.2 Surrogate Data II.....	110
4.2 Results.....	112
4.2.1 Results of Run Test.....	112
4.2.2 Results of Ensemble Average Analysis	112
4.2.3 Sign Test of the Results of Run Test and Ergodicity Analysis.....	117
5.DISCUSSION	122
REFERENCES.....	133

APPENDICES

A:RUN TEST DEMONSTRATION 143

B:THE RUN DISTRIBUTION TABLE..... 147

C:ANOVA TEST 148

D:TRAPEZOID RULE 152

E:DERIVATION OF THE SPECTRAL ESTIMATE..... 154

F:SIGN TEST 156

G:CONFIDENCE INTERVAL ESTIMATION BY BOOTSTRAPPING
TECHNIQUE..... 158

H:KRUSKAL-WALLIS TEST..... 159

I:DERIVATION OF SURROGATE DATA WITH PHASE RANDOMIZATION 163

J:THE KNOWLEDGE ABOUT THE SUBJECTS 168

K:ALTERNATIVE ALGORITHM FOR CONVERGENCE 173

LIST OF TABLES

Table 2.1 Age, height, and weight statistics of the subjects and the groups.....	15
Table 3.1(a) Standard deviation values of the CoP_x signals in millimeters.....	38
Table 3.1(b) Standard deviation values of the CoP_y signals in millimeters.....	39
Table 3.2 Run Test Results in <i>total run</i>	42
Table 3.3 (a) p -values obtained from the two-way ANOVA of T matrix for CoP_x	43
Table 3.3 (b) p -values obtained from the two-way ANOVA of T matrix for CoP_y ...44	44
Table 3.3 (c) Sign Test Table.....	48
Table 3.3 (d) Run Test Results for varying data window size (w.s.) for the CoP_x signal.....	49
Table 3.3 (e) Run Test Results for varying data window size (w.s.) for the CoP_y signal.....	50
Table 3.4 (a) The ratios of the power of the signal at 0-0.1 Hz (R1) frequency band to the power in the whole frequency spectrum for the CoP_x	55
Table 3.4 (b) The ratios of the power of the signal at 0-1 Hz (R2) frequency band to the power in the whole frequency spectrum for the CoP_x	56
Table 3.5 (a) The ratios of the power of the signal at 0-0.1 Hz (R1) frequency band to the power in the whole frequency spectrum for the CoP_y signals.....	57
Table 3.5 (b) The ratios of the power of the signal at 0-1 Hz (R2) frequency band to the power in the whole frequency spectrum for the CoP_y signals.....	58
Table 3.6 Time delays (τ) of the first trials of 28 subjects for varying m	61
Table 3.7 Time delays (τ) of the second trials of 28 subjects for varying m	62
Table 3.8 Time delays (τ) of the third trials of 28 subjects for varying m	63
Table 3.9 Time delays (τ) of the fourth trials of 28 subjects for varying m	64
Table 3.10 Time delays (τ) of the fifth trials of 28 subjects for varying m	65

Table 3.11 τ_w for the first trials of 28 subjects for varying m	66
Table 3.12 τ_w for the second trials of 28 subjects for varying m	67
Table 3.13 τ_w for the third trials of 28 subjects for varying m	68
Table 3.14 τ_w for the fourth trials of 28 subjects for varying m	69
Table 3.15 τ_w for the fifth trials of 28 subjects for varying m	70
Table 3.16 Saturation points in embedding dimension of 136 converged trials.....	84
Table 3.17 Results of Convergence	86
Table 3.18 D_2 values of the converged trials.....	88
Table 4.1 Run Test Results in <i>total run</i>	114
Table 4.2 p -values obtained from the two-way ANOVA of T matrix for the shuffled CoP_x	115
Table 4.3 p -values obtained from the two-way ANOVA of T matrix for the phase-randomized CoP_x	116
Table 4.4 Sign Test Table for shuffled CoP_x	119
Table 4.5 Sign Test Table for phase-randomized CoP_x	120
Table 4.6 Sign Test Results for experimental, shuffled, and phase-randomized CoP_x	121

LIST OF FIGURES

Figure 2.1 The Biomechanics Laboratory.....	12
Figure 2.2 Center of Pressure.....	16
Figure 2.3(a) Anatomical planes described for the human body.....	17
Figure 2.3(b) Sagittal and coronal planes on force plate.....	17
Figure 2.4 A typical representative 180 sec long CoP_x [11 th S, F, 28] time series.....	18
Figure 2.5 A typical representative 180 sec long CoP_y [11 th S, F, 28] time series.....	18
Figure 2.6 Concept of ensemble averaging.....	23
Figure 2.7 Possible attractor.....	30-32
Figure 3.1 FFTs (left panel), corresponding PSDs (right panel) of the CoP_x signal...53	53
Figure 3.2 FFTs (left panel), corresponding PSDs (right panel) of the CoP_y signal...54	54
Figure 3.3 τ for varying dimensions, m [Group 1, 1 st S, F, 6 years old].....	71
Figure 3.4 τ_w for varying dimensions, m [Group 1, 1 st S, F, 6 years old].....	71
Figure 3.5 τ for varying dimensions, m [Group 2, 8 th S, M, 21 years old].....	72
Figure 3.6 τ_w for varying dimensions, m [Group 2, 8 th S, M, 21 years old].....	72
Figure 3.7 τ for varying dimensions, m [Group 3, 16 th S, M, 42 years old].....	73
Figure 3.8 τ_w for varying dimensions, m [Group 3, 16 th S, M, 42 years old].....	73
Figure 3.9 τ for varying dimensions, m [Group 4, 22 th S, F, 65 years old].....	74
Figure 3.10 τ_w for varying dimensions, m [Group 4, 22 th S, F, 65 years old].....	74
Figure 3.11 Step 1 - Curve $\ln C(r)$ versus $\ln r$ for the first trial of S-11 at $m=2$	77
Figure 3.12 Step 2 - Curve $\ln C(r)$ versus $\ln r$ for the first trial of S-11 at $m=2$	78

Figure 3.13 Step 3 - Curve $\ln C(r)$ versus $\ln r$ for the first trial of S-11 at $m=2$	79
Figure 3.14 Step 4 - Computed D_2 estimates for varying dimensions, m	80
Figure 3.15 D_2 estimate curve (poor fit of one exponential model) of the S-11, t_1 ...	81
Figure 3.16 D_2 estimate curve (experimental and modeled by Equation (3.1)) of the S-11, t_1	82
Figure 3.17 The line m versus $(m-1)/2$ and D_2 estimate curve of the S-11, t_1 . The marker “+” is the saturation point right to the intersection point of the line $D_2(m)$ with D_2 estimates curve.....	83
Figure 3.18 Modeled D_2 estimate curve of 1 st trial of 1 st S (black line), fitted line (red line).....	85
Figure 3.19 Curves $\ln C(r)$ versus $\ln r$ for varying m [11 th S, F, 28, 1 st trial].....	90
Figure 3.20 Curves $\ln C(r)$ versus $\ln r$ for varying m [11 th S, F, 28, 5 th trial].....	91
Figure 3.21 Curves $\ln C(r)$ versus $\ln r$ for varying m [14 th S, M, 39, 1 st trial].....	91
Figure 3.22 Computed D_2 estimates of five trials for varying m [5 th S, F, 11].....	92
Figure 3.23 Computed D_2 estimates of five trials for varying m [12 th S, M, 31].....	92
Figure 3.24-27 Computed D_2 estimates of the converged-trials of Group 1-4.....	93-94
Figure 3.28. Computed D_2 estimates of all converged trials.....	95
Figure 3.29-3.56 Fitted D_2 estimates of Subject 1-28 for varying m	96-109
Figure 4.1 Time series (first column), amplitude distributions (second column), and Fast Fourier Transformations (third column) of the experimental, shuffled (Surrogate Data I), and phase randomized (Surrogate Data II) CoP_x signals.....	111

CHAPTER 1

INTRODUCTION

1.1 General Overview

Even it looks easy to stand in upright stance, many researcher have tried to understand the complex behavior of human erect posture. A definition of posture can be stated as the position of the body and limbs with respect to each other and the environment. Even in static conditions, human upright posture exhibits an everlasting oscillatory behavior of complex nature, called as the *postural sway*.

The exploration of the dynamics, physiology and sensory motor control of human posture emphasizes importance in many areas of science such as neuroscience and its clinical applications (e.g., neurology, rehabilitation and prevention of fall); physical education, sport, and motor development (e.g., physical culture and education); ergonomics, industrial design (e.g., prosthesis and robotics); and ecology and adaptive biology (e.g., space studies).

To be in a static equilibrium, the forces and moments acting on a body must be zero. However, a person cannot stand in a static equilibrium but rather sway. Both intrinsic (e.g., mechanics of muscles; noise, delays and nonlinearities in the control system of human upright stance) and extrinsic factors (e.g., external forces acting on the body) may cause disruptions at the static equilibrium in standing.

The human upright posture is controlled by the central nervous system (CNS). To ensure the upright posture, CNS uses the information which comes from

somatosensory, vestibular, visual systems and control of the muscles. The proprioceptive system sends information about the changes of the positions of the body segments to the CNS [1]. The vestibular system can sense the linear and angular acceleration of the head and feedback this information to the CNS [2]. By the visual system, CNS has information about the position and velocity of the head [3]. The information comes from different sensory systems and is continuously re-weighted and integrated by the CNS to control the upright stance [4,5,6].

Alteration in sensory condition results in changes on postural sway. Kuo et al. (1998) [7] showed that subjects swayed more when either somatosensory or visual information has been disrupted. In addition, loss of a sensory system may lead changes in the nature of re-weighting mechanism. Peterka (2002) [4] claimed that stimulus-response characteristics of vestibular loss subjects was quiet linear because they cannot perform re-weighting of sensory information; however, for the healthy subjects stimulus-response characteristics was non-linear due to re-weighting. Besides, not the changes in the parameters that characterize the stability of postural control system but the changes in coupling coefficients (e.g., visual gain affected from touch motion amplitude) is proposed to be the primary reason of the changes in the gains used in the postural control system among different stimuli conditions [6].

Large amount of information from different senses is sent to CNS continuously. But, what is more important may be, how this information is perceived in our mind. CNS must adapt to variations in the body, environment and the task while solving motor control “problems” of voluntary or involuntary origin. That might be the perception that allows for adaptation of movement patterns to the variations in the body, the environment, and the task [8].

Many attempts were allocated to model postural control system (PCS). Johansson et al. (1988) [9] used an inverted pendulum to model postural body mechanism of their

subjects stimulated by the vibrators attached to their calf muscle. They made parametric identification of transfer function (TF) of the dynamics of the inverted pendulum. In another study, it was claimed that postural sway results from the impulsive control of calf muscle activity [10]. Peterka (2000) [11] modelled the postural control system with a PID (Proportional, Integral, Derivative) controller used to control the body, which is assumed to be an inverted pendulum. Kiemel et al. (2002) [5] modelled PCS as a modified optimal controller with computational noise (inaccuracies in neural computations). Park et al. (2004) [12] suggested that postural control system can be described by a single feedback controller with scalable gains through a biomechanical model which was composed of 3 inverted pendulums. In all of the aforementioned models, the feedback is continuous (closed loop control scheme); however, Collins et al. (1994 and 1995) [13,14] declared that feedback mechanisms is not continuous in time; ie, both open and closed loop dynamics co-existing simultaneously for postural control. Recently, Bottaro et al. (2005) [15] proposed a sliding mode control (a control strategy that first drives system to a stable manifold and then slide to equilibrium [16]), where the feedback is not continuous; as the system switches among stable manifolds [16] in time for PCS. Another control model is based on a set-point model proposed by Zatsiorsky et al. (1999 and 2000) [17,18]. They decomposed the stabilograms into two parts as rambling and trembling. They suggested CNS to set a reference point (rambling) and the body to sway with respect to the reference point (trembling) defined. Recently, Gürses et al. (2002 and 2006) [19,20] have suggested a closed loop nonlinear control scheme with stationary dead-zone (threshold) dynamics for position and velocity feedbacks.

On the contrary to the classical inverted pendulum model for the postural dynamics, mechanisms with higher degrees-of-freedom were also suggested for postural body dynamics. Creath et al. (2005) [21] and Colobert et al. (2006) [22] modelled human body upright posture dynamics with two inverted pendulums jointed at ankle and hip.

In another study, Alexandrov et al. (2005) [23] used three inverted pendulum model jointed at ankle, knee, and hip.

To study the human upright posture, a technique called stabilography has widely been accepted and used [24]. The method is used to obtain the projection of center-of-mass (CoM) in the horizontal plane. CoP is the application point of the resultant force-moments system created by the distributed forces and moments of standing subjects on the support surface [25]. That is the Center-of-Pressure (CoP) with its variations in its position on the horizontal plane (generally a force plate), which have been used to describe the human postural sway. There are many scientific researches that examined CoP to study human upright posture.

1.2 Motivation of the Thesis

1.2.1 Dynamics of the Human Postural Sway: Determinism versus Stochasticity

Newell and Corcos [26] said that “*Variability is inherent within and between all biological systems. The considerable differences that may be discerned among the motor abilities of humans is strong testament to this observation, as is the fact that it seems impossible for a given individual to generate identical movement patterns on successive attempts at performing the same task*”. The variability on a motor control system has two main sources. One of them is the noise in the multi-degrees of freedom sensorimotor system. And, the second one is the nonlinear oscillations of a control system [26]. This phenomenon can be exemplified by considering the sensors in the postural control system. The noise in the sensors [5,6] may lead measurement errors on the postural control system. On the other hand, the architecture of the sensors e.g., threshold on the sensors (e.g., [19,20]) may lead nonlinear oscillations for the PCS. Both may be the reasons of that an individual cannot generate identical movement trajectories on successive attempts at biped upright quiet stance. To study

motor control behaviour, generally the outputs of the motor control system (signals) was recorded and analyzed. The signals recorded demonstrate both deterministic and stochastic characteristics [27]. Center-of-Pressure (CoP) signal is the most common signal recorded to study the human postural sway. CoP is the collective output of postural control system and the force of gravity; and also includes dynamical components due to the body acceleration [28]. Subsequently, it can be suggested that the variability in the CoP signal has two main sources as well: noise in the sensorimotor system and nonlinear oscillations of the postural control system. In order to search the determinism versus stochastic features in the CoP signal, many research (e.g., Zatsiorsky and Duarte (e.g., [28,29]); Collins and De Luca (e.g., [13,14]); Kiemel, Oie, and Jeka (e.g., [5,6]); Newell, Slobounov, Slobounova (e.g., [30])) have been done since 1994 [13]. However, there is still not a universal consensus on the time period of the experimental trials performed to study the CoP signal. Trials from 30-second [31] up to 200-second [32] for quiet stance and 1800-second long [28,29] for unconstrained prolonged stance were used to study the CoP signal dynamics.

Determinism may be originated either from a linear or a nonlinear system. Nonlinear systems include both non-oscillatory systems: stable or unstable fixed points, saddle points (hyperbolic solutions); and oscillatory systems: periodic (e.g., limit cycle) and quasi-periodic (e.g., torus two-incommensurate-periodic), chaotic (e.g, strange attractors) [33]. Chaos in a system can be identified by showing existence of an attractor with fractal dimension [34] and sensitivity to the initial conditions. One may estimate the correlation dimension (D_2) [35] of a system to search for an attractor with fractal dimension and positive Lyapunov exponent (LE) for showing sensitivity to initial conditions [36]. For this purpose, the observed signal from a dynamical system is firstly reconstructed in m -dimensional state space for further analysis [37,38]. After calculation of nonlinear measures (e.g., D_2 and LE), the method of surrogate data is commonly applied to the calculated measures to justify the

nonlinearity [39]. Surrogate data sets are created by modelling the experimental data with some linear processes (preserving/destroying some features of the experimental data), then surrogate and experimental data are compared in terms of computed statistical measures to assess the difference/similarity between them. The nonlinear tools developed for physical sciences and engineering was also used widely to conceptualize biological systems (e.g., [40,41]).

Some examples of studies on the deterministic and stochastic characteristics of human postural sway have previously been mentioned. Collins et al. (1994) [13] tried to estimate correlation dimension (D_2) and Lyapunov exponent (LE) of the 90-second long CoP signals. However, they reported that D_2 estimate cannot be calculated since there was no clear linear scaling region and also D_2 estimates did not converge to a value for increasing embedding dimension (m) [42]. Also for the LE, they couldn't find significant difference between the calculated LEs from experimental records and the ones calculated from phase randomized surrogates [39]. They then concluded that postural control system (PCS) dynamics should not be modelled as a chaotic system. They then tried to model CoP trajectories with a correlated random walk model. For this purpose they calculated H exponent [43] and showed the significant difference between experimental records and shuffled surrogates on this measure [44]. They found $H > 0.5$, which means that past and future increments are positively correlated in the short-term region (< 1 second); while $H < 0.5$, which means that past and future increments are negatively correlated in the long-term (> 1 second) period. In the light of these findings, they proposed their famous theory about the PCS, which is stating that postural control system utilizes open-loop and closed-loop control strategies for short-term and long-term intervals respectively. In another study in 1994, Collins et al. [14] solidify their previous findings by using one and two dimensional random walk models (fractional Brownian motion [45]). Their findings suggested that postural control system has a memory, which means that past increments in displacements are correlated with future increments.

On the other hand, Yamada (1995) [32] has proposed that postural sway is chaotic. He calculated D_2 and LE for the 200-second long trials obtained from 5 subjects. He found fractal correlation dimension values and positive Lyapunov exponents. He suggested that to assure the “talk” between the postural control system and the body with its environment, the structure of postural sway should be chaotic rather than a limit cycle or a point attractor.

Duarte et al. (2000) [28] studied fractal properties of CoP trajectories for unconstrained prolonged standing (30 minutes). Their results suggested that postural control system presents long-range correlations from 10 seconds to 10 minutes. In a following study by Duarte et al. in 2001 [29], detrended fluctuation analysis (DFA) and power spectral analysis (PSA) were applied to the same 30-minutes signals. By this study, they claimed that postural control system can be explained by $1/f$ noise which is also observed in many other processes in the human.

Recently, Pascolo et al. (2005) [46] have estimated correlation dimension values and Lyapunov exponent for both healthy subjects and the subject who have Parkinson’s disease and found no significance difference between two groups on the measures (D_2 and LE). Roerdink et al. (2006) [31] calculated nonlinear measures as D_2 , LE, exponent H, and sample entropy [47] for healthy and stroke-after patients and they reported substantial differences between two groups on the mentioned measures.

On the other hand, stochastic models that are different than random walk were also used to model CoP trajectories. Two examples may be as follows: Chow et al. (1999) [48] used fluctuation-dissipation theorem (FDT presents the linear relation between the correlated fluctuations in the system and the response of the system to an external stimuli) Newell et al. (1997) [30] used Ornstein-Uhlenbeck model (a linear model in

which successive displacements of sway are governed by only a stiffness term) describe postural sway.

1.2.2 Stationarity of the CoP Signals

Most of the methods and measures described in previous section are valid if the CoP signal is stationary. In other words, they are justified with the implicit assumption of stationarity. So, it is critical to assess the stationarity of the CoP signals explicitly. For this reason, one of the first analyses applied to signal is the stationarity analysis. A stationary signal is a trend-free signal that has time-invariant statistical properties. CoP signal is generally accepted as a stationary signal (e.g., [13,28,29,31,32,46]), however, there are studies against this view. For example, Carroll et al. (1993) [49] expressed that one minute long CoP x or y time series are non-stationary since the mean and the variance of the postural sway is not time-invariant. They presented that there is a transition period (from non-stationarity to stationarity) in the time series for the mean and the variance measures. Also, Schumann et al. (1995) [50] demonstrated that CoP trajectories show non-stationary characteristics by time-frequency analysis, which is a technique to quantify changes in the spectral characteristic of a signal in time, for 100-second long trials. In another study, Loughlin et al. (1996) [51] studied CoP time series collected from both healthy and vestibularly-impaired subjects. Their results suggested that CoP time series are non-stationary for 90 seconds long trials (first 30-seconds quiet standing followed by a 60-seconds visually induced standing) by using time-frequency analysis. Also, there were time and frequency dependent differences in visually induced standing but not in quiet standing between normal and impaired subjects. So, why stationarity is an issue on this study? Because, if one intends to suggest deterministic chaos for the CoP signal by calculating fractal D_2 and positive LE, then he/she must show that the signal used for the analyses is stationary. Since, proposing *a number* for the mentioned measures has the inherent necessity that it is fixed during the measurement period.

1.2.3 Aging and Human Upright Posture

Many changes occur in human body and mind in many aspects (e.g., psychological, physiological) for many reasons by aging (e.g., [52,53,54,55]). This may also be the case for postural control (e.g., [56,57,58,59]). Infants learn to stand in their first years by falling and trying again [60]. However, falling may be lethal or cause impairments in the elderly (e.g., [61,62,63]); falls are the leading cause of nonfatal medically attended injuries in the United States [64]). Deterioration of the sensory systems in the postural adaptation (e.g., [65,66]), weakness of the muscles (e.g., [67,68]), and age-related pathologies like Parkinson's disease etc. may lead slight balance impairment (e.g., [69,70]). Several studies devoted to study postural control with aging are presented in the following paragraphs.

Woollacott et al. (1990) [71] worked on changes in postural control according to age and come up with the following conclusions:

- Older adults have more difficulty to stand when one or more sensory information is missing.
- Muscle weakness is a factor of postural trouble (difficulty in maintaining upright posture) in older adults.
- Older adults' muscles give later response to external threats to balance.
- A similarity between young children and older adults observed was using the co-activation of agonist and antagonist muscles when compared with young adults.

In another study by Amiridis et al. (2003) [72], young (20 subjects with a mean age of 20.1 years) and old adults (19 subjects with a mean age of 70.1 years) compared in 3 different stance (a) normal quiet stance (b) tandem Romberg stance (non-dominant heel in front of the dominant toe, arms on the hips) (c) one-legged stance. They used

CoP variations, electromyography (EMG) activity of hip and ankle muscles, kinesiograms (a kinematic analysis method used to measure displacements in joints) as the measures for looking difference between young and old adults. They found more CoP excursion, EMG activity, and joint displacement (ankle, knee, and hip displacements) in the old adults when compared to young adults.

Recently, Heldberg et al. (2007) [73] experimented with 13 infants in two different stances as with and without support on a movable platform (can make back and forward move in horizontal plane) in a longitudinal study (at 8th, 10th, 12th, 14th months of infants). They placed electrodes to the muscles placed in ankle, hip, lumbar region, and arm to record EMG activity. They concluded that postural adjustments were task and direction specific (response to stimuli with activation of agonist or antagonist muscle according to the direction of stimuli) and also changing with increasing age.

In this study, various measures have been used to understand the human postural sway. It has also been searched in this study whether any significant changes occur in these measures due to aging. Since, it may be crucial to use these measures to understand changes in the postural control system by aging.

1.3 Aim and Scope of the Thesis

The main aim of this work was searching dynamical and/or statistical measures of the CoP signal to build up a framework to understand human movement and perception. Both linear and nonlinear analytical methods were applied to CoP signals to obtain the relevant dynamical measures of the signal. This work covers the signal processing of the Center-of-Pressure in time, frequency, and state-space domains. In the time domain, to look for amount of postural sway, standard deviation values [74] of the time average detrended 180 sec long CoP signals were calculated. Also to interpret about the stationarity of the signal, Run Test [75] analysis; to evaluate ergodicity,

ensemble averages [76] were used in time domain. In the frequency domain, frequency content of the dynamics of the signal was searched by Fast Fourier Transformation [77] and the power distribution of the signal according to the spectral frequencies has been investigated by Welch's method [78].

In the state-space domain (the space in which the dynamical system evolves topologically rather; i.e., time is implicit); time delays (if $x(t)$ is the observed signal; then $x(t+\tau)$, $x(t+2\tau)$, ... , are constructed state-variables by time delay, τ) [37,38], and correlation dimension estimates [35] were calculated. Also parametric and non-parametric statistical tools were applied to search for the significant differences in the dynamical measures estimated over the trials of a subject (intra-subject), the subjects in the age-groups (inter-subject), and the groups (inter-group) formed with respect to the age.

1.4 Outline of the Study

The study is composed of 5 Chapters. Chapter 1 is the Introduction that offers information about the human postural dynamics and control system as well as introducing the global outcome of the human postural sway defined as Center-of-Pressure (CoP). In Chapter 2, the dynamical and statistical methods used to analyze the CoP signal are described. The Results obtained by analyzing the CoP signal collected from 28 subjects whose ages ranged from 6 to 84 are presented in Chapter 3. Chapter 4 includes modeling attempts of the statistical and dynamical behavior of the CoP_x (the x coordinate of CoP, refer to Chapter 2 Section 2.1.3) signal. Finally, in Chapter 5, the results found are discussed in the light of previous work done on human postural system.

CHAPTER 2

MATERIALS and METHODS

2.1 Data Acquisition

2.1.1 The Experimental Set-up

The experiments were performed at the Biomechanics Laboratory (Figure 2.1) of Mechanical Engineering Department of Middle East Technical University (METU).



Figure 2.1 The Biomechanics Laboratory. Left: A side (from left to right) view of the laboratory while the subjects are standing still; Right: Back to front view of the laboratory with respect to the standing subjects with the scene presented to the subjects during the data collection.

Signals from the ground reactions forces (F_x , F_y , F_z) and moments (M_x , M_y , M_z) were acquired by using Bertec[®] force platform while the subjects were standing at biped quiet stance. The analog signals were first amplified with a pre-amplifier embedded to the force platform, then, a second amplification was performed by a stand-alone amplifier with a cut-off frequency at 500 Hz, which have adjustable gains and can be

auto-zeroed. Filtered analog signals were sampled at 50 Hz with a 16-bit A/D converter card (DAQ PCI-6224 NI[®]), which is mounted into the computer (Pentium IV, Windows XP[®]). Data has been collected by using Matlab[®] (Data Acquisition Toolbox). The digitized signals were stored in the hard-disk of the computer and have been further manipulated and processed with the software Matlab[®].

2.1.2 Subjects and the Experimental Procedure

The signals were collected from 28 healthy subjects (14 male and 14 female). All subjects gave informed consent according to the guidelines of the Human Research Ethics Board of Middle East Technical University to participate in this study. 28 subjects were equally divided into 4 groups according to their ages. Group 1 (Children) was composed of 7 subjects with their ages 6 to 15 years old. Group 2 (Young Adults) comprised 7 subjects whose ages were between 20 and 40 years old. Other 7 subjects with their ages ranging from 41 to 60 years old made up the Group 3 (Adults). The last group (Group 4) was the Elderly Group, which had 7 subjects older than or at 65 years old.

The sex, age, height, and weight statistics of the subjects and the groups are given in Table 2.1. The average age, weight, and height of all subjects were 40.2 ± 24.5 (mean \pm standard deviation) years (ranging from 6 to 84 years old), 162.4 ± 16.4 cm (ranging from 119 to 183 cm), and 64.9 ± 16.6 kg (ranging from 25 to 88 kg) respectively.

Each subject has been instructed to stand still as quiet as possible with an upright posture on the force platform at two-leg (tandem) stance without wearing shoes and with their eyes open. A series of five successive 180 seconds long trials were recorded from each of the 28 subjects. The sampling frequency of the data collection was 50 Hz. 180 seconds long resting gaps were allowed between the successive trails of the subjects. After the experiments, two questions were asked to the subjects. First

one was “Have you been tired in the experiments?” and the other one was “What did you pay attention during the experiments?” The answers of the subjects to the questions and the other knowledge about the subjects are given in the Appendix J.

Table 2.1 Age, height, and weight statistics of the subjects and the groups

Subject	Group	Sex*	Age [years]	Height [cm]	Weight [kg]
1	Group 1	F	6	119	25
2		M	7	130	43
3		M	9	137	31
4		M	10	140	42
5		F	11	142	41
6		M	14	174	86
7		F	14	162	61
Group 1 Means			10.1 ± 3.1	143.4 ± 18.8	47.0 ± 20.6
8	Group 2	M	21	183	85
9		F	25	174	63
10		F	27	162	68
11		F	28	170	53
12		M	31	183	70
13		F	35	160	60
14		M	39	180	88
Group 2 Means			29.4 ± 6.1	173.1 ± 9.6	69.6 ± 12.8
15	Group 3	F	41	175	70
16		M	42	176	76
17		F	43	168	67
18		F	54	168	67
19		M	48	174	75
20		M	50	178	75
21		F	55	154	78
Group 3 Means			47.6 ± 5.7	170.4 ± 8.2	72.6 ± 4.5
22	Group 4	F	65	158	69
23		M	65	161	82
24		M	68	176	78
25		M	73	170	81
26		M	78	167	75
27		F	83	153	54
28		F	84	154	56
Group 4 Means			73.7 ± 8.1	162.7 ± 8.6	70.7 ± 11.6

* F, denotes Female and M, denotes Male

2.1.3 Center-of-Pressure

Center-of-Pressure (CoP) (Figure 2.2 (c)) is the application point of the resultant force-couple system (Figure 2.2 (b)) created by the distributed forces beneath the feet of standing subjects on the support surface (Figure 2.2 (a)). Variations in the position of the Center-of-Pressure (CoP) were used to describe the human postural sway [24,25]. F_z , M_x , and M_y signals were used to construct the time series CoP_x and CoP_y which are the x and y coordinates of CoP respectively (Equations (2.1) and (2.2)). Each of the signals, CoP_x and CoP_y time series were composed of 9000 samples (180-sec long trial with the sampling frequency of 50 Hz). The x- and y- components of the CoP signal give knowledge about the sway dynamics mapped to the sagittal and coronal planes respectively (Figure 2.3 (a) and (b)). CoP_x and CoP_y time series were used for further analysis of human postural sway.

$$CoP_x(i) = -\frac{M_y(i)}{F_z(i)}, i = 1 \dots 9000 \quad (2.1)$$

$$CoP_y(i) = \frac{M_x(i)}{F_z(i)}, i = 1 \dots 9000 \quad (2.2)$$

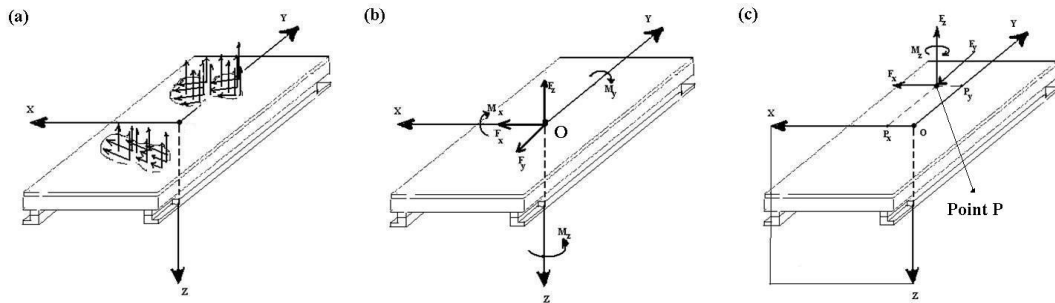


Figure 2.2 (a) Distributed forces at the foot-base (b) The resultant force-couple system of the distributed forces at the mid-point (origin) of the platform (Point O) (c) The resultant force-couple system has been moved to Point P (Center of Pressure), where M_x and M_y were zero [19,79]

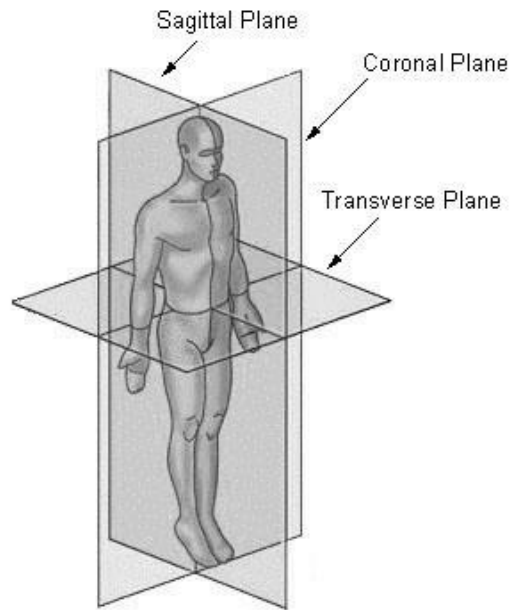


Figure 2.3(a) Anatomical planes described for the human body

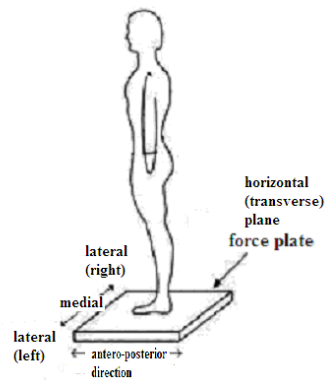


Figure 2.3(b) Sagittal and coronal planes on force plate

Examples of CoP_x and CoP_y signals are presented in Figure 2.4 and 2.5. The exemplar CoP signals belong to the first trial of Subject 11 (Table 2.1).

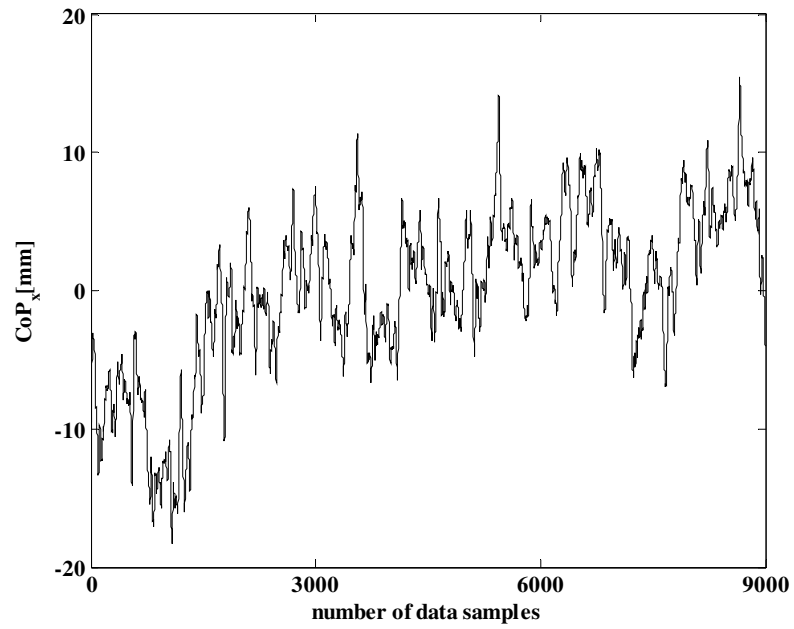


Figure 2.4 A typical representative 180 sec long CoP_x [11th subject, F, 28] time series

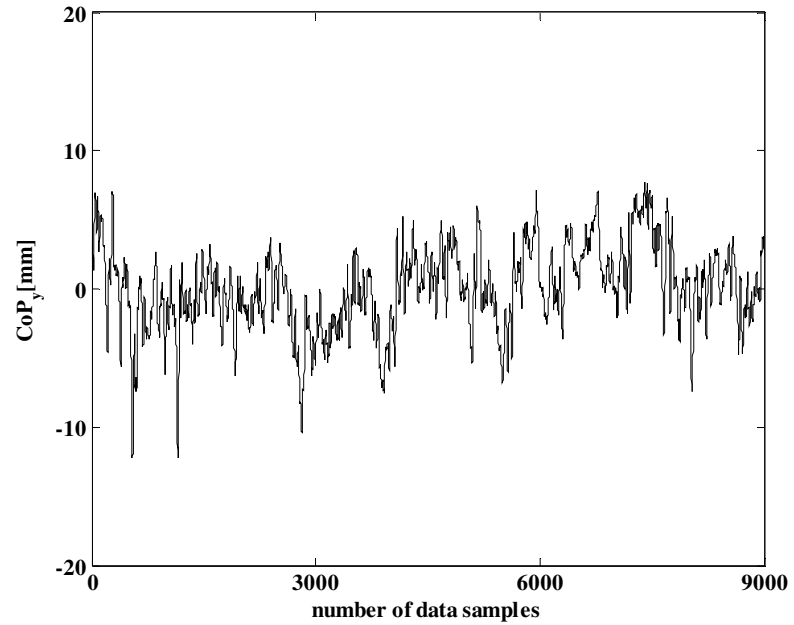


Figure 2.5 A typical representative 180 sec long CoP_y [11th subject, F, 28] time series

2.2 Analysis of the Signals

The CoP_x or CoP_y signals were abbreviated by the symbol X for the signal analysis. Also, X_i is the amplitude of the i^{th} sample of the signal and $X_{i,j}$ is the amplitude of the i^{th} sample of the j^{th} trial, if not otherwise stated.

2.2.1 Linear Analysis

2.2.1.1 Time Domain Analysis

2.2.1.1.1 Mean and Variance

The first step in the statistical analysis of the time series was to compute the mean and variance (CoP_x and CoP_y). The mean value (time average) of the signals, which represents the central tendency in the signals, was computed. “Central tendency is a statistical measure to determine a single score that defines the center of a distribution [80]”. The mean value of CoP signal was estimated by computing the arithmetic average of all sample values in the trial (Equation (2.3)). Since the mean value of CoP signal is a static measure, which indicates the arbitrary position of the subject while standing on the platform during the test, it has been subtracted from the corresponding signal; i.e., signals which were used in the further analysis have been detrended. The standard deviation and the variance (Equation (2.4)) of the CoP signals were also computed. Standard deviation/variance is a measure of dispersion of the distribution [74]. In our case, it is a measure of variability or amount of postural sway.

$$\bar{X} = \frac{1}{n} \sum_{i=1}^n X_i, \quad i = 1 \dots 9000 \quad (2.3)$$

$$\sigma_x^2 = \frac{1}{n-1} \sum_{i=1}^n (X_i - \bar{X})^2, \quad i=1 \dots 9000 \quad (2.4)$$

2.2.1.1.2 Run Test

Run test is a non-parametric statistical test to examine whether a signal carries a trend or not. A signal can be categorized as being *non-stationary* or *stationary* depending on whether it carries a trend or not, respectively [76]. A formal definition of stationarity by Kantz et al [81] is as follows; “a signal is called stationary if all joint probabilities of finding the system at some time in one state and at some later time in another state are independent of time within the observation period, i.e. when calculated from the data”.

The procedure to apply the Run Test to the CoP time series has been described below [75]. Also, a demonstration of application of the Run Test has been given in Appendix A.

1) CoP_x (or CoP_y) signal which was composed of 9000 samples (180 seconds x 50 Hz) has been divided into 18 equal segments each containing 10 second-long data. The mean square of each segment (Ψ^2) was computed (Equation 2.5). Thus a series of 18 elements each being an estimate of the segmental mean square was computed (Equation (2.6)).

$$\Psi_r^2, \quad r=1 \dots 18 \quad (2.5)$$

$$\Psi_r^2 = \frac{1}{500} \sum_i^w X_i^2 \quad (2.6)$$

where $i = (r-1) \cdot 500 + 1$, $w = r \cdot 500$, $r = 1 \dots 18$

2) The median of the series was calculated (Equation (2.7)).

$$\text{median}(\Psi_r^2, r = 1 \dots 18) \quad (2.7)$$

3) In order to apply the non-parametric statistical Run Test, the elements of the series (Equation 2.5), which are larger than the median of the series (Equation 2.7) were marked with the symbol '+'; while the elements of the series, which are less than the median of the series were marked with the symbol '-'.

4) Sequences of '+'s and '-'s were grouped separately and each group is counted as a *run*. By this way, the value of the *total run* was found.

5) The *null hypothesis* of the Run Test is that the signal does not carry a trend. The null hypothesis has been tested by comparing the value of the total run with the interval estimated (Equation 2.8) in the *Run Distribution Table*. The Run Distribution Table (given in Appendix B) presents the intervals estimated at different confidence levels to reject or accept the null hypothesis for the value of the total run computed.

In this study, the confidence level has been selected as 95% and the number of elements in the series ($\Psi_r^2, r=1 \dots 18$) was 18. The interval to accept the null hypothesis (Equation (2.8)) is given in the 'Run Distribution Table' (refer to Appendix B). If the condition defined in Equation (2.8) is satisfied, then it can be concluded that the signal does not carry a trend. Thus it is called a *stationary signal*. On the other hand, if the condition defined in Equation (2.8) is not satisfied, then it is concluded that the signal carries a trend, which states that the signal is *non-stationary*. Two intervals for the signal to be non-stationarity are given in Equation (2.9) and Equation (2.10). It has been defined that if the condition given in Equation (2.9) holds, then the signal is said to be *non-stationary from the left-side* and if the

condition given in Equation (2.10) holds, then the signal is said to be *non-stationary from the right-side* [84].

$$5 < r \leq 14 \quad (2.8)$$

$$0 < r \leq 5 \quad (2.9)$$

$$14 < r \leq 18 \quad (2.10)$$

2.2.1.1.3 Ensemble Average

In the further statistical analysis, “*Ensemble Average*” of the CoP signal was used to check whether the signals are *ergodic* or not. Ensemble average is defined as an average over trials at a given instant in time [76]. In other words, ensemble average is measured across the trials ($x_1(t)$, $x_2(t)$, $x_3(t)$, $x_4(t)$, $x_5(t)$) at a particular instant of time (t_1 or t_2) (Figure 2.6) or at a particular frame [82]. A frame is a data window composed of a fixed number of data samples. *Stationary signals* are called *ergodic* if the ensemble average is equal to the time average obtained from one of the trial ($x_i(t)$), and the time average obtained from one frame to the next is the same [76].

In order to apply the method, a number of frames were to be composed from the CoP signals. The data window width has been chosen to be consisting of 500 data samples. It has been shown that the dynamics in the CoP_x signal collected during quiet stance, consists of at least two natural frequencies in the frequency band of 0.1-1 Hz [4,21]. Thus, a data window with a width of 500 data samples, which has been sampled with a frequency of 50 Hz would then cover a full cycle of CoP dynamics reported. Because the CoP signals were composed of 9000 samples and the width of data window has been chosen to be 500 data samples, the total number of frames came out to be 18. There was no overlap between the two successive frames.

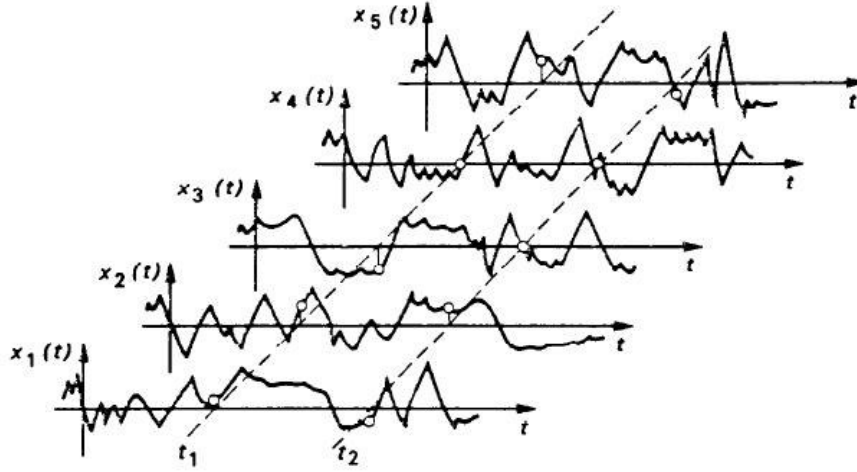


Figure 2.6 Concept of ensemble averaging [10]. $x_1(t)$, $x_2(t)$, $x_3(t)$, $x_4(t)$, $x_5(t)$ are the trials and t_1 or t_2 are the instants in time (t)

The procedure to check ergodicity by computing the ensemble average is symbolically presented below.

1) Frames (F) were started to be composed from the first trial's data ($i = 1$ to 9000 data samples and $j = 1$) of a subject. Each frame ($F_{i,j}$, Equation (2.11)) has 500 samples. The first frame consisted of data samples from 1st to 500th of the first trial. The second frame has data samples starting from 501th data sample to 1000th data sample of the first trial and so on. Thus, there were a total number of 18 frames within a trial. The same procedure was repeated for the other 4 trials (Equation 2.12).

$$\overline{F}_{i,j} = [X_{(i-1) \cdot 500 + 1, j}, \dots, X_{i \cdot 500, j}], \quad i = 1 \dots 5, \quad j = 1 \dots 18 \quad (2.11)$$

$$\overline{F} = \begin{pmatrix} \overline{F}_{1,1} & \dots & \overline{F}_{1,18} \\ \vdots & \ddots & \vdots \\ \overline{F}_{5,1} & \dots & \overline{F}_{5,18} \end{pmatrix} \quad (2.12)$$

All of the frames obtained from CoP signals of five of the successive trials of one subject composed the frame matrix F defined in Equation (2.12).

2) Time average ($T_{i,j}$) of each frame ($F_{i,j}$) was computed and time average matrix (T) was composed.

$$T_{i,j} = \frac{1}{500} \sum_{(i-1) \cdot 500 + 1}^{i \cdot 500} X_{i,j}, \quad i = 1 \dots 5, \quad j = 1 \dots 18 \quad (2.13)$$

$$\bar{T} = \begin{pmatrix} T_{1,1} & \dots & T_{1,18} \\ \vdots & \ddots & \vdots \\ T_{5,1} & \dots & T_{5,18} \end{pmatrix} \quad (2.14)$$

3) A two-way analysis of variance (ANOVA) was applied to T matrix in order to check whether averages on columns and rows are significantly different or not. A p -value less than 0.05 was accepted as an indication of significant difference (Appendix C).

4) The null hypothesis of the statistical test has been defined as the CoP signals of a subject are ergodic. The null hypothesis has been checked by comparing the p -values obtained from the two-way ANOVA test of T matrix of a subject at the confidence level, α set to 0.05. The null hypothesis has been accepted if the p -values for both columns and rows are greater than 0.05.

2.2.1.2 Frequency Domain Analysis

Detrended CoP_x and CoP_y signals were used in the frequency domain analysis. CoP_x and CoP_y signals were filtered with a digital 3rd-order low-pass Butterworth filter, with a cut-off frequency of 8 Hz [4,21].

2.2.1.2.1 Fast Fourier Transformation

To explore the frequency content of the CoP_x and CoP_y signals, Fast Fourier Transformation (FFT) analysis was applied [77]. The built-in function (fft) in the software Matlab[®], which is based on Cooley-Tukey algorithm [83] has been used. The discrete Fourier coefficients of the transformation are defined in Equation (2.15).

$$C_k = \frac{1}{N} \sum_{i=0}^{N-1} X_i e^{-j(2\pi ki/N)}, \quad k = 0, 1, 2, \dots, (N-1) \quad (2.15)$$

where $j = \sqrt{-1}$ and N is the length of the signal in samples.

2.2.1.2.2 Power Spectral Density Estimates

Power Spectral Density (PSD) estimates via *Welch's method* [78] were computed to quantify the distribution of the power of the signals in frequency spectrum. The built-in function (pwelch) of Matlab[®] was used for computing PSD estimates. By using Equations (2.16) and (2.17) the ratio of the power between 0-0.1 Hz and 0-1 Hz frequency band to the power involved in the signal at the entire frequency spectrum of the signal (0-25 Hz) were defined respectively. These two frequency bands (0-0.1 Hz and 0.1-1 Hz) which have been used to compute the power ratios, involve the two natural frequencies of the CoP_x dynamics [4,21]. The integrals in Equations (2.16) and (2.17) were computed numerically by using *Trapezoid Rule* (presented in Appendix D).

$$\int_0^{0.1} \hat{P}(f) \cdot df \Big/ \int_0^{25} \hat{P}(f) \cdot df \quad (2.16)$$

$$\int_0^1 \hat{P}(f) \cdot df \Big/ \int_0^{25} \hat{P}(f) \cdot df \quad (2.17)$$

The derivation and definition of the estimator $P(f)$ [78] were given in Appendix E.

2.2.2 Nonlinear Analysis

In the previous part of the study, linear methods were introduced for the analysis of the CoP signals. However, the linear analyses are not adequate to explain the complex structure of the CoP signals (e.g., [13,28,29,32,46]). In this part of the study, nonlinear methods are presented to study the complexity in the structure of the CoP signals.

2.2.2.1 Correlation Dimension

Complex and chaotic systems are usually characterized by searching for the existence and the properties of an attractor [33,76,85,87]. An *attractor* is the smallest set of the phase points to which all of the system trajectories eventually converge [33]. The space in which the dynamical system evolves is called the state space of the dynamical system and the ordered points in this space are called as the phase points, which constitute the dynamical system trajectories in the state space [76].

“The dimension of an attractor determines the minimum number of essential variables required to describe the dynamics on the attractor [76]”. Generally, dimension estimates [85] are used to search and quantify the properties of an attractor. In this

study, a widely used dimension estimate, correlation dimension estimate (D_2) [35] has been used to search and quantify the properties of the possible attractor. Independent m -signals are needed in order to compute an estimate of the dimension of an attractor [86]. It follows that the dynamics of the CoP_x signal is to be reconstructed in a m -dimensional state space.

2.2.2.2 Reconstruction of Dynamics in m -dimensional Embedding State Space

Experimentally obtained CoP_x signals (Section 2.1.3) were utilized as the observable state of the human postural sway. The observable state of a dynamical system is the dynamical variable which is measured in the experiment to describe the phenomenon studied [76]. In our case, the studied phenomenon was the human postural sway and the dynamical variable measured in the experiments has been the CoP_x signal. However, it is not possible to estimate the dimension of a possible attractor, which has a dimension larger than 1 through a single time series; thus the dynamics from the observable state should be reconstructed in a m -dimensional state space [86]. Packard et al. [29] and Takens [30] suggested a way to reconstruct the dynamics from the observable state in m -dimensional state space by selecting a fixed time delay, τ . The method is called *method of time delay* [87], by which $x(t), x(t+\tau), x(t+2\tau), \dots$ become the new independent variables obtained from a single time series, $x(t)$. The amplitudes of the data samples (X_i) in the original time series of measurements, which have been collected by using a fixed time interval (Δt), are represented by Equation (2.18), where N is the total number of the data points in the time signal.

$$X_1 = x(t_0), X_2 = x(t_0 + \Delta t), X_3 = x(t_0 + 2\Delta t), \dots, X_N = x(t_0 + (N-1)\Delta t) \quad (2.18)$$

By selecting a fixed time delay τ , m vectors (ξ) of fixed length k have been constructed (Equation (2.19)); where $k = N-(m-1)\tau$.

$$\begin{aligned}
\bar{\xi}_1 &= \{X_1 \ X_2 \ \dots \ X_{N-(m-1)\tau}\} \\
\bar{\xi}_2 &= \{X_{1+\tau} \ X_{2+\tau} \ \dots \ X_{N-(m-1)\tau+\tau}\} \\
&\vdots \\
\bar{\xi}_m &= \{X_{1+(m-1)\tau} \ X_{2+(m-1)\tau} \ \dots \ X_N\}
\end{aligned} \tag{2.19}$$

Then the first elements of the vectors, ξ_i where $i=1\dots m$ define the coordinates of the first *phase point* ($X_1, X_{1+\tau}, \dots, X_{1+(m-1)\tau}$) in the m -dimensional state space, second elements of the vectors, ξ_i are the coordinates of the second phase point ($X_2, X_{2+\tau}, \dots, X_{2+(m-1)\tau}$) and it goes on (Equation (2.20)).

$$\begin{aligned}
X_{m,1} &= (X_1, X_{1+\tau}, \dots, X_{1+(m-1)\tau}) \\
X_{m,2} &= (X_2, X_{2+\tau}, \dots, X_{2+(m-1)\tau}) \\
&\vdots \\
X_{m,N-(m-1)\tau} &= (X_{N-(m-1)\tau}, X_{N-(m-1)\tau+\tau}, \dots, X_N)
\end{aligned} \tag{2.20}$$

where N is the length of the experimental time series and τ is the time delay introduced. $X_{m,k}$ is the k^{th} phase point in m -dimensional state space, where $k = N-(m-1)\tau$. Subsequently, in order to be able to use the *method of time delay*, a proper time delay should be determined.

2.2.6.2 Estimate of Time Delay (τ)

In order to embed CoP_x dynamics in m -dimensional state space, a proper time delay (τ) should be selected. Choosing a proper time delay (τ) is critical in reconstructing the CoP_x dynamics. If τ is chosen to be too small, it leads to a *redundancy* between the successive delay coordinates (Equation (2.19)), which causes the possible attractor to be represented in the state space as the *identity line* (Figure 2.7 (a)) [88]. In other words, if τ had been chosen to be too small, the variables (ξ) would not behave as independent signals [88]. On the other hand, if τ had been chosen to be too

large, then, it would lead to *irrelevance* in successive delay coordinates. To put it in another way, it would cause the independent variables (ξ) to be dynamically unrelated (Figure 2.7 (b)). The dynamics of the CoP_x signal in m -dimensional state-space wouldn't have been represented properly in both of the above two cases. Thus, the strategy to choose the proper time delay τ , should be to search for expanding the possible attractor sufficiently away from the identity line without losing relevance to the dynamics. Rosenstein et al. [88] stated that expansion of the attractor from the identity line is best quantified by measuring the average displacement (S_m , Equation (2.21)). The average displacement is a multidimensional measure that quantifies the difference between delay coordinates (ξ) [88].

$$S_m(\tau) = \frac{1}{M} \sum_{i=1}^M \sqrt{\sum_{j=1}^{m-1} (X_{i+jJ} - X_i)^2} \quad (2.21)$$

where J is related to the time delay in samples by Equation (2.22) and M is the number of pairs of phase points in m -dimensional state space.

$$J = \tau / \Delta t \quad (2.22)$$

The value of τ_c (the subscript ‘‘c’’ denotes the critical time delay) for a given dimension m was quantified by the point where the slope of the curve $S_m(\tau)$, obtained by plotting the average displacement S_m (Equation (2.21)) against varying time delays (τ), first decreased to less than 40% of its initial value. Further, a *reconstruction window*, τ_w (Equation (2.23)) has been proposed to be defined as a system invariant when the system dynamics is to be reconstructed in a m -dimensional embedding state-space [88,89].

$$\tau_w = \tau_c \cdot (m-1) \quad (2.23)$$

Average displacement ($S_m(\tau)$) curves were computed for varying embedding dimensions ($m=2,3,4,5,6,8,9,10,12,15,18,20$) from CoP_x signals at each of the trial of every subject. Then, the critical time delays (τ_c) were determined by using the curve, $S_m(\tau)$. The existence of reconstruction windows (τ_w) [88,89] were searched in our particular problem. Time delays were used to embed CoP_x dynamics in m -dimensional state-space, so the correlation dimension estimates could be computed.

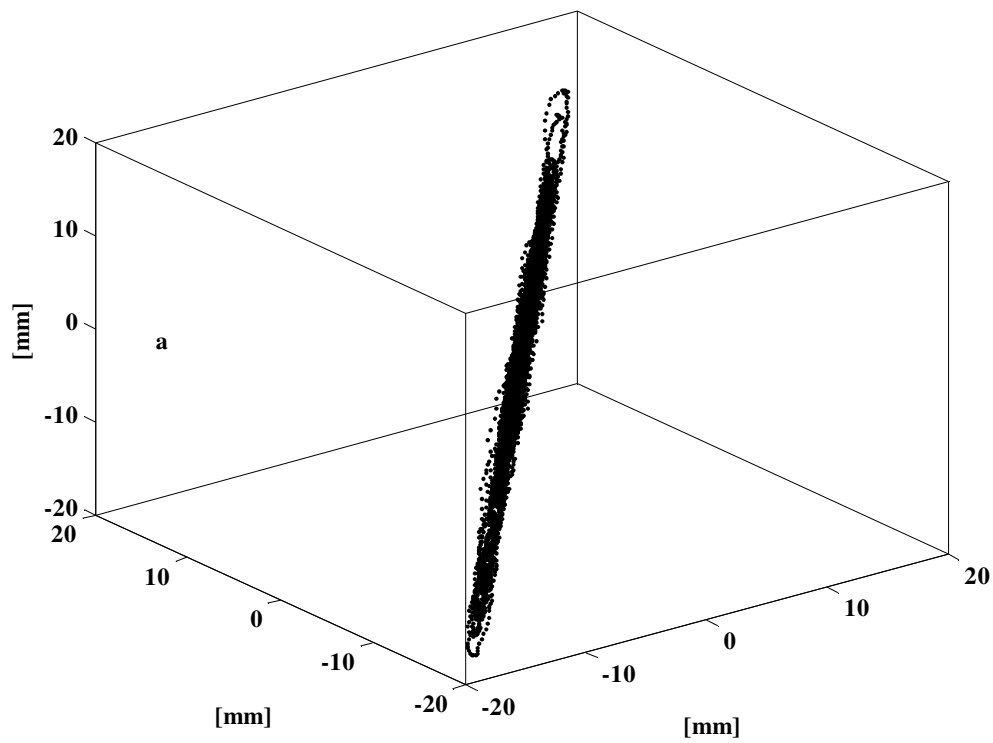


Figure 2.7 (a) The figure shows how the pattern of the possible attractor changes by selecting the time delay τ , too small (1/10 of the proper time delay).

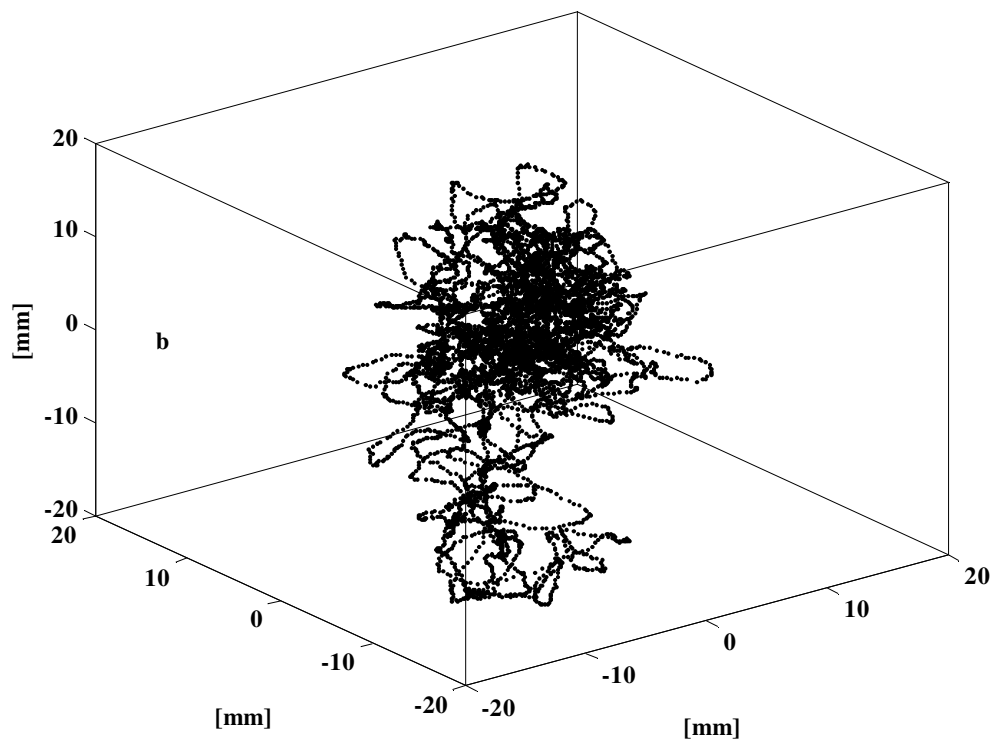


Figure 2.7 (b) The figure shows how the pattern of the possible attractor changes by selecting the time delay τ , too large (10 times the proper time delay).

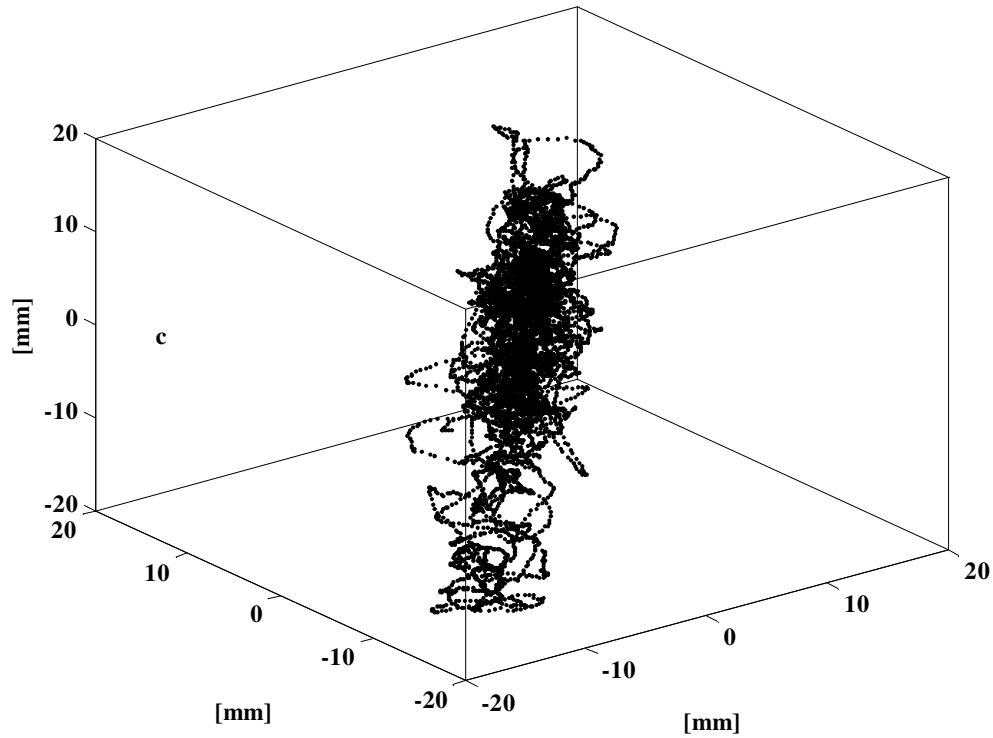


Figure 2.7 (c) The figure shows how the pattern of the possible attractor changes by selecting the time delay τ , properly [88,91]. The plots in the figure have been generated by plotting the three successive delay coordinates against each other (ξ_1 , ξ_2 and ξ_3 in Equation (2.19)) of the reconstructed CoP_x signal [11th subject, F, 28] in 3-dimensional embedding state space ($m=3$) with the time delay (τ) values taken as (a) 2 (b) 190 (c) 19 in number of data samples.

2.2.6.3 Correlation Dimension Estimates

Correlation dimension is a measure obtained by considering spatial correlations between the phase points on the attractor [35]. In order to compute the correlation dimension (D_2) estimate from a time series, the correlation function, $C(r)$ is defined as the spatial correlations between the pairs of phase points (Equation (2.24)) in the m -dimensional embedded dynamics (Equation (2.20)). The correlation function, $C(r)$ is computed by constructing a sphere of radius r around each point X_i in the state

space of the possible attractor and counting the number of points within the sphere [76].

$$C(r) = \lim_{N \rightarrow \infty} \left[\frac{1}{N^2} \sum_{i=1}^N \sum_{j=1}^N H(r - |X_i - X_j|) \right] \quad (2.24)$$

where H is the Heaviside function defined as

$$H(u) = \begin{cases} 0 & \text{if } u < 0 \\ 1 & \text{if } u \geq 0 \end{cases} \quad (2.25)$$

and $|X_i - X_j|$ is Euclidean norm [90] and defined in Equation (2.26).

$$|X_i - X_j| = \sqrt{(X_i - X_j)^2} \quad (2.26)$$

Then, the correlation dimension D_2 is defined as:

$$D_2 = \lim_{r \rightarrow 0} \frac{\ln C(r)}{\ln(r)} \quad (2.27)$$

The correlation dimension (D_2) has been computed from the slope of the linear portion of the curve obtained by plotting the natural logarithm of the correlation function, $C(r)$ against the natural logarithm of varying tolerance distances, r ; i.e., curve $\ln C(r)$ as a function of $\ln(r)$. To estimate D_2 , the slope of the linear portion of the curve $\ln C(r)$ versus $\ln(r)$ must have a significant length (a length of $\Delta \ln(r) = 1.6$ is the minimum acceptable scaling length) [42]. Furthermore, D_2 estimates must be robust against variations in embedding dimension, m [42]. Thus the correlation

dimension estimates were computed for the embedding dimensions,
 $m=2,3,4,5,6,8,9,10,12,15,18,20$.

CHAPTER 3

RESULTS

3.1 Results of the Linear Analysis

3.1.1 Results of the Time Domain Analysis

3.1.1.1 Variance/Standard Deviation of the Signals

The variance/standard deviation statistics (Section 2.2.1.1.1) for both detrended CoP_x and CoP_y signals (Section 2.1.3) are presented in this section. Variance values of the CoP_x and CoP_y signals are measures of amount of postural sway in the antero-posterior and medio-lateral directions at the horizontal plane respectively (Figure 2.3(b)) in Chapter 2 Section 2.1.3). The standard deviation values of the CoP_x and CoP_y signals for five successive trials of each of 28 subjects are presented in Table 3.1 and 3.2 respectively.

3.1.1.1.1 Standard Deviation of the CoP_x Signals

The maximum standard deviation value for detrended CoP_x signals was 16.0 mm, which belongs to the fourth trial of 6 years old, female subject (Subject 1 in Table 3.1(a)). On the other hand, the minimum of the standard deviation values for CoP_x signals was 2.9 mm, which was demonstrated by two subjects. One of the subjects was Subject 14 (39 years old, Male, Table 3.1(a)) while the other one was Subject 27 (83 years old, Female, Table 3.1(a)).

When the mean of standard deviation values of five trials of the subjects considered, the maximum mean value was 12.5 ± 2.4 which was performed by the 1st subject (Female, 6 years old) (Table 3.1(a)). Also, the minimum mean value was 3.5 which was demonstrated by two subjects (Subject 9: Female 25 years old, Subject 14: Male, 39 years old) in Group 2 (Table 3.1(a)).

A 2-way ANOVA test performed on the standard deviation values of CoP_x signals were found to be significantly different on subjects ($p < 0.000$) but not significantly different on trials ($p < 0.195$). In addition, 1-way ANOVA test was used to search for the group differences on the standard deviation values. The results of 1-way ANOVA test, where the groups were the main effect and the trials have been the repeated measures, indicated that standard deviation values were not significantly different on the groups ($p < 0.414$).

3.1.1.1.2 Standard Deviation of the CoP_y Signals

The maximum standard deviation value of the detrended CoP_y signals was 23.3 mm, which has been observed in the second trial of the 7 years old, male subject (Subject 2 in Table 3.1(b)). On the other hand, the minimum of the standard deviation values of CoP_y signals was 1.2 mm, which has been demonstrated by two subjects as well. The first subject was the same subject as in the case of minimum CoP_x performance; i.e., Subject 14 (39, Male) while the other subject was Subject 19 (48, Male).

Similar to the CoP_x signal, the maximum mean value of standard deviations in CoP_y signals was 10.8 ± 4.7 which was performed by the Subject 1 (Female, 6 years old) (Table 3.1(b)). Similarly, the minimum mean value was 1.5 ± 0.4 which was made by the Subject 14 (39, Male) (Table 3.1(b)).

Similarly, a 2-way ANOVA test applied on the standard deviation values of CoP_y signals were found to be significantly different on subjects ($p < 0.000$) but not significantly different on trials ($p < 0.511$). Besides, 1-way ANOVA test was performed to search for the group differences on the standard deviation values. The results of 1-way ANOVA test, where the groups were the main effect and the trials have been the repeated measures, showed that standard deviation values were not significantly different on the groups ($p < 0.112$).

Table 3.1(a) Standard deviation values of the CoP_x signals in millimeters

Subject	Group	T 1	T 2	T 3	T 4	T 5	Means *	StDevs *
1	Group 1	9.8	11.0	12.0	16.0	13.9	12.5	2.4
2		6.8	7.9	6.2	7.5	6.7	7.0	0.7
3		5.1	6.1	5.1	5.1	7.0	5.7	0.9
4		7.2	9.0	8.9	10.0	8.3	8.7	1.0
5		4.7	4.4	4.2	5.6	5.4	4.8	0.6
6		7.8	8.9	5.2	7.4	5.8	7.0	1.5
7		6.4	6.6	5.1	6.3	7.0	6.3	0.7
8	Group 2	4.4	5.8	9.2	11.8	7.1	7.7	2.9
9		3.1	3.1	3.8	3.9	3.9	3.5	0.4
10		7.8	10.7	12.1	11.2	12.3	10.8	1.8
11		6.0	7.0	5.9	6.4	7.8	6.6	0.8
12		7.3	5.0	4.2	3.5	4.7	4.9	1.4
13		4.0	3.9	6.3	4.4	3.4	4.4	1.1
14		4.1	3.1	3.6	2.9	3.9	3.5	0.5
15	Group 3	5.4	5.0	5.4	5.8	5.1	5.3	0.3
16		4.1	4.6	3.6	3.1	3.9	3.8	0.5
17		3.8	4.0	4.9	4.5	3.4	4.1	0.6
18		11.2	8.4	7.0	8.9	6.9	8.5	1.8
19		4.1	4.6	7.7	4.7	5.7	5.3	1.4
20		8.2	7.2	7.1	8.2	7.3	7.6	0.6
21		4.1	3.6	4.3	4.5	3.9	4.1	0.3
22	Group 4	4.0	4.0	4.5	5.7	5.3	4.7	0.8
23		3.4	5.4	4.1	4.4	4.7	4.4	0.7
24		8.5	9.3	8.4	10.9	8.9	9.2	1.0
25		5.5	11.1	7.1	6.6	4.4	6.9	2.5
26		9.1	7.1	5.2	7.5	7.0	7.1	1.4
27		3.9	3.0	2.9	4.9	4.3	3.8	0.9
28		4.4	3.8	4.2	4.4	3.7	4.1	0.3

*Means and StDevs indicate the mean and the standard deviation value of five successive trials of a subject respectively.

Table 3.1(b) Standard deviation values of the CoP_y signals in millimeters

Subject	Group	T 1	T 2	T 3	T 4	T 5	Means *	StDevs *
1	Group 1	6.0	7.1	9.9	13.6	17.4	10.8	4.7
2		5.9	23.3	6.0	6.9	5.5	9.5	7.7
3		3.5	2.7	3.8	3.5	4.2	3.5	0.5
4		4.0	5.2	4.5	6.0	4.9	4.9	0.7
5		2.8	3.1	2.8	2.0	1.9	2.5	0.5
6		3.8	2.2	2.8	2.7	2.5	2.8	0.6
7		5.3	4.6	3.3	5.5	4.8	4.7	0.9
8	Group 2	5.0	4.1	3.5	2.9	3.2	3.7	0.8
9		2.1	2.9	2.3	2.5	2.0	2.4	0.3
10		3.8	2.8	3.3	4.1	3.6	3.5	0.5
11		3.0	4.5	6.9	5.8	5.7	5.2	1.5
12		2.8	1.4	2.5	1.9	2.0	2.1	0.5
13		1.8	1.5	2.7	2.1	2.5	2.1	0.5
14		1.2	1.2	1.7	1.5	2.0	1.5	0.4
15	Group 3	2.5	4.0	3.2	2.8	2.0	2.9	0.8
16		1.7	2.0	1.4	3.3	2.9	2.3	0.8
17		2.5	2.2	2.2	2.8	2.9	2.5	0.3
18		5.5	3.2	5.6	7.3	6.1	5.6	1.5
19		1.2	2.4	2.4	1.4	2.2	1.9	0.5
20		5.2	5.5	5.1	4.9	6.0	5.3	0.4
21		2.3	1.8	1.8	1.7	2.3	2.0	0.3
22	Group 4	2.9	2.1	3.1	1.8	3.4	2.7	0.7
23		2.5	5.3	3.2	2.4	3.7	3.4	1.2
24		6.1	5.7	3.7	4.8	7.1	5.5	1.3
25		1.9	3.4	1.8	1.7	1.3	2.0	0.8
26		6.3	5.9	4.9	5.2	5.5	5.6	0.6
27		3.2	4.2	4.0	6.6	7.1	5.0	1.7
28		2.0	2.0	2.1	3.0	1.9	2.2	0.5

*Means and StDevs indicate the mean and the standard deviation values of five successive trials of a subject respectively.

3.1.1.2 Results of Run Test

Run Test (Section 2.2.1.1.2) was applied to detrended CoP_x and CoP_y signals obtained from 5 successive trials of each of 28 subjects (140 CoP_x and 140 CoP_y signals altogether). The results of the *Run Test* were given in *total run* (Chapter 2 Section 2.2.1.1.2) in Table 3.2. The test results for the CoP_x signal has shown that 4 out of 140 trials, which belong to four different subjects (Subjects 5, 7, 23, and 24) were non-stationary from the left-side (refer to Chapter 2 Section 2.2.1.1.2). Thus, 136 of the CoP_x signals recorded during 140 of 180-sec long quiet stance trials (97.1%) were stationary. On the other hand, CoP_y signals' *Run Test* results demonstrated that 11 out of 28 subjects presented non-stationarity in at least one of their five successive trials and totally 14 CoP_y signals were non-stationary from the left-side among 140 trials. Thus, 126 of the CoP_y signals (90.0%) were stationary. None of the 280 signals of CoP_x and CoP_y were non-stationary from the right-side.

3.1.1.3 Results of Ensemble Average Analysis

The *ensemble average* analysis (Section 2.2.1.1.3) has been applied to the CoP signals that belong to the subjects who demonstrated stationary signal characteristics in each of the five successive experimental trials [76]; i.e., 24 out of 28 subjects have been evaluated for CoP_x signal (Subject 5,7,23,24 excluded) and 17 out of 28 subjects have been evaluated for CoP_y signal (Subject 1,8,9,13,15,17,18,19,20,21,23 excluded). The reason for excluding the subjects who demonstrated at least one non-stationary trial in their five successive trials is that when the mean value CoP estimate changes with respect to time in a trial, it doesn't make sense to search for trends with respect to time over the trials; subsequently, it becomes unnecessary to make an ergodicity analysis for these subjects. The results were presented in p -values (Table 3.3 (a) and (b)) obtained from 2-way ANOVA test performed on T matrix (Section 2.2.1.1.3, Equation (2.14)). The results for the CoP_x signal (Table 3.3 (a)) revealed that 13 subjects (Subjects 2, 3, 9, 11, 12, 13, 14, 15, 19, 20, 22, 26, and 27) have p

values less than 0.05 on columns. Thus, the CoP_x signals which belong to these Subjects were not ergodic. As a result, 11 out of 28 subjects (Subjects 1, 4, 6, 8, 10, 16, 17, 18, 21, 25, and 28) had stationary ergodic CoP_x signals.

Similarly, the CoP_y signals of Subjects 3, 4, 7, 11, and 27 have p values less than 0.05 on columns (Table 3.3). Thus, the CoP_y signals which belong to Subjects 3, 4, 7, 11, and 27 were not ergodic. Subsequently, CoP_y signals of 12 subjects (Subjects 2,5,6,10,12,14,16,22,24,25,26, and 28) were stationary and ergodic.

Table 3.2 Run Test Results in *total run*

Subject	Group	CoP _x					CoP _y				
		T 1	T 2	T 3	T 4	T 5	T 1	T 2	T 3	T 4	T 5
1	Group 1	7	11	10	6	10	11	4*	8	6	10
2		9	10	11	6	12	9	7	7	10	11
3		8	10	8	6	7	6	9	7	8	7
4		9	6	14	8	8	12	6	8	9	9
5		8	5*	10	9	7	7	7	9	9	8
6		9	8	9	11	12	7	7	10	8	7
7		8	10	8	10	5*	8	11	13	10	7
8	Group 2	10	9	6	6	8	5*	9	7	10	6
9		7	9	10	7	11	6	12	4*	8	8
10		11	6	6	8	10	8	8	12	9	6
11		9	7	8	12	10	10	6	9	6	7
12		9	7	8	11	10	12	8	7	7	9
13		8	11	7	7	7	6	13	4*	6	5*
14		11	8	7	9	7	8	6	7	9	6
15	Group 3	7	7	6	8	6	4*	7	5*	7	4*
16		14	7	10	11	7	6	8	10	6	9
17		14	8	7	8	9	10	9	7	5*	6
18		9	10	11	7	13	7	6	7	9	5*
19		9	13	11	12	7	7	12	6	8	5*
20		9	8	9	10	11	6	10	9	9	4*
21		9	12	12	9	7	9	6	8	7	5*
22	Group 4	9	7	11	8	10	6	9	6	8	7
23		10	9	10	8	5*	5*	11	6	7	9
24		9	5*	6	7	8	6	9	10	8	11
25		8	10	8	12	7	9	9	7	9	9
26		7	9	12	13	7	13	10	10	10	8
27		7	12	8	8	7	9	6	10	12	12
28		8	9	7	8	7	6	10	8	6	8

*indicates non-stationary trials

Table 3.3 (a) p -values obtained from the two-way ANOVA of T matrix for CoP_x

Subject	p_{columns}	p_{rows}
1	0.44	1.00
2	0.00	1.00
3	0.00	1.00
4	0.15	1.00
6	0.53	1.00
8	0.09	1.00
9	0.01	1.00
10	0.06	1.00
11	0.00	1.00
12	0.00	1.00
13	0.00	1.00
14	0.00	1.00
15	0.00	1.00
16	0.19	1.00
17	0.26	1.00
18	0.06	1.00
19	0.00	1.00
20	0.03	1.00
21	0.62	1.00
22	0.00	1.00
25	0.14	1.00
26	0.00	1.00
27	0.01	1.00
28	0.86	1.00

Table 3.3 (b) p -values obtained from the two-way ANOVA of T matrix for CoP_y

Subject	p_{columns}	p_{rows}
2	0.39	1.00
3	0.00	1.00
4	0.03	1.00
5	0.95	1.00
6	0.62	1.00
7	0.04	1.00
10	0.70	1.00
11	0.04	1.00
12	1.00	1.00
14	0.06	1.00
16	0.39	1.00
22	0.97	1.00
24	0.06	1.00
25	0.65	1.00
26	0.31	1.00
27	0.00	1.00
28	0.76	1.00

3.1.1.4 Sign Test of the Results of Run Test and Ergodicity Analysis

In this part of the analysis, a sign test based on the direction of the differences between two measures has been applied to the results obtained from the stationarity and ergodicity analysis. The trials of a subject were named as fully-stationary if all of the 5 successive trials are stationary (indicated with '+' in Table 3.3(c), Column 'Stationarity'). However, even if one of the five successive trials of a subject were to be found non-stationary, then the trials of that subject were called as not-fully-stationary (indicated with '-' in Table 3.3(c), Column 'Stationarity'). Furthermore, subjects who demonstrated ergodic trials were recorded with a '+' sign, while the subjects who had non-ergodic trials were recorded with a '-' sign in Table 3.3(c), Column 'Ergodicity'. The last column (Sign Test) of the Table 3.3(c) has been composed either for CoP_x or CoP_y signals in such a way that:

- 1) If the CoP_x (or CoP_y) signals of a subject were fully-stationary and ergodic, then a '+' sign has been used
- 2) If the CoP_x (or CoP_y) signals of a subject were fully-stationary but non-ergodic, then a '-' sign has been used
- 3) If the CoP_x (or CoP_y) signals of a subject were not-fully-stationary, then a '0' sign has been used

The results revealed that 11 out of 24 subjects' CoP_x signals have been marked with a '+' sign, which means that the one-tailed probability of the case "fully-stationary and ergodic" was 0.419 by reference to the binomial distribution (Appendix F). Similarly, the results showed that 12 out of 17 subjects' CoP_y signals were marked with a '+' sign, which means that the one-tailed probability of the case "fully-stationary and ergodic" has been 0.975 for CoP_y signal by reference to the binomial distribution (Appendix F).

On the other hand, Group 2 and 3 differed significantly ($p < 0.05$) from the other groups in terms of demonstrating fully-stationary CoP_x signal characteristics, since the one-tailed probability of the case “fully-stationary signal characteristics own by all of seven of the subjects in Group 2 or 3” was 0.008 by reference to the binomial distribution (Appendix F). Lastly, Group 3 differed considerably from other groups in terms of the not-fully-stationary characteristics of CoP_y signals, since the one-tailed probability of the case “fully-stationary signal characteristics of only one subject out of 7” was 0.062 by reference to the binomial distribution (Appendix F).

3.1.1.5 Robustness of Run Test Results

To check the robustness of the Run Test results, the same test was applied to the CoP_x and CoP_y signals, but with different window sizes. In the previous analysis the window size has been used as 500 data samples. The window size was changed from 500 to 550 data samples by 10 data sample increments for the robustness test of the Run Test results.

For the CoP_x signal, the results showed that 18 out of 28 subjects had 5 stationary trials for all of the five different window sizes (Table 3.3(d)). 16 out of these 18 subjects had also five successive stationary CoP_x trials by the Run Test, which has been made by using 500 data samples window size (Chapter 3 Section 3.1.1.2). Thus, 16 out of 24 subjects' trials were robust to changes in window size.

Group 3 behavior in CoP_x fully stationary signal characteristics was shown to be robust until the data window size has reached to 530 data samples, while the significant difference observed in Group 2 through sign test was not robust to data window size change. Similarly, the considerable difference observed in the behavior of Group 3 CoP_y signals as being not-fully stationary was shown not to be robust to the change in the data window size.

Similarly, for the CoP_y signal, the results indicated that 7 out of 28 subjects had 5 stationary trials for all of the five different window sizes (Table 3.3(e)). 6 out of these 7 subjects had also five successive stationary CoP_y trials by the Run Test has made with 500 data samples window size (Chapter 3 Section 3.1.1.2).

Table 3.3 (c) Sign Test Table

Subjects	Group	Stationarity		Ergodicity		Sign Test	
		CoP _x	CoP _y	CoP _x	CoP _y	CoP _x	CoP _y
1	Group 1	+	-	+	-	+	0
2		+	+	-	+	-	+
3		+	+	-	-	-	-
4		+	+	+	-	+	-
5		-	+	-	+	0	+
6		+	+	+	+	+	+
7		-	+	-	-	0	-
8	Group 2	+	-	+	-	+	0
9		+	-	-	-	-	0
10		+	+	+	+	+	+
11		+	+	-	-	-	-
12		+	+	-	+	-	+
13		+	-	-	-	-	0
14		+	+	-	+	-	+
15	Group 3	+	-	-	-	-	0
16		+	+	+	+	+	+
17		+	-	+	-	+	0
18		+	-	+	-	+	0
19		+	-	-	-	-	0
20		+	-	-	-	-	0
21		+	-	+	-	+	0
22	Group 4	+	+	-	+	-	+
23		-	-	-	-	0	0
24		-	+	-	+	0	+
25		+	+	+	+	+	+
26		+	+	-	+	-	+
27		+	+	-	-	-	-
28		+	+	+	+	+	+

Table 3.3 (d) Run Test Results for varying data window size (w.s.) for the CoP_x signal

Subject	Group	w.s.=510	w.s.=520	w.s.=530	w.s.=540	w.s.=550
1	Group 1	+	+	+	+	+
2		-	-	+	+	+
3		+	+	+	+	+
4		+	+	-	-	-
5		-	+	+	+	+
6		+	+	+	+	+
7		+	+	+	+	+
8	Group 2	+	+	+	+	+
9		+	+	+	+	+
10		-	-	+	-	-
11		+	+	+	+	+
12		+	+	+	+	+
13		-	-	+	-	+
14		+	+	+	+	+
15	Group 3	+	+	-	-	-
16		+	+	+	+	+
17		+	+	+	+	+
18		+	+	-	-	-
19		+	+	+	+	+
20		+	+	+	+	+
21		+	+	+	+	+
22	Group 4	+	+	+	+	+
23		+	+	+	+	+
24		+	-	+	+	+
25		+	+	+	+	-
26		+	+	+	+	+
27		+	+	+	+	+
28		+	-	+	+	+

‘+’ indicates fully-stationary; ‘-’ indicates not-fully-stationary

Table 3.3 (e) Run Test Results for varying data window size (w.s.) for the CoP_y signal

Subject	Group	w.s.=510	w.s.=520	w.s.=530	w.s.=540	w.s.=550
1	Group 1	+	-	-	-	-
2		+	+	+	+	+
3		-	-	+	-	-
4		+	+	+	-	+
5		+	+	-	+	-
6		+	+	+	+	+
7		+	+	+	-	+
8	Group 2	+	+	+	+	+
9		-	-	-	-	-
10		+	+	+	+	+
11		+	+	+	-	-
12		+	+	-	-	+
13		-	-	-	-	-
14		-	+	-	-	+
15	Group 3	-	-	-	-	-
16		+	+	-	+	-
17		-	-	+	-	-
18		+	+	+	-	-
19		-	-	-	-	-
20		-	-	-	-	+
21		+	+	-	-	-
22	Group 4	+	+	+	-	-
23		+	+	+	-	+
24		+	+	+	+	+
25		+	+	+	+	+
26		+	+	+	+	+
27		+	-	+	-	+
28		-	+	+	+	+

‘+’ indicates fully-stationary; ‘-’ indicates not-fully-stationary

3.1.2 Results of Frequency Domain Analysis

3.1.2.1 Fast Fourier Transformation and Power Spectral Density estimates

Fast Fourier Transformation (FFT) and *Power Spectral Density estimates* (PSD) analysis (Section 2.2.1.2) of 140 CoP_x and 140 CoP_y signals were performed to explore the frequency content and the distribution of the power of the signals in frequency spectrum respectively. Figure 3.1 is a typical example of FFT and PSD of CoP_x signals, which belongs to the five successive trials of the 11th subject (Female, 28). Similarly, Figure 3.2 illustrates a typical FFT and PSD pattern for CoP_y signals (the same subject). In addition, Table 3.4 ((a) and (b)) and Table 3.5 ((a) and (b)) show the ratios of the power between 0-0.1 Hz (R1) and 0-1 Hz (R2) band to the power in the entire frequency spectrum (0-25 Hz) for the CoP_x and CoP_y signals respectively. (see Equations (2.16) and (2.17)).

The power ratios' results of the CoP_x signal show that the signal demonstrates dynamics in different frequencies but the dynamics involved in the CoP_x signal has mostly settled at 0-1 Hz frequency band. The amplitude of the dynamics was larger at lower frequencies for all trials and for all subjects. The ratios of the power of the signal at 0-0.1 Hz and 0-1 Hz frequency band to the whole frequency spectrum for all trials of all subjects had a grand mean of 0.48 ± 0.08 and 0.98 ± 0.02 respectively (these values were computed from the "Mean" column of the Table 3.4(a) and Table 3.4(b) respectively). Fifth trial of the Subject 27 was the minimum value of ratios of the power of the signal at 0-0.1 Hz, as being 14%. Also, 89% was the minimum value of ratios of the power of the signal at 0-1 Hz (Subject 2, trial 2, Table 3.4(b)).

The power ratios' results of the CoP_y signals demonstrated that the CoP_y signal also contained dynamics in different frequencies. Similar to the CoP_x signal, the dynamics of the CoP_y signals existed mostly at 0-1 Hz frequency band. The lower frequencies contained the higher amplitudes of motion in CoP_y dynamics. The ratios of the power

of the signal at 0-0.1 Hz and 0-1 Hz frequency band to the whole frequency spectrum for all trials of all subjects had a grand mean of 0.47 ± 0.09 and 0.98 ± 0.02 respectively (these values were computed from the “Mean” column of the Table 3.5(a) and Table 3.5(b) respectively). Like the CoP_x signal, fifth trial of the Subject 27 has shown the minimum value of ratios of the power of the signal at 0-0.1 Hz, as being 9%. Further, 81% was the minimum value of ratios of the power of the signal at 0-1 Hz (Subject 8, trial 4, Table 3.5(b)).

A 2-way analysis of variance (ANOVA) test on PSD R1 ratios of CoP_x signals (Table 3.4 (a)) were significantly different on subjects ($p < 0.000$) but not significantly different on trials ($p < 0.800$). Further, 1-way ANOVA test where groups were the main effect and the trials were the repeated measures, on PSD R1 ratios of CoP_x signals demonstrated that the groups were not significantly different ($p < 0.098$).

Similarly, a 2-way analysis of variance (ANOVA) test on PSD R2 ratios of CoP_x signals (Table 3.4 (b)) were significantly different on subjects ($p < 0.000$) but not significantly different on trials ($p < 0.617$). Additionally, 1-way ANOVA test where groups were the main effect and the trials were the repeated measures, on PSD R2 ratios of CoP_x signals indicated that the groups were not significantly different ($p < 0.158$).

In the same way, a 2-way analysis of variance (ANOVA) test on PSD R1 ratios of CoP_y signals (Table 3.5 (a)) were significantly different on subjects ($p < 0.000$) but not significantly different on trials ($p < 0.825$). Moreover, 1-way ANOVA test where groups were the main effect and the trials were the repeated measures, on PSD R1 ratios of CoP_y signals showed that the groups were not significantly different ($p < 0.604$).

Lastly, a 2-way analysis of variance (ANOVA) test on PSD R2 ratios of CoP_y signals (Table 3.5 (b)) were significantly different on subjects ($p < 0.000$) but not significantly different on trials ($p < 0.609$). Furthermore, 1-way ANOVA test where groups were the main effect and the trials were the repeated measures, on PSD R2 ratios of CoP_y signals demonstrated that the groups were significantly different ($p < 0.044$). Group 1 and Group 3 were significantly different from each other for the measure PSD R2 ratios.

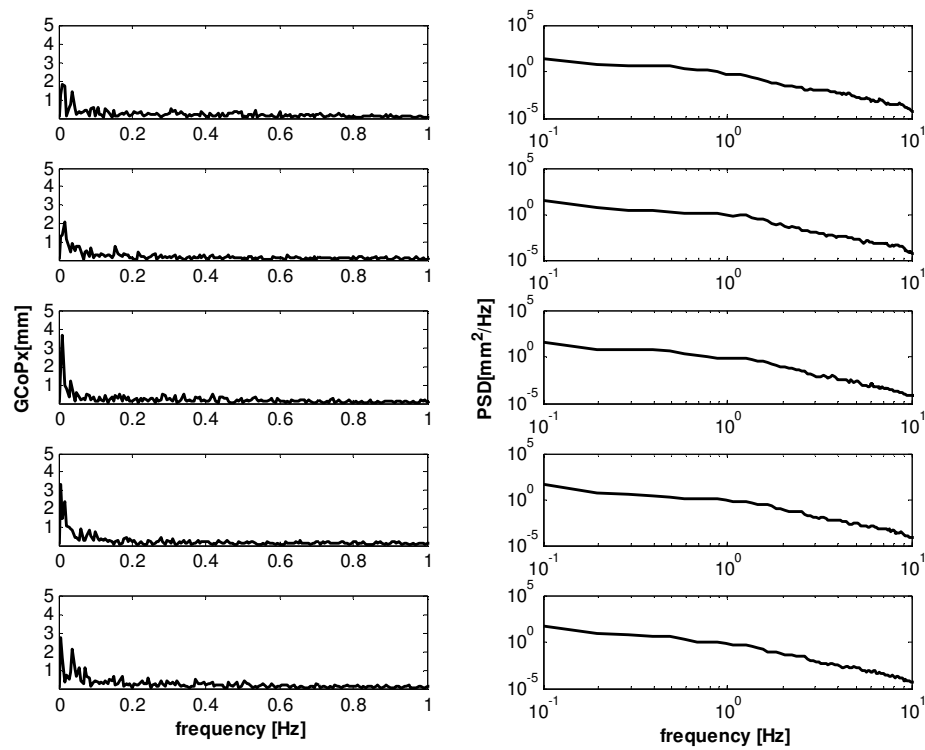


Figure 3.1 FFTs (left panel) and corresponding PSDs (right panel) of the five successive trials of the CoP_x signal [9th subject, F, 25]. PSDs are in log-log scale.

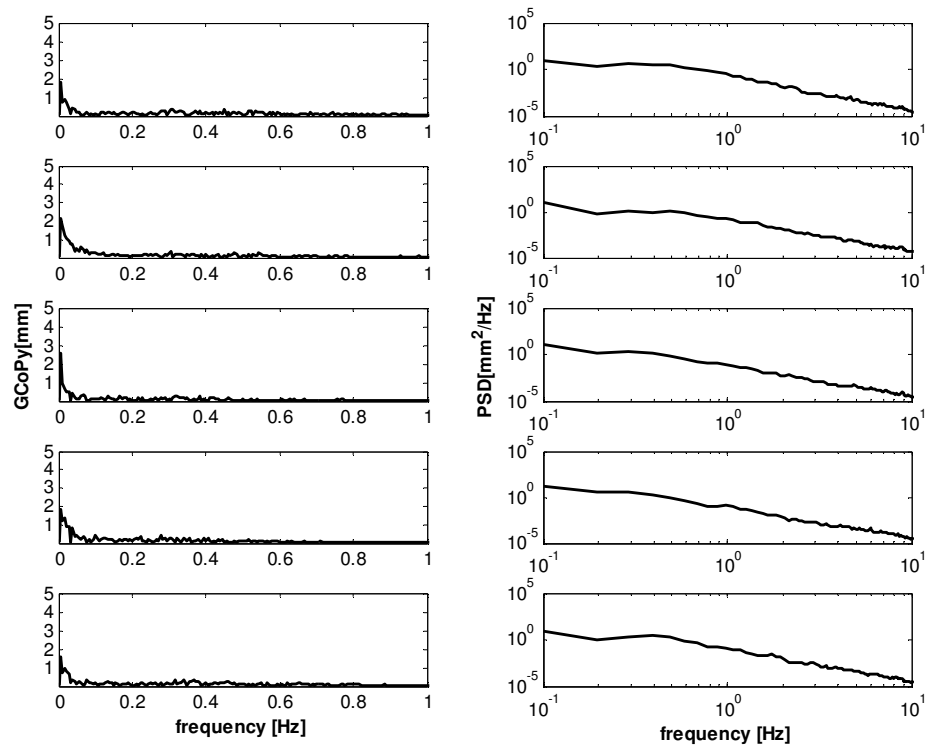


Figure 3.2 FFTs (left panel) and corresponding PSDs (right panel) of the five successive trials of the CoPy signal [9th subject, F, 25]. PSDs are in log-log scale.

Table 3.4 (a) The ratios of the power of the signal at 0-0.1 Hz (R1) frequency band to the power in the whole frequency spectrum for the CoP_x

Subject	Group	T 1	T 2	T 3	T 4	T 5	Mean	StDev
1	Group 1	0.50	0.39	0.37	0.34	0.25	0.37	0.09
2		0.33	0.31	0.31	0.38	0.36	0.34	0.03
3		0.53	0.42	0.31	0.41	0.51	0.44	0.09
4		0.51	0.57	0.52	0.52	0.52	0.53	0.02
5		0.51	0.35	0.41	0.47	0.46	0.44	0.06
6		0.52	0.61	0.46	0.54	0.47	0.52	0.06
7		0.53	0.55	0.42	0.42	0.51	0.49	0.06
8	Group 2	0.20	0.50	0.60	0.68	0.56	0.51	0.19
9		0.44	0.47	0.53	0.58	0.51	0.51	0.05
10		0.57	0.62	0.66	0.60	0.60	0.61	0.03
11		0.58	0.68	0.61	0.60	0.65	0.62	0.04
12		0.58	0.56	0.41	0.34	0.53	0.48	0.10
13		0.59	0.47	0.67	0.53	0.45	0.54	0.09
14		0.55	0.51	0.56	0.43	0.62	0.53	0.07
15	Group 3	0.33	0.32	0.50	0.49	0.27	0.38	0.11
16		0.46	0.49	0.40	0.29	0.48	0.43	0.08
17		0.32	0.47	0.49	0.46	0.40	0.43	0.07
18		0.64	0.56	0.44	0.58	0.49	0.54	0.08
19		0.49	0.54	0.64	0.50	0.58	0.55	0.06
20		0.51	0.56	0.58	0.64	0.59	0.58	0.05
21		0.23	0.26	0.37	0.38	0.32	0.31	0.07
22	Group 4	0.36	0.44	0.48	0.59	0.55	0.48	0.09
23		0.45	0.56	0.47	0.45	0.48	0.48	0.05
24		0.51	0.61	0.57	0.62	0.58	0.58	0.04
25		0.46	0.65	0.53	0.54	0.33	0.50	0.12
26		0.47	0.49	0.35	0.53	0.48	0.46	0.07
27		0.55	0.31	0.33	0.36	0.14	0.34	0.15
28		0.45	0.45	0.46	0.49	0.51	0.47	0.03

Table 3.4 (b) The ratios of the power of the signal at 0-1 Hz (R2) frequency band to the power in the whole frequency spectrum for the CoP_x

Subject	Group	T 1	T 2	T 3	T 4	T 5	Mean	StDev
1	Group 1	0.98	0.97	0.97	0.97	0.95	0.97	0.01
2		0.95	0.89	0.95	0.95	0.95	0.94	0.03
3		0.98	0.96	0.94	0.96	0.97	0.96	0.01
4		0.99	0.98	0.98	0.98	0.97	0.98	0.01
5		0.95	0.95	0.94	0.96	0.94	0.95	0.01
6		0.98	0.98	0.96	0.98	0.97	0.98	0.01
7		0.99	0.98	0.98	0.98	0.98	0.98	0.01
8	Group 2	0.97	0.98	0.99	0.99	0.99	0.98	0.01
9		0.97	0.95	0.96	0.97	0.98	0.96	0.01
10		0.99	1.00	1.00	1.00	1.00	1.00	0.00
11		0.99	1.00	0.99	0.99	1.00	0.99	0.00
12		0.99	0.99	0.98	0.98	0.99	0.99	0.00
13		0.99	0.98	0.99	0.98	0.96	0.98	0.01
14		0.99	0.98	0.98	0.96	0.99	0.98	0.01
15	Group 3	0.99	0.99	0.99	0.99	0.99	0.99	0.00
16		0.99	0.99	0.98	0.97	0.98	0.98	0.01
17		0.97	0.98	0.99	0.98	0.97	0.98	0.01
18		0.99	0.99	0.99	0.99	0.99	0.99	0.00
19		0.99	0.99	1.00	0.99	0.99	0.99	0.00
20		0.99	0.99	0.99	0.99	0.99	0.99	0.00
21		0.92	0.94	0.95	0.95	0.92	0.93	0.01
22	Group 4	0.97	0.97	0.98	0.98	0.98	0.98	0.01
23		0.97	0.97	0.97	0.97	0.96	0.97	0.01
24		0.99	1.00	0.99	1.00	0.99	0.99	0.00
25		0.94	0.97	0.95	0.95	0.90	0.94	0.03
26		0.98	0.99	0.98	0.99	0.99	0.99	0.00
27		0.99	0.98	0.97	0.98	0.98	0.98	0.01
28		0.96	0.95	0.96	0.97	0.97	0.96	0.01

Table 3.5 (a) The ratios of the power of the signal at 0-0.1 Hz (R1) frequency band to the power in the whole frequency spectrum for the CoP_y signals

Subject	Group	T 1	T 2	T 3	T 4	T 5	Mean	StDev
1	Group 1	0.39	0.26	0.27	0.26	0.19	0.27	0.07
2		0.35	0.37	0.33	0.31	0.33	0.34	0.02
3		0.42	0.33	0.46	0.53	0.59	0.46	0.10
4		0.55	0.63	0.50	0.56	0.51	0.55	0.05
5		0.46	0.52	0.48	0.38	0.39	0.45	0.06
6		0.56	0.34	0.54	0.52	0.48	0.49	0.09
7		0.61	0.54	0.42	0.43	0.49	0.50	0.08
8	Group 2	0.56	0.48	0.40	0.25	0.33	0.40	0.12
9		0.41	0.62	0.62	0.54	0.48	0.53	0.09
10		0.57	0.33	0.48	0.48	0.52	0.48	0.09
11		0.38	0.59	0.63	0.54	0.55	0.54	0.10
12		0.37	0.35	0.52	0.40	0.46	0.42	0.07
13		0.43	0.29	0.47	0.42	0.60	0.44	0.11
14		0.43	0.43	0.56	0.39	0.62	0.48	0.10
15	Group 3	0.54	0.67	0.65	0.64	0.46	0.59	0.09
16		0.55	0.40	0.43	0.62	0.53	0.51	0.09
17		0.41	0.37	0.38	0.59	0.41	0.43	0.09
18		0.61	0.45	0.49	0.60	0.61	0.55	0.08
19		0.27	0.39	0.55	0.27	0.45	0.39	0.12
20		0.64	0.51	0.50	0.60	0.55	0.56	0.06
21		0.52	0.45	0.47	0.48	0.64	0.51	0.08
22	Group 4	0.66	0.47	0.61	0.58	0.66	0.59	0.08
23		0.48	0.59	0.65	0.54	0.45	0.54	0.08
24		0.50	0.59	0.54	0.46	0.57	0.53	0.05
25		0.35	0.55	0.29	0.41	0.32	0.39	0.11
26		0.38	0.46	0.48	0.47	0.40	0.44	0.04
27		0.30	0.23	0.15	0.11	0.09	0.17	0.09
28		0.50	0.45	0.49	0.61	0.56	0.52	0.06

Table 3.5 (b) The ratios of the power of the signal at 0-1 Hz (R2) frequency band to the power in the whole frequency spectrum for the CoP_y signals

Subject	Group	T 1	T 2	T 3	T 4	T 5	Mean	StDev
1	Group 1	0.97	0.97	0.96	0.97	0.97	0.97	0.00
2		0.96	0.97	0.97	0.91	0.93	0.95	0.03
3		0.99	0.98	0.98	0.98	0.99	0.98	0.01
4		0.98	0.98	0.95	0.98	0.97	0.97	0.01
5		0.95	0.95	0.95	0.92	0.93	0.94	0.01
6		0.97	0.95	0.98	0.98	0.97	0.97	0.01
7		0.99	0.99	0.97	0.98	0.99	0.98	0.01
8	Group 2	0.97	0.97	0.97	0.81	0.95	0.93	0.07
9		0.98	0.98	0.99	0.99	0.99	0.99	0.01
10		0.99	0.98	0.98	0.99	0.99	0.99	0.00
11		0.94	0.99	0.99	0.98	0.99	0.98	0.02
12		0.98	0.93	0.98	0.98	0.96	0.97	0.02
13		0.98	0.97	0.98	0.98	0.99	0.98	0.01
14		0.98	0.99	1.00	0.99	1.00	0.99	0.00
15	Group 3	0.99	1.00	0.99	0.99	0.99	0.99	0.00
16		0.99	0.99	0.98	1.00	0.99	0.99	0.00
17		0.99	0.99	0.98	0.99	0.99	0.98	0.01
18		1.00	0.99	1.00	1.00	1.00	1.00	0.00
19		0.99	1.00	0.99	0.99	0.99	0.99	0.00
20		1.00	0.99	0.99	0.99	0.99	0.99	0.00
21		0.99	0.99	0.98	0.97	0.99	0.98	0.01
22	Group 4	0.99	0.98	0.99	0.99	1.00	0.99	0.01
23		0.99	0.99	1.00	0.99	0.99	0.99	0.00
24		1.00	1.00	1.00	1.00	1.00	1.00	0.00
25		0.96	0.98	0.93	0.95	0.93	0.95	0.02
26		0.98	0.99	0.99	0.99	0.99	0.99	0.01
27		0.99	0.99	0.99	0.99	0.99	0.99	0.00
28		0.96	0.96	0.97	0.99	0.97	0.97	0.01

3.2 Results of the Nonlinear Analysis

3.2.1 Results of the Time Delays (τ)

Time delays (τ) were computed to embed the CoP_x dynamics into m -dimensional state space (Chapter 2 Section 2.2.2.2). Time delays were calculated for 136 CoP_x signals which belong to 28 subjects' five successive trials at 12 different embedding dimensions; i.e., $m=2,3,4,5,6,8,9,10,12,15,18,20$. 4 trials: 2nd trial of Subject 5, 5th trial of Subject 7, 5th trial of Subject 23, and 2nd trial of Subject 24 was excluded as they were non-stationary trials. For embedding dimension, $m=2,3,4,5,6,8,9,10,12,15,18,20$ was selected as they are the exact dividers of 9000 (number of data samples).

The results of the time delays were given in Tables 3.6, 3.7, 3.8, 3.9, and 3.10 for the 1st, 2nd, 3rd, 4th, and 5th trials of the subjects respectively.

The minimum time delay (τ) value (Tables 3.6, 3.7, 3.8, 3.9, and 3.10) was 3 data samples, which belongs to the first trial of Subject 21 at $m=20$; the first, third, and fifth trial of Subject 25 at $m=18$; the first, third, fourth and fifth trial of Subject 25 at $m=20$, while the maximum time delay value (Tables 3.7) was 44 data samples that belongs to the second trial of Subject 15 at $m=2$. The grand mean of time delay values was 9.7 data samples (0.194 seconds) with a standard deviation of 6.5 data samples (0.130 seconds).

Moreover, for each time delay value, a reconstruction window value (τ_w) has been evaluated according to Equation (2.6) in Chapter 2, Section 2.2.2. The results are presented in Tables 3.11, 3.12, 3.13, 3.14, and 3.15 for the 1st, 2nd, 3rd, 4th, and 5th trials of the subjects respectively.

Figures 1 – 8 show the τ (Figures 3.3,3.5,3.7,3.9) and τ_w (Figures 3.4,3.6,3.8,3.10) values for 5 trials (trial-1:green, trial-2:blue, trial-3:cyan, trial-4:magenta, trial-5:red in color for line and markers in Figures 3.3-3.10) of 4 subjects from different groups with error bars (error bars are drawn for τ only). The strategy to define the error bars for the time delays:

- The mean (μ_τ) and standard deviation (σ_τ) value of five different time delay (τ) values for 5 successive trials at each embedding dimension was calculated.
- The mean values (μ_τ) were indicated with the black triangular marker in the Figures 3.3,3.5,3.7,3.9
- The error bars (also in black color) had a total length of two standard deviation (σ_τ) and each error bar was symmetric with respect to the black triangular marker in the Figures 3.3,3.5,3.7,3.9 at each m .
- An error bar was drawn for each m in Figures 3.3,3.5,3.7,3.9.

Table 3.6 Time delays (τ) of the first trials of 28 subjects for varying m

Subject	Group	$m=2$	$m=3$	$m=4$	$m=5$	$m=6$	$m=8$	$m=9$	$m=10$	$m=12$	$m=15$	$m=18$	$m=20$
1	Group 1	29	19	14	12	10	9	8	8	7	6	6	5
2		19	13	10	8	7	6	6	5	5	4	4	4
3		20	15	12	10	9	7	6	6	6	5	5	4
4		29	22	17	14	12	10	9	9	8	7	6	6
5		17	11	8	7	6	5	5	4	4	4	4	4
6		21	14	11	9	8	7	6	6	6	6	6	6
7		27	19	14	12	10	8	8	7	7	6	6	6
8	Group 2	24	16	13	10	9	7	7	6	6	5	4	4
9		20	14	11	9	8	6	6	5	5	4	4	4
10		36	24	18	14	12	10	9	8	7	6	6	6
11		26	19	14	12	10	8	8	7	7	6	6	6
12		28	21	17	14	12	10	9	8	7	6	6	6
13		26	20	16	13	11	9	8	8	7	6	6	5
14		22	16	13	11	9	8	7	7	6	6	5	5
15	Group 3	40	27	20	16	14	11	10	9	8	7	6	6
16		38	24	18	15	13	10	9	8	7	6	6	5
17		27	18	14	12	10	9	8	7	7	6	5	5
18		26	16	13	10	9	7	7	6	6	5	5	5
19		31	22	17	15	13	10	10	9	8	7	6	6
20		35	27	21	18	15	13	12	12	11	10	9	9
21		20	13	10	8	7	5	5	5	4	4	4	3
22	Group 4	23	15	11	9	8	7	6	6	5	5	5	5
23		17	12	10	9	8	7	7	6	6	6	5	5
24		40	33	25	20	17	13	12	11	10	8	8	7
25		16	11	9	7	6	5	5	4	4	4	3	3
26		26	17	13	10	9	7	6	6	5	5	4	4
27		28	19	15	12	10	8	8	7	6	6	5	5
28		12	8	8	7	7	6	6	5	5	6	6	6

Table 3.7 Time delays (τ) of the second trials of 28 subjects for varying m

Subject	Group	$M=2$	$m=3$	$m=4$	$m=5$	$m=6$	$m=8$	$m=9$	$m=10$	$m=12$	$m=15$	$m=18$	$m=20$	
1	Group 1	20	14	11	9	8	7	7	7	6	6	6	6	
2		15	10	8	7	6	5	5	5	4	4	4	4	
3		21	14	11	9	8	6	6	6	5	5	5	5	
4		19	15	12	10	9	7	7	7	6	6	5	5	
5														
6		18	12	10	8	7	6	6	5	5	5	5	5	5
7		22	15	12	10	8	7	7	6	6	6	5	5	5
8	Group 2	23	17	13	11	9	7	7	6	6	5	5	5	
9		17	11	8	7	6	5	5	4	4	4	4	4	
10		36	25	19	15	13	11	10	9	8	7	7	6	
11		29	19	14	12	10	8	7	7	6	5	5	5	
12		21	17	15	13	11	9	8	8	7	6	6	5	
13		26	17	13	11	9	7	7	6	6	5	5	4	
14		18	14	12	10	9	8	7	7	6	6	6	6	
15	Group 3	44	28	21	16	14	11	9	9	7	6	6	5	
16		29	21	16	13	11	9	8	8	7	6	5	5	
17		24	16	13	11	9	7	7	7	6	6	5	5	
18		28	18	14	12	10	8	7	7	6	6	6	5	
19		27	19	14	12	10	8	7	7	6	6	6	6	
20		26	18	14	12	10	9	8	8	7	7	7	8	
21		19	13	10	8	7	6	5	5	5	5	4	5	
22	Group 4	19	13	10	8	7	6	6	5	5	5	5	5	
23		17	11	9	8	7	6	6	5	5	5	4	4	
24														
25		15	10	8	7	6	5	5	4	4	4	4	4	
26		31	20	15	12	10	8	7	7	6	5	5	5	
27		30	19	14	11	10	8	7	6	6	5	4	4	
28		9	8	7	6	6	6	6	6	6	6	6	6	6

Table 3.8 Time delays (τ) of the third trials of 28 subjects for varying m

Subject	Group	$m=2$	$m=3$	$m=4$	$m=5$	$m=6$	$m=8$	$m=9$	$m=10$	$m=12$	$m=15$	$m=18$	$m=20$
1	Group 1	20	14	12	10	9	8	7	7	7	6	5	5
2		20	13	10	8	7	6	6	5	5	5	5	5
3		20	13	10	8	7	5	5	5	4	4	4	5
4		17	13	10	9	8	7	6	6	5	5	5	5
5		18	12	9	7	6	5	5	5	4	4	4	4
6		19	12	10	8	7	6	6	5	5	5	4	4
7		23	16	12	10	9	7	7	6	6	5	5	5
8	Group 2	23	17	13	11	9	8	7	7	6	5	5	5
9		17	12	9	8	7	6	5	5	5	5	5	4
10		40	27	21	17	14	11	11	10	9	8	8	8
11		33	21	16	13	11	9	8	7	7	6	6	6
12		27	19	15	12	10	8	7	7	6	5	5	5
13		21	14	11	9	8	6	6	5	5	5	4	4
14		15	13	11	10	9	8	7	7	6	6	5	5
15	Group 3	36	25	19	16	13	10	10	9	8	7	6	6
16		27	19	15	12	11	9	8	8	7	6	6	5
17		30	20	16	13	11	9	8	8	7	6	6	5
18		34	22	17	14	12	9	8	8	7	6	6	5
19		39	27	21	17	15	12	11	10	9	8	8	8
20		26	17	12	10	9	7	6	6	5	5	4	4
21		17	12	9	7	6	5	5	5	5	5	5	5
22	Group 4	18	13	10	9	8	6	6	6	5	5	5	5
23		17	11	10	8	8	7	7	7	6	6	6	5
24		29	20	15	12	10	8	8	7	7	7	7	7
25		15	10	8	7	6	5	5	4	4	4	3	3
26		30	20	15	12	10	8	8	7	6	6	5	5
27		27	17	13	10	9	7	6	6	5	5	4	4
28		13	9	8	8	7	6	6	6	5	5	5	5

Table 3.9 Time delays (τ) of the fourth trials of 28 subjects for varying m

Subject	Group	$m=2$	$m=3$	$m=4$	$m=5$	$m=6$	$m=8$	$m=9$	$m=10$	$m=12$	$m=15$	$m=18$	$m=20$
1	Group 1	21	15	11	9	8	7	6	6	6	5	5	5
2		18	13	10	8	7	6	5	5	5	4	4	4
3		20	13	10	8	7	6	5	5	5	4	4	4
4		22	15	12	10	8	7	6	6	5	5	5	4
5		19	13	10	8	7	5	5	5	4	4	4	4
6		20	14	10	9	8	6	6	6	5	5	5	5
7		24	17	13	11	9	8	7	7	6	5	5	5
8	Group 2	19	13	10	9	8	6	6	6	5	5	5	5
9		17	11	9	7	6	5	5	5	4	4	4	4
10		42	29	22	18	15	12	11	11	10	8	8	7
11		30	21	15	12	10	8	7	7	6	6	5	5
12		29	21	16	14	12	9	8	8	7	6	5	5
13		22	15	11	9	8	7	6	6	5	5	5	5
14		20	14	11	9	8	6	6	6	5	5	4	4
15	Group 3	34	22	17	14	12	9	8	8	7	6	5	5
16		26	17	13	10	9	7	6	6	5	5	4	4
17		22	15	12	10	8	7	6	6	6	5	5	5
18		37	25	18	15	12	10	9	8	7	6	5	5
19		34	24	19	15	13	11	10	9	8	7	7	7
20		23	15	12	10	8	7	6	6	5	5	5	5
21		20	13	10	8	7	6	5	5	5	4	4	4
22	Group 4	17	12	10	8	7	6	6	5	5	5	5	4
23		17	13	10	9	8	7	7	7	6	6	5	5
24		32	23	17	14	12	10	9	8	8	7	6	6
25		16	11	8	7	6	5	5	4	4	4	4	3
26		35	22	17	14	12	9	9	8	7	6	6	5
27		31	19	14	11	9	7	7	6	5	5	4	4
28		10	9	8	7	7	7	7	6	6	6	6	5

Table 3.10 Time delays (τ) of the fifth trials of 28 subjects for varying m

Subject	Group	$m=2$	$m=3$	$m=4$	$m=5$	$m=6$	$m=8$	$m=9$	$m=10$	$m=12$	$m=15$	$m=18$	$m=20$
1	Group 1	20	14	11	9	8	6	6	6	5	5	4	4
2		18	12	10	8	7	6	6	5	5	5	4	4
3		22	14	10	8	7	6	5	5	4	4	4	4
4		19	13	10	9	8	6	6	6	5	5	5	5
5		17	11	9	7	6	5	5	4	4	4	4	4
6		18	13	10	8	7	6	5	5	5	5	5	5
7													
8	Group 2	21	15	11	9	8	7	6	6	5	5	5	5
9		21	15	11	9	8	6	6	6	5	5	5	5
10		43	31	24	19	16	13	12	11	10	9	8	8
11		41	26	20	17	14	11	10	9	8	8	7	7
12		24	18	14	12	10	8	7	7	6	5	5	5
13		20	13	10	8	7	6	5	5	5	4	4	4
14		21	15	11	9	8	7	6	6	6	5	5	5
15	Group 3	42	28	21	16	14	11	9	9	7	6	6	5
16		24	16	13	10	9	7	7	6	6	5	5	5
17		22	15	11	9	8	6	6	5	5	4	4	4
18		37	24	18	14	12	9	9	8	7	6	5	5
19		39	26	20	16	14	11	10	9	8	7	6	6
20		23	16	12	10	8	7	6	6	5	5	5	5
21		18	12	9	7	6	5	5	4	4	4	4	4
22	Group 4	19	13	10	9	8	6	6	6	5	5	5	4
23													
24		27	19	15	12	11	9	8	8	8	8	7	7
25		16	11	8	7	6	5	5	4	4	4	3	3
26		37	24	18	15	12	10	9	8	7	7	6	6
27		31	19	14	11	9	7	6	6	5	4	4	4
28		8	8	8	8	8	7	7	7	6	6	6	5

Table 3.11 Reconstruction window (τ_w) for the first trials of 28 subjects for varying m

Subject	Group	$m=2$	$m=3$	$m=4$	$m=5$	$m=6$	$m=8$	$m=9$	$m=10$	$m=12$	$m=15$	$m=18$	$m=20$
1	Group 1	29	38	42	48	50	63	64	72	77	84	102	95
2		19	26	30	32	35	42	48	45	55	56	68	76
3		20	30	36	40	45	49	48	54	66	70	85	76
4		29	44	51	56	60	70	72	81	88	98	102	114
5		17	22	24	28	30	35	40	36	44	56	68	76
6		21	28	33	36	40	49	48	54	66	84	102	114
7		27	38	42	48	50	56	64	63	77	84	102	114
8	Group 2	24	32	39	40	45	49	56	54	66	70	68	76
9		20	28	33	36	40	42	48	45	55	56	68	76
10		36	48	54	56	60	70	72	72	77	84	102	114
11		26	38	42	48	50	56	64	63	77	84	102	114
12		28	42	51	56	60	70	72	72	77	84	102	114
13		26	40	48	52	55	63	64	72	77	84	102	95
14		22	32	39	44	45	56	56	63	66	84	85	95
15	Group 3	40	54	60	64	70	77	80	81	88	98	102	114
16		38	48	54	60	65	70	72	72	77	84	102	95
17		27	36	42	48	50	63	64	63	77	84	85	95
18		26	32	39	40	45	49	56	54	66	70	85	95
19		31	44	51	60	65	70	80	81	88	98	102	114
20		35	54	63	72	75	91	96	108	121	140	153	171
21		20	26	30	32	35	35	40	45	44	56	68	57
22	Group 4	23	30	33	36	40	49	48	54	55	70	85	95
23		17	24	30	36	40	49	56	54	66	84	85	95
24		40	66	75	80	85	91	96	99	110	112	136	133
25		16	22	27	28	30	35	40	36	44	56	51	57
26		26	34	39	40	45	49	48	54	55	70	68	76
27		28	38	45	48	50	56	64	63	66	84	85	95
28		12	16	24	28	35	42	48	45	55	84	102	114

Table 3.12 Reconstruction window (τ_w) of the second trials of 28 subjects for varying m

Subject	Group	$m=2$	$m=3$	$m=4$	$m=5$	$m=6$	$m=8$	$m=9$	$m=10$	$m=12$	$m=15$	$m=18$	$m=20$
1	Group 1	20	28	33	36	40	49	56	63	66	84	102	114
2		15	20	24	28	30	35	40	45	44	56	68	76
3		21	28	33	36	40	42	48	54	55	70	85	95
4		19	30	36	40	45	49	56	63	66	84	85	95
5													
6		18	24	30	32	35	42	48	45	55	70	85	95
7		22	30	36	40	40	49	56	54	66	84	85	95
8	Group 2	23	34	39	44	45	49	56	54	66	70	85	95
9		17	22	24	28	30	35	40	36	44	56	68	76
10		36	50	57	60	65	77	80	81	88	98	119	114
11		29	38	42	48	50	56	56	63	66	70	85	95
12		21	34	45	52	55	63	64	72	77	84	102	95
13		26	34	39	44	45	49	56	54	66	70	85	76
14		18	28	36	40	45	56	56	63	66	84	102	114
15	Group 3	44	56	63	64	70	77	72	81	77	84	102	95
16		29	42	48	52	55	63	64	72	77	84	85	95
17		24	32	39	44	45	49	56	63	66	84	85	95
18		28	36	42	48	50	56	56	63	66	84	102	95
19		27	38	42	48	50	56	56	63	66	84	102	114
20		26	36	42	48	50	63	64	72	77	98	119	152
21		19	26	30	32	35	42	40	45	55	70	68	95
22	Group 4	19	26	30	32	35	42	48	45	55	70	85	95
23		17	22	27	32	35	42	48	45	55	70	68	76
24													
25		15	20	24	28	30	35	40	36	44	56	68	76
26		31	40	45	48	50	56	56	63	66	70	85	95
27		30	38	42	44	50	56	56	54	66	70	68	76
28		9	16	21	24	30	42	48	54	66	84	102	114

Table 3.13 Reconstruction window (τ_w) of the third trials of 28 subjects for varying m

Subject	Group	$m=2$	$m=3$	$m=4$	$m=5$	$m=6$	$m=8$	$m=9$	$m=10$	$m=12$	$m=15$	$m=18$	$m=20$
1	Group 1	20	28	36	40	45	56	56	63	77	84	85	95
2		20	26	30	32	35	42	48	45	55	70	85	95
3		20	26	30	32	35	35	40	45	44	56	68	95
4		17	26	30	36	40	49	48	54	55	70	85	95
5		18	24	27	28	30	35	40	45	44	56	68	76
6		19	24	30	32	35	42	48	45	55	70	68	76
7		23	32	36	40	45	49	56	54	66	70	85	95
8	Group 2	23	34	39	44	45	56	56	63	66	70	85	95
9		17	24	27	32	35	42	40	45	55	70	85	76
10		40	54	63	68	70	77	88	90	99	112	136	152
11		33	42	48	52	55	63	64	63	77	84	102	114
12		27	38	45	48	50	56	56	63	66	70	85	95
13		21	28	33	36	40	42	48	45	55	70	68	76
14		15	26	33	40	45	56	56	63	66	84	85	95
15	Group 3	36	50	57	64	65	70	80	81	88	98	102	114
16		27	38	45	48	55	63	64	72	77	84	102	95
17		30	40	48	52	55	63	64	72	77	84	102	95
18		34	44	51	56	60	63	64	72	77	84	102	95
19		39	54	63	68	75	84	88	90	99	112	136	152
20		26	34	36	40	45	49	48	54	55	70	68	76
21		17	24	27	28	30	35	40	45	55	70	85	95
22	Group 4	18	26	30	36	40	42	48	54	55	70	85	95
23		17	22	30	32	40	49	56	63	66	84	102	95
24		29	40	45	48	50	56	64	63	77	98	119	133
25		15	20	24	28	30	35	40	36	44	56	51	57
26		30	40	45	48	50	56	64	63	66	84	85	95
27		27	34	39	40	45	49	48	54	55	70	68	76
28		13	18	24	32	35	42	48	54	55	70	85	95

Table 3.14 Reconstruction window (τ_w) of the fourth trials of 28 subjects for varying m

Subject	Group	$m=2$	$m=3$	$m=4$	$m=5$	$m=6$	$m=8$	$m=9$	$m=10$	$m=12$	$m=15$	$m=18$	$m=20$
1	Group 1	21	30	33	36	40	49	48	54	66	70	85	95
2		18	26	30	32	35	42	40	45	55	56	68	76
3		20	26	30	32	35	42	40	45	55	56	68	76
4		22	30	36	40	40	49	48	54	55	70	85	76
5		19	26	30	32	35	35	40	45	44	56	68	76
6		20	28	30	36	40	42	48	54	55	70	85	95
7		24	34	39	44	45	56	56	63	66	70	85	95
8	Group 2	19	26	30	36	40	42	48	54	55	70	85	95
9		17	22	27	28	30	35	40	45	44	56	68	76
10		42	58	66	72	75	84	88	99	110	112	136	133
11		30	42	45	48	50	56	56	63	66	84	85	95
12		29	42	48	56	60	63	64	72	77	84	85	95
13		22	30	33	36	40	49	48	54	55	70	85	95
14		20	28	33	36	40	42	48	54	55	70	68	76
15	Group 3	34	44	51	56	60	63	64	72	77	84	85	95
16		26	34	39	40	45	49	48	54	55	70	68	76
17		22	30	36	40	40	49	48	54	66	70	85	95
18		37	50	54	60	60	70	72	72	77	84	85	95
19		34	48	57	60	65	77	80	81	88	98	119	133
20		23	30	36	40	40	49	48	54	55	70	85	95
21		20	26	30	32	35	42	40	45	55	56	68	76
22	Group 4	17	24	30	32	35	42	48	45	55	70	85	76
23		17	26	30	36	40	49	56	63	66	84	85	95
24		32	46	51	56	60	70	72	72	88	98	102	114
25		16	22	24	28	30	35	40	36	44	56	68	57
26		35	44	51	56	60	63	72	72	77	84	102	95
27		31	38	42	44	45	49	56	54	55	70	68	76
28		10	18	24	28	35	49	56	54	66	84	102	95

Table 3.15 Reconstruction window (τ_w) of the fifth trials of 28 subjects for varying m

Subject	Group	$m=2$	$m=3$	$m=4$	$m=5$	$m=6$	$m=8$	$m=9$	$m=10$	$m=12$	$m=15$	$m=18$	$m=20$
1	Group 1	20	28	33	36	40	42	48	54	55	70	68	76
2		18	24	30	32	35	42	48	45	55	70	68	76
3		22	28	30	32	35	42	40	45	44	56	68	76
4		19	26	30	36	40	42	48	54	55	70	85	95
5		17	22	27	28	30	35	40	36	44	56	68	76
6		18	26	30	32	35	42	40	45	55	70	85	95
7													
8	Group 2	21	30	33	36	40	49	48	54	55	70	85	95
9		21	30	33	36	40	42	48	54	55	70	85	95
10		43	62	72	76	80	91	96	99	110	126	136	152
11		41	52	60	68	70	77	80	81	88	112	119	133
12		24	36	42	48	50	56	56	63	66	70	85	95
13		20	26	30	32	35	42	40	45	55	56	68	76
14		21	30	33	36	40	49	48	54	66	70	85	95
15	Group 3	42	56	63	64	70	77	72	81	77	84	102	95
16		24	32	39	40	45	49	56	54	66	70	85	95
17		22	30	33	36	40	42	48	45	55	56	68	76
18		37	48	54	56	60	63	72	72	77	84	85	95
19		39	52	60	64	70	77	80	81	88	98	102	114
20		23	32	36	40	40	49	48	54	55	70	85	95
21		18	24	27	28	30	35	40	36	44	56	68	76
22	Group 4	19	26	30	36	40	42	48	54	55	70	85	76
23													
24		27	38	45	48	55	63	64	72	88	112	119	133
25		16	22	24	28	30	35	40	36	44	56	51	57
26		37	48	54	60	60	70	72	72	77	98	102	114
27		31	38	42	44	45	49	48	54	55	56	68	76
28		8	16	24	32	35	49	56	54	66	84	85	95

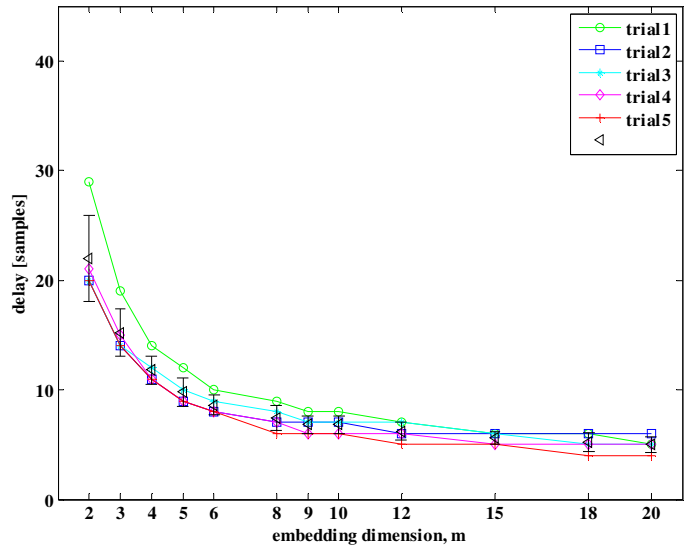


Figure 3.3 τ for varying dimensions, m [Group 1, 1st subject, F, 6 years old, 5 trials]

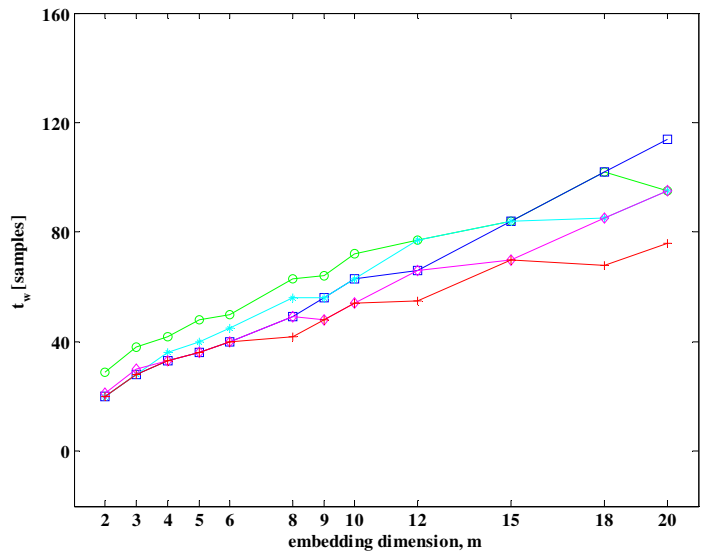


Figure 3.4 τ_w for varying dimensions, m [Group 1, 1st subject, F, 6 years old, 5 trials]

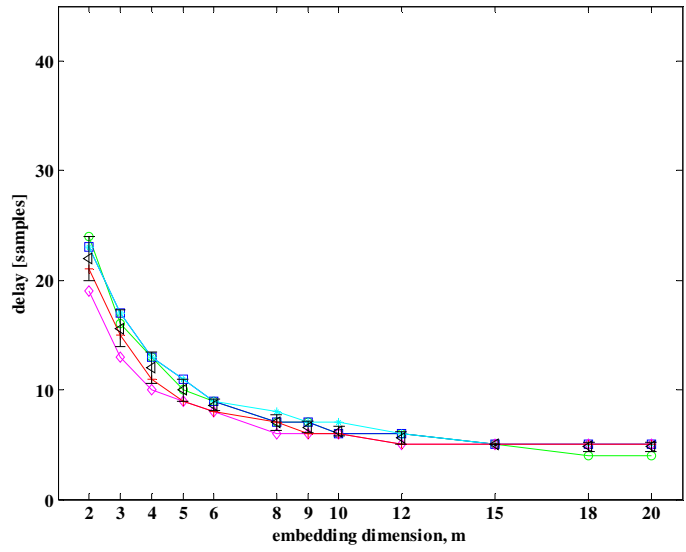


Figure 3.5 τ for varying dimensions, m [Group 2, 8th subject, M, 21 years old, 5 trials]

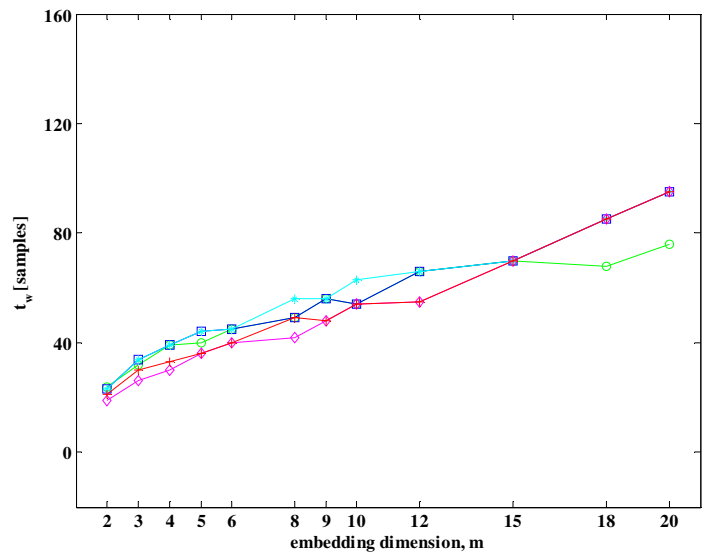


Figure 3.6. τ_w for varying dimensions, m [Group 2, 8th subject, M, 21 years old, 5 trials]

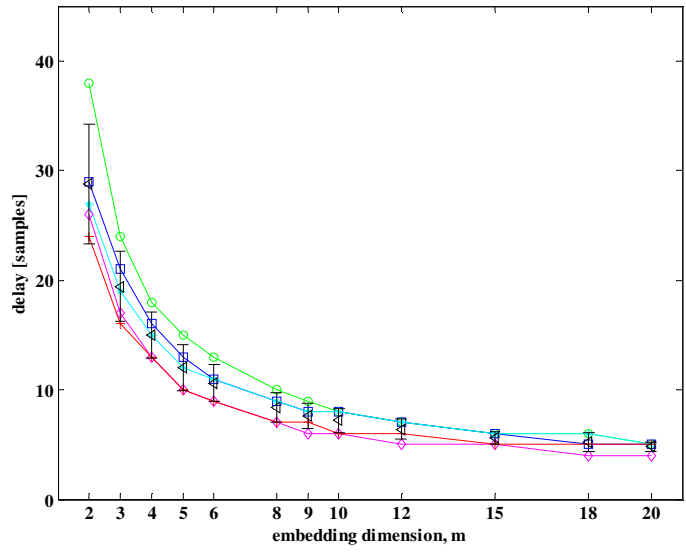


Figure 3.7. τ for varying dimensions, m [Group 3, 16th subject, M, 42 years old, 5 trials]

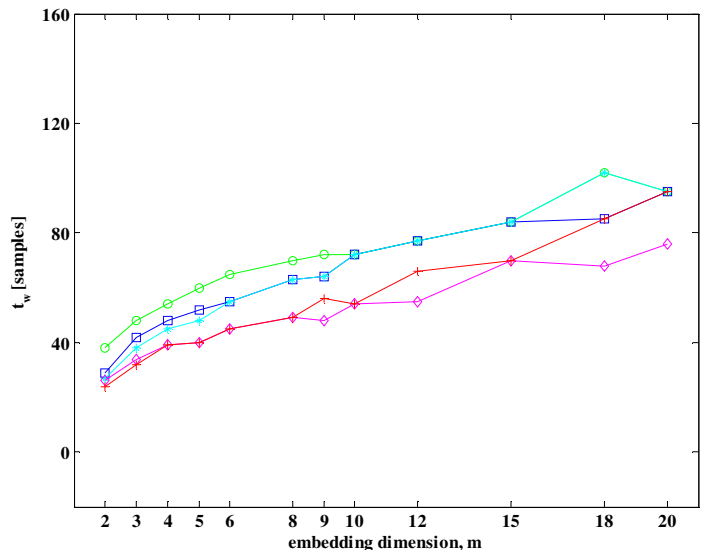


Figure 3.8. τ_w for varying dimensions, m [Group 3, 16th subject, M, 42 years old, 5 trials]

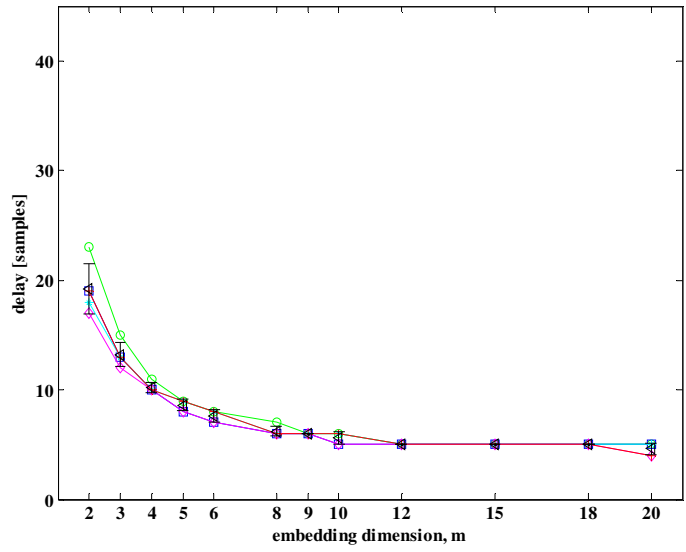


Figure 3.9. τ for varying dimensions, m [Group 4, 22th subject, F, 65 years old, 5 trials]

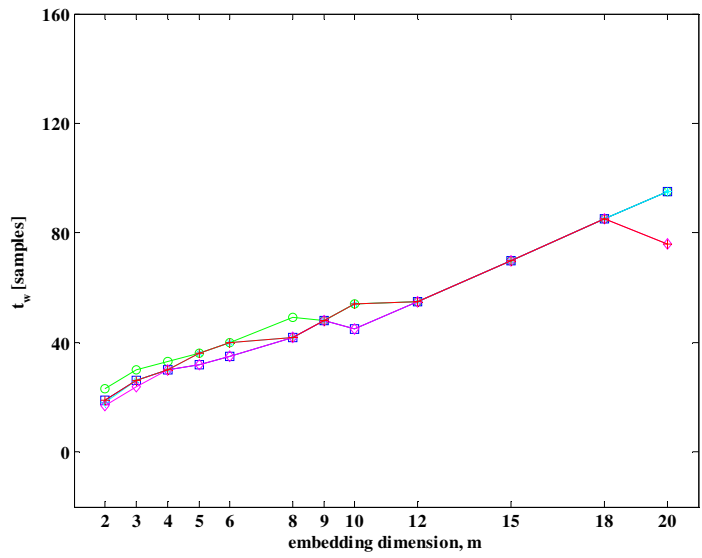


Figure 3.10 τ_w for varying dimensions, m [Group 4, 22th subject, F, 65 years old, 5 trials]

3.2.2 Correlation Dimension Estimates

Correlation dimension estimates (D_2) from 136 CoP_x signals have been computed according to the following steps. 4 trials: 2nd trial of Subject 5, 5th trial of Subject 7, 5th trial of Subject 23, and 2nd trial of Subject 24 were excluded as they were non-stationary trials.

1. The dynamics from the CoP_x signal has been reconstructed in the phase space by using the method of time delays (Chapter 2, Section 2.2.2.2).
2. Spatial correlations between the phase points on the possible attractor have been explored by the algorithm proposed by Grassberger and Procaccia [35]. In order to compute the correlation dimension (D_2) estimate from a time series, the correlation function, $C(r)$ is defined as the spatial correlations between the pairs of phase points (Equation (2.24) in Chapter 2, Section 2.2.6.3) in the m -dimensional embedded dynamics (Equation (3.3) in Chapter 2, Section 2.2.6.3). The correlation function, $C(r)$ is computed by constructing a sphere of radius r around each point X_i in the state space of the possible attractor and counting the number of points within the sphere [76].
3. The correlation dimension (D_2) was estimated from the slope of the linear portion of the curve obtained by plotting the natural logarithm of the correlation function, $C(r)$ against the natural logarithm of varying tolerance distances, r ; i.e., curve $\ln C(r)$ as a function of $\ln(r)$.
4. Besides, three criteria introduced by Rapp et al. [42] have been used in order to compute correlation dimension estimates (Chapter 2, Section 2.2.6.3). The three criteria were given below.
 - i) The scaling region of the curve $\ln C(r)$ versus $\ln(r)$ must be linear.
 - ii) Scaling region must be of significant length (a length of $\Delta \ln r = 1.6$ is the minimally acceptable scaling length).

iii) The estimate of dimension should be robust against variations in the embedding dimension, m .

The three steps in order to compute D_2 estimate from a CoP_x signal of one trial of a subject are as follows:

- The first step is plotting the curve $\ln C(r)$ versus $\ln r$ (Figure 3.11).
- The second step is detecting the linear scaling region with the significant length (Criteria i,ii) (Figure 3.12).
- The final step is to compute D_2 estimate from the slope of the linear scaling region (Figure 3.13).

The procedure described above in three steps has been repeated at 12 different embedding dimensions, $m=2,3,4,5,6,8,9,10,12,15,18,20$ for each trial of a subject. Lastly, the third criterion (Criteria iii) has been checked whether D_2 estimates converged to a value for the corresponding trial. If D_2 estimates were found to converge to a value against variations in the embedding dimensions, m ; and then this value was accepted as the correlation dimension of the corresponding CoP_x signal. (Figure 3.14). This procedure has been repeated for each stationary CoP_x signal of 28 subjects.

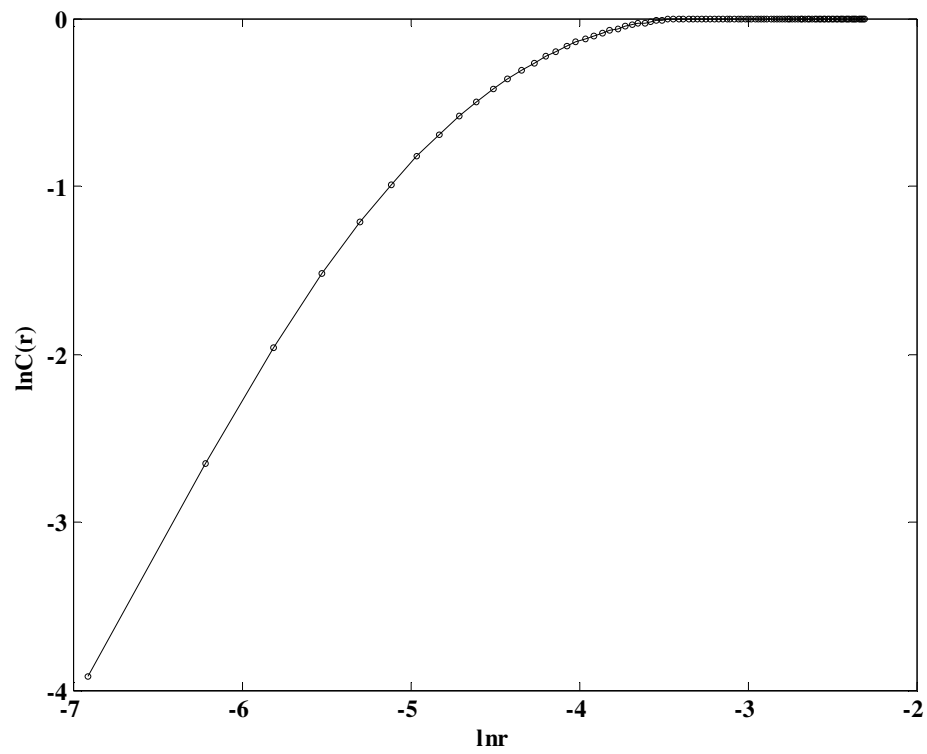


Figure 3.11. Step 1 - Curve $\ln C(r)$ versus $\ln r$ for the first trial of Subject 11 at $m=2$

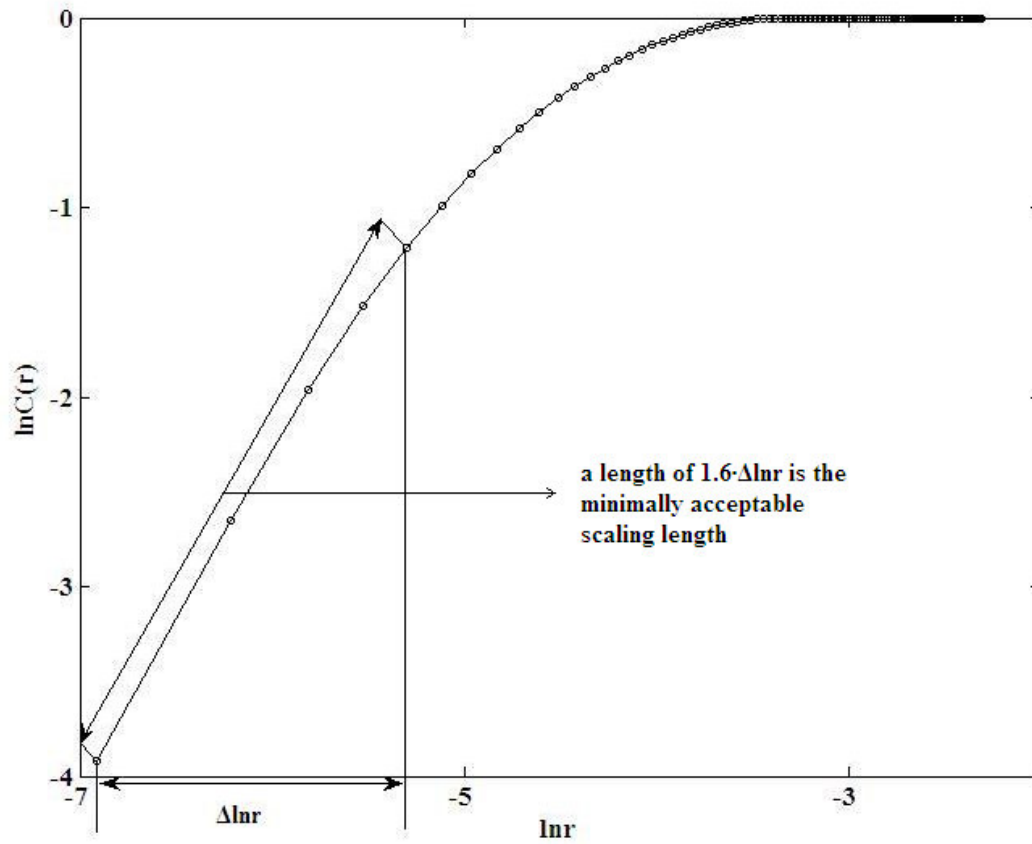


Figure 3.12. Step 2 - Curve $\ln C(r)$ versus $\ln r$ for the first trial of Subject 11 at $m=2$

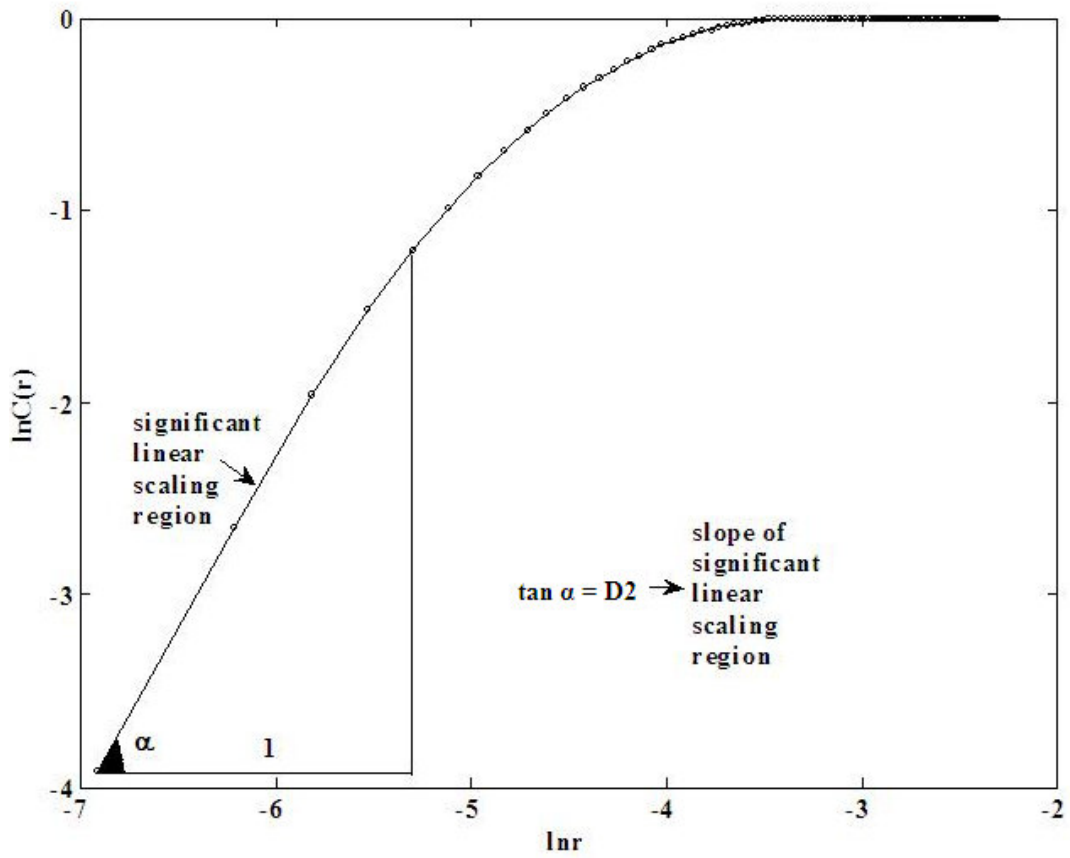


Figure 3.13. Step 3 - Curve $\ln C(r)$ versus $\ln r$ for the first trial of Subject 11 at $m=2$

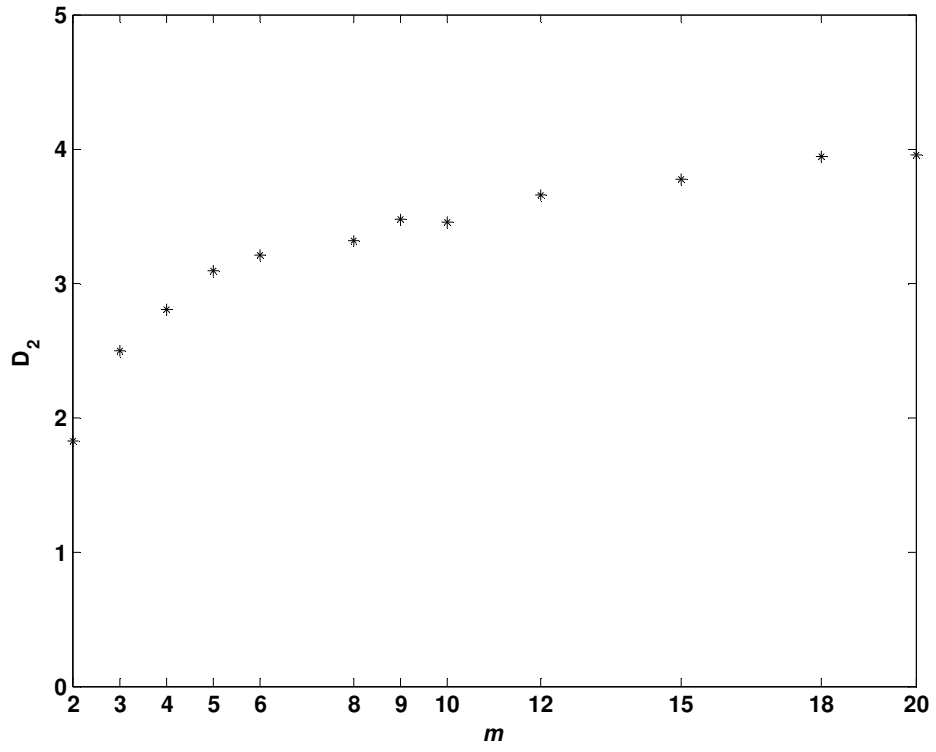


Figure 3.14. Step 4 - Computed D_2 estimates for varying dimensions, m [11th subject, F, 28, 1st trial]

In order to define a criterion for convergence of the D_2 estimate curves, the following algorithm has been developed:

Step 1. The D_2 estimate curves were fitted to the double exponential model (due to poor fit of one exponential model, Figure 3.15) defined in Equation (3.1) for each of 136 saturated trials (Figure 3.16). The constants (a, b, c, d) were calculated by using the built-in function, “fit” of the software Matlab[®].

$$D_2 = a \cdot e^{b \cdot m} + c \cdot e^{d \cdot m} \quad (3.1)$$

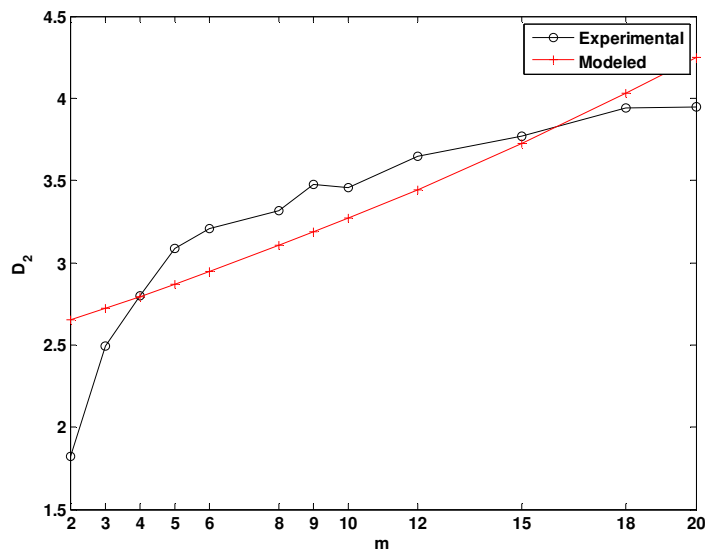


Figure 3.15. D_2 estimate curve (poor fit of one exponential model) of the Subject 11, trial 1

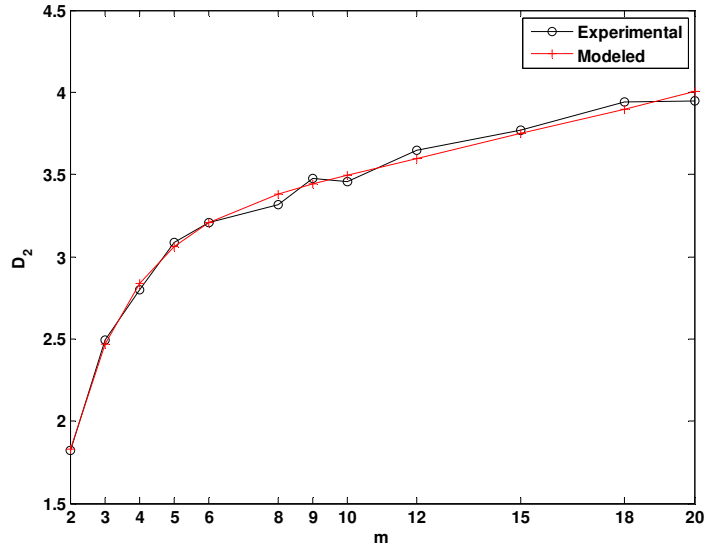


Figure 3.16. D_2 estimate curve (experimental and modeled by Equation (3.1)) of the Subject 11, trial 1

Step 2. The embedding dimension at which modeled D_2 estimate curves are to be accepted as *saturated* has to be decided. The modeled D_2 estimate curves are accepted as saturated when the criterion defined in Equation (3.2) is satisfied [114]. In Equation (3.2), m is embedding dimension and n is topological dimension.

$$m \geq 2n + 1 \quad (3.2)$$

In the place of n , D_2 estimates were used. The line m versus $(m-1)/2$ (derived from Equation (3.2) by solving for n) was drawn for each of 136 stationary trials. The intersection point of the line, $D_2(m)$; ie, m versus $(m-1)/2$ (red line in Figure 3.17) and the D_2 estimate curves (black line in Figure 3.17) has been found. Then, the saturation point in embedding dimension (blue plus marker in Figure 3.17) has been accepted as the first embedding dimension value which is in the right side of the intersection point. The saturation points found accordingly in embedding dimension, m of 136 converged trials were given in Table 3.16.

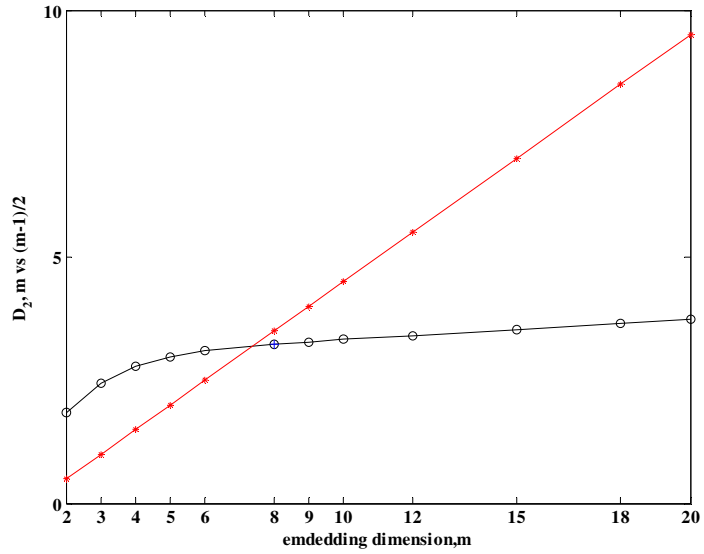


Figure 3.17. The line m versus $(m-1)/2$ and D_2 estimate curve of the Subject 11, trial 1. The marker “+” is the saturation point right to the intersection point of the line $D_2(m)$ with D_2 estimates curve.

Table 3.16. Saturation points in embedding dimension of 136 converged trials

Subjects	t1	t2	t3	t4	t5
1	8	9	9	9	8
2	8	8	8	8	9
3	8	9	8	8	8
4	8	9	8	8	9
5	9	n	9	8	8
6	8	8	9	9	9
7	8	9	9	8	n
8	9	9	8	8	9
9	9	8	8	8	8
10	8	8	8	8	8
11	8	8	8	8	8
12	8	8	9	9	9
13	8	8	8	8	8
14	9	9	9	9	8
15	9	8	8	9	8
16	8	8	9	9	9
17	9	8	8	9	9
18	8	8	8	8	8
19	9	8	8	8	8
20	9	8	8	8	8
21	9	9	9	9	9
22	9	9	9	9	9
23	10	9	10	10	n
24	8	n	8	8	8
25	9	9	9	9	8
26	8	8	9	8	8
27	9	9	9	9	9
28	12	12	12	12	12

'n' indicates non-stationary trials

Step 3. The values of modeled D_2 estimates starting from the saturation point (in embedded dimensions m , larger than $2D_2 + 1$) to $m=20$ have been fitted to a line (linear regression, Equation 3.3, Figure 3.18) to search for a linear trend. Similarly, the constants a and b were calculated by using the built-in function, “fit” of the software Matlab[®].

$$D_2 = a \cdot m + b \tag{3.3}$$

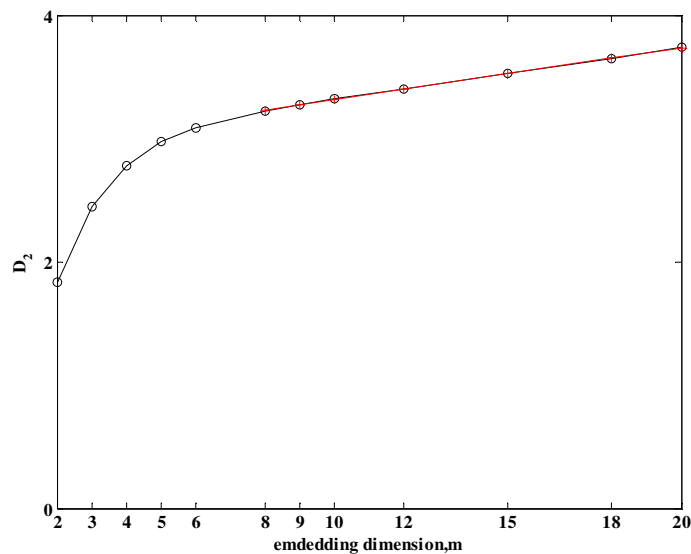


Figure 3.18. Modeled D_2 estimate curve of 1st trial of 1st subject (black line), fitted line (red line)

The convergence criterion is then defined as: D_2 estimate curves are accepted as “converged” if the slope of the fitted line (a in Equation (3.3)) to D_2 estimates starting from the saturation point on (in embedded dimensions m , larger than $2D_2 + 1$), is less than the slope of the double exponential model fit to D_2 estimates at the same saturation point. The convergence test has been applied to only the trials that possess stationary CoP_x signal characteristics. By this method, 112 out of 136 trials passed the convergence test (Table 3.17).

Table 3.17. Results of Convergence

Subjects	t1	t2	t3	t4	t5
1	c	c	c	c	c
2	c	c	nc	nc	c
3	c	nc	nc	c	c
4	c	c	c	c	c
5	nc	n	nc	nc	nc
6	c	c	c	c	nc
7	c	c	c	c	n
8	c	c	c	c	c
9	c	nc	nc	c	nc
10	c	c	c	nc	c
11	c	c	c	c	nc
12	c	c	c	c	c
13	c	c	nc	c	c
14	c	c	c	c	c
15	c	c	c	c	c
16	c	c	c	c	c
17	c	c	c	c	nc
18	c	c	c	c	c
19	c	nc	c	c	c
20	c	c	c	c	nc
21	c	c	nc	c	nc
22	nc	c	c	c	c
23	c	c	c	c	n
24	c	n	nc	c	c
25	c	nc	c	c	nc
26	c	c	c	c	c
27	c	c	c	c	c
28	c	c	c	c	c

‘n’ indicates non-stationary trials, ‘nc’ not-converged trials, ‘c’ converged trials

Finally, the D_2 value of a trial is defined as the mean value of the D_2 estimates starting from the saturation point (in embedded dimensions m , larger than $2D_2 + 1$) to $m=20$ (Table 3.18). The grand mean of D_2 values of 112 converged trials was 3.78 with a standard deviation of 0.45 (Table 3.18). The minimum D_2 value computed was 2.88 (Subject 18, t1, Female, 54), while the maximum D_2 value was 5.28 (Subject 28, t5, Female, 84) among D_2 values of 112 converged trials of stationary saturated CoP_x

signals (Table 3.18). D_2 values exhibited diversity within the population studied (Table 3.18). However, there existed similarities in the computed D_2 values also (Table 3.18). 83 D_2 values out of 112 were among 3-4 (3 and 4 included), while 23 of the D_2 values were between 4 and 5. Furthermore, 3 trials demonstrated D_2 values among 2-3 and among 5-6 (Table 3.18).

Table 3.18. D_2 values of the converged trials

Subject	Group	t1	t2	t3	t4	t5
1	Group 1	3.45	3.99	3.95	3.84	3.63
2		3.72	3.60	-	-	4.06
3		3.63	-	-	3.76	3.79
4		3.67	3.90	3.73	3.63	3.96
5		-	-	-	-	-
6		3.87	3.82	4.00	4.01	-
7		3.66	3.92	3.87	3.65	-
8	Group 2	3.90	4.04	3.70	3.65	3.90
9		3.89	-	-	3.79	-
10		3.17	3.05	2.98	-	2.93
11		3.65	3.11	3.18	3.36	-
12		3.50	3.60	3.79	3.82	3.87
13		3.53	3.68	-	3.72	3.72
14		3.82	4.13	4.22	4.09	3.78
15	Group 3	3.81	3.33	3.66	3.69	3.50
16		3.55	3.66	4.00	3.79	4.03
17		3.92	3.62	3.41	3.87	-
18		2.88	3.05	3.17	3.17	3.16
19		3.83	-	3.03	3.52	3.60
20		3.81	3.49	3.18	3.29	-
21		3.88	4.11	-	4.01	-
22	Group 4	-	4.28	4.21	4.17	4.16
23		4.52	4.18	4.51	4.65	-
24		3.47	-	-	3.42	3.59
25		4.09	-	4.11	4.23	-
26		3.10	3.58	3.95	3.38	3.29
27		3.90	3.69	3.99	3.72	3.79
28		5.27	5.15	4.83	4.92	5.28

Another similarity for correlation dimension analysis was the behavior of the correlation integral curves; i.e., $\ln C(r)$ versus $\ln r$ were similar among the trials (intra-subject) and the subjects (inter-subject). Figure 3.19 and 3.20 show the behavior of the curves $\ln C(r)$ versus $\ln r$ for the first and the fifth trials of an exemplar subject (Subject 11) for varying embedding dimensions, m respectively. Figure 3.21 shows

the behavior of the curves $\ln C(r)$ versus $\ln r$ for the first trial of a different subject (Subject 14) for varying embedding dimensions, m . This similarity in the behavior of the curves of $\ln C(r)$ versus $\ln r$ has existed in all of the trials of all subjects.

On the other hand, Figure 3.22 and 3.23 present D_2 estimates computed from five successive trials of Subjects 5 and 12 for varying embedding dimensions, m respectively. Although D_2 estimates look similar, the behavior of the D_2 estimates is different in terms of convergence (Figure 3.22 and 3.23). Since none of the five successive trials of Subject 5 (Female, 11) has converged (Figure 3.22), while all of the five successive trials of Subject 12 (Male, 31) have converged (Figure 3.23).

Figures 3.24,3.25,3.26,3.27 presented the converged D_2 estimates of the Groups 1,2,3,4 respectively. There were 24 converged trials out of 35 for the Group 1 with an average D_2 value of 3.80 ± 0.16 (mean \pm std). Also, for the Group 2, the number of converged trials was 29 out of 35, and the mean value was 3.64 ± 0.35 . The largest number of converged trials was owned by the Group 3 with 30 trials and mean of them was 3.57 ± 0.34 . Lastly, the Group 4 had 29 converged trials with the mean 4.12 ± 0.59 . Also, Figure 3.28 showed all converged D_2 estimates.

In addition, Figures 3.29 – 3.56 show fitted D_2 estimates for varying embedding dimensions, m of each subjects' first, second, third, fourth, and fifth trials. The non-stationary trials showed green in color, not converged trials were red in color, and the converged trials were black in color. In addition, the line m versus $(m-1)/2$ was blue in color and the blue plus markers indicate saturation point in embedding dimension. Finally, the double exponential curve fitting to D_2 estimates didn't work well for one of the trials of three of the subjects (Subject 9,13,25). These curves were shown in dashed lines rather than solid lines.

Finally, a Kruskal-Wallis (KW) test (analog to 1-way ANOVA, but data replaced by their ranks, go to Appendix H for a more detailed description) [92] on the D_2 values of the converged trials of the CoP_x signals (Table 3.18) were significantly different on subjects ($p < 0.000$). Furthermore, another Kruskal-Wallis test was applied to search for significance difference between groups on the D_2 values of the converged trials of the CoP_x signals (Table 3.18) resulted in a way that groups were significantly different ($p < 0.000$). Group 4 has been found to be significantly different than Group 2 and 3 for the measure of D_2 values.

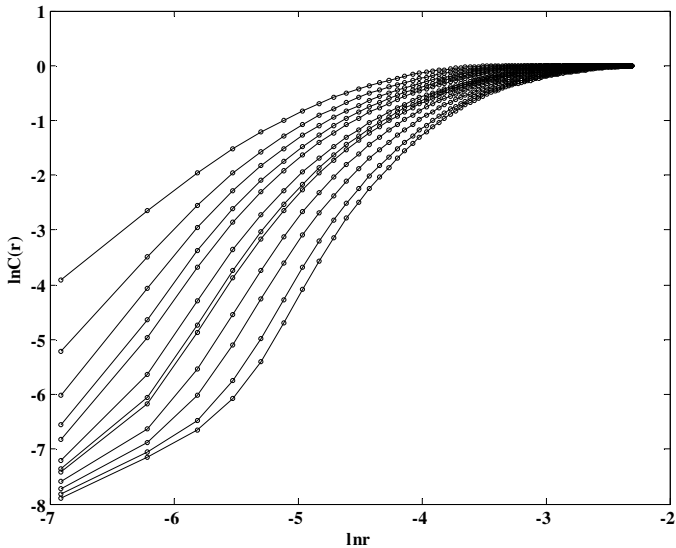


Figure 3.19. Curves $\ln C(r)$ versus $\ln r$ for varying m [11th subject, F, 28, 1st trial]

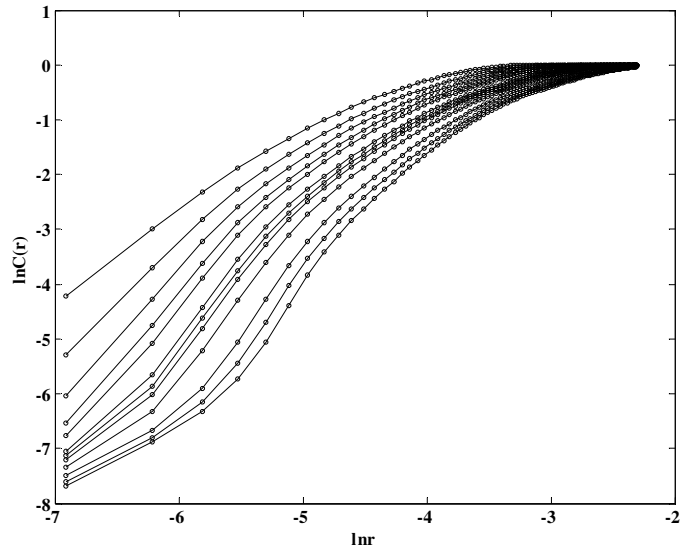


Figure 3.20. Curves $\ln C(r)$ versus $\ln r$ for varying m [11th subject, F, 28, 5th trial]

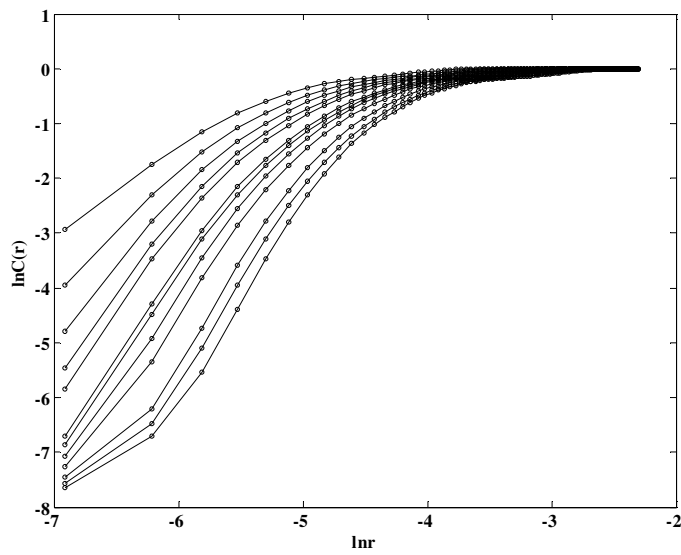


Figure 3.21. Curves $\ln C(r)$ versus $\ln r$ for varying m [14th subject, M, 39, 1st trial]

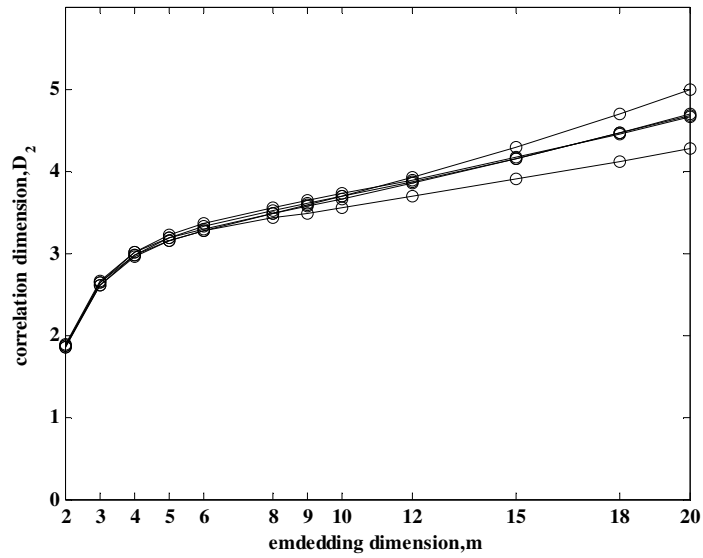


Figure 3.22. Computed D_2 estimates of five trials for varying m [5th subject, F, 11]

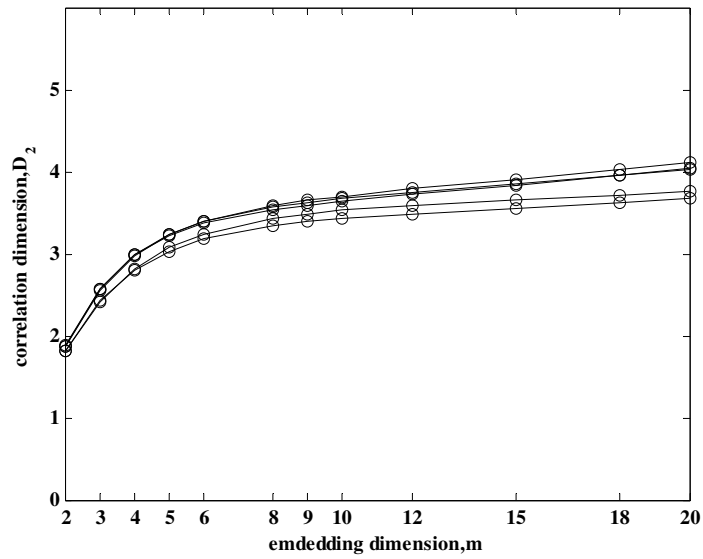


Figure 3.23. Computed D_2 estimates of five trials for varying m [12th subject, M, 31]

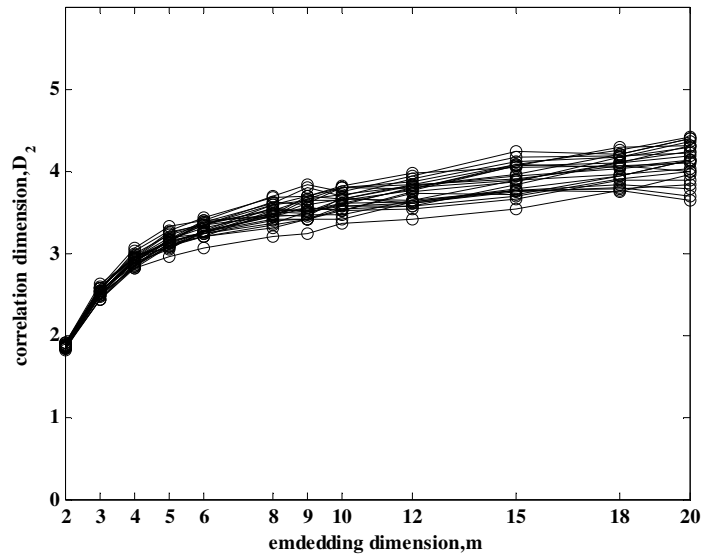


Figure 3.24. Computed D_2 estimates of the converged trials for the Group 1

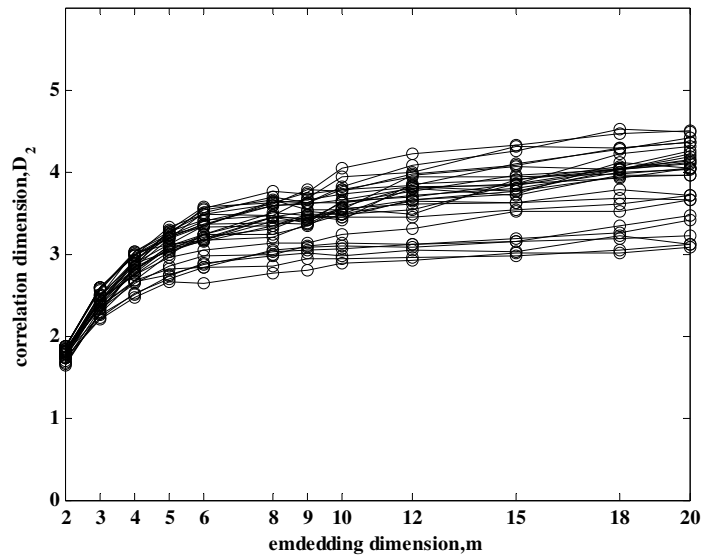


Figure 3.25. Computed D_2 estimates of the converged trials for the Group 2

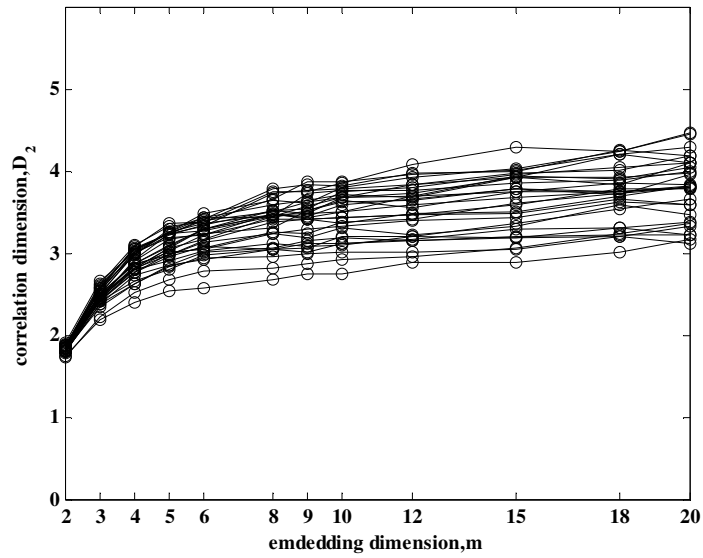


Figure 3.26. Computed D_2 estimates of the converged trials for the Group 3

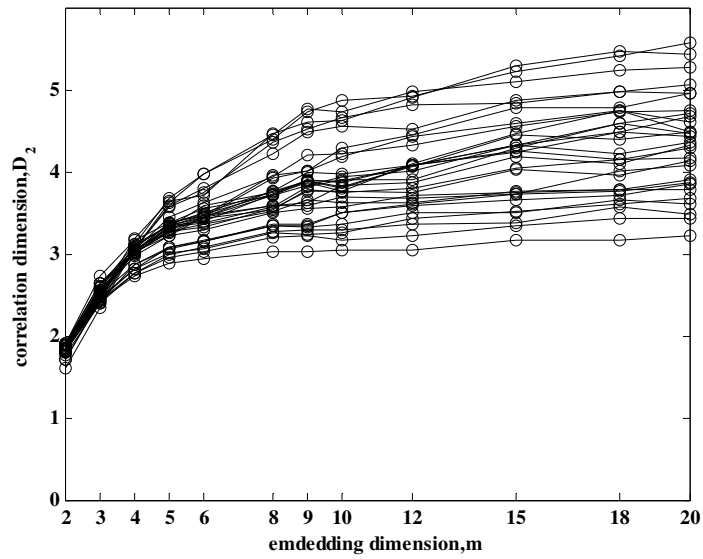


Figure 3.27. Computed D_2 estimates of the converged trials for the Group 4

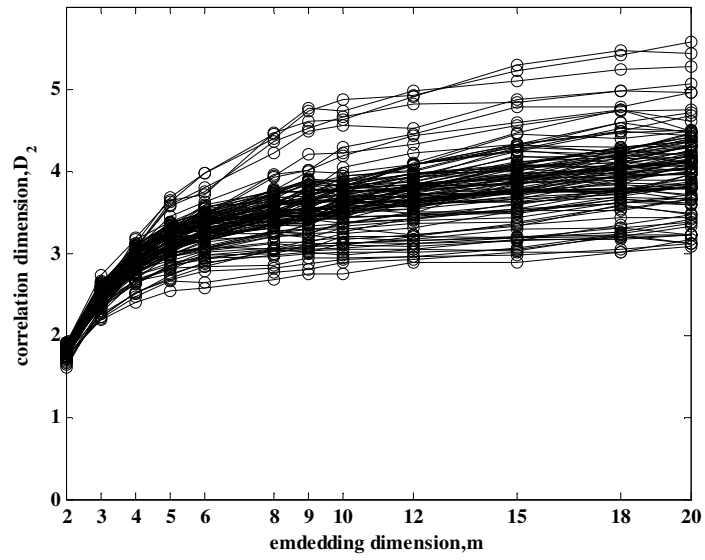


Figure 3.28. Computed D_2 estimates of all converged trials

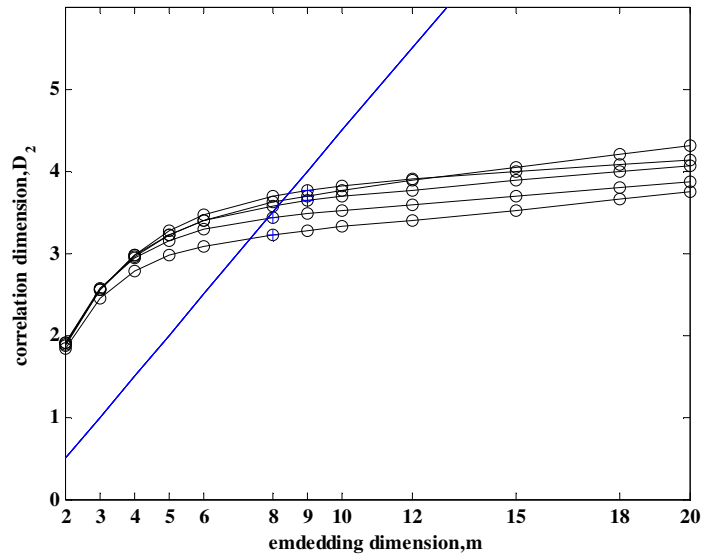


Figure 3.29 Fitted D_2 estimates of Subject 1 for varying m

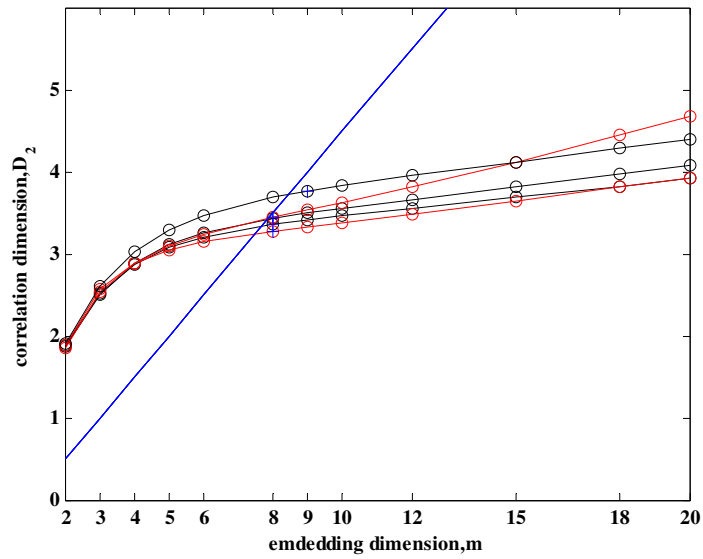


Figure 3.30. Fitted D_2 estimates of Subject 2 for varying m

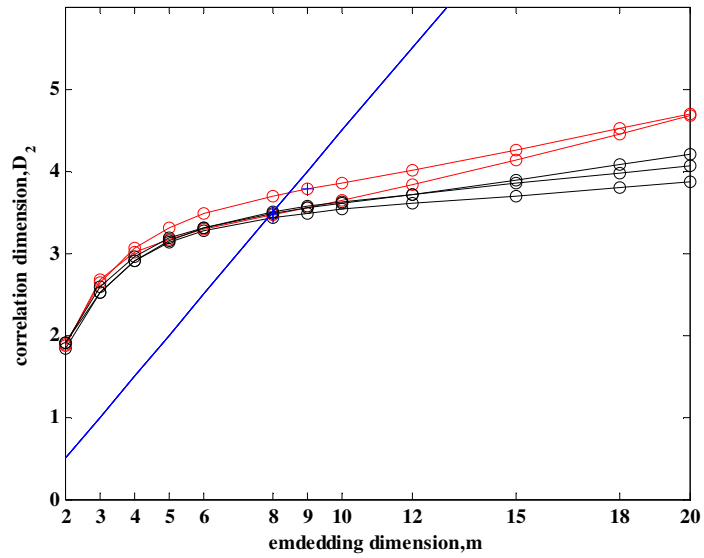


Figure 3.31. Fitted D_2 estimates of Subject 3 for varying m

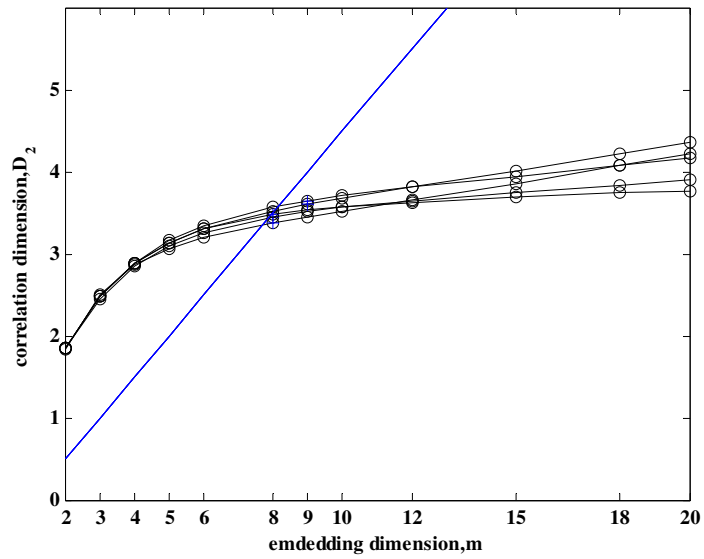


Figure 3.32. Fitted D_2 estimates of Subject 4 for varying m

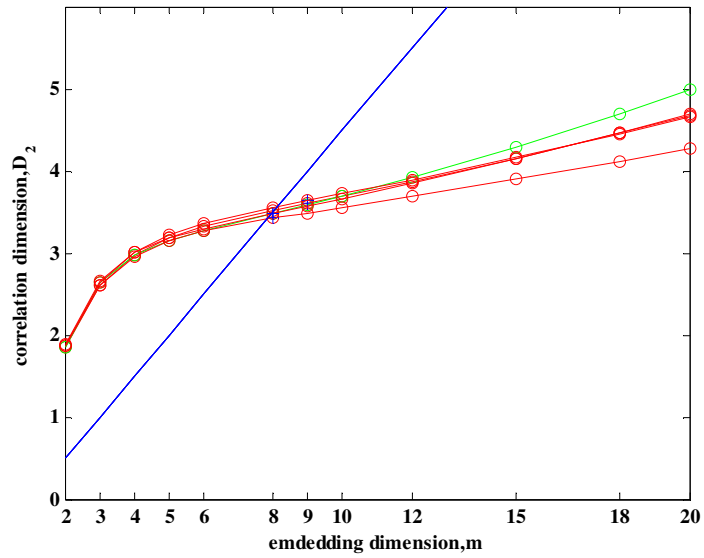


Figure 3.33. Fitted D_2 estimates of Subject 5 for varying m

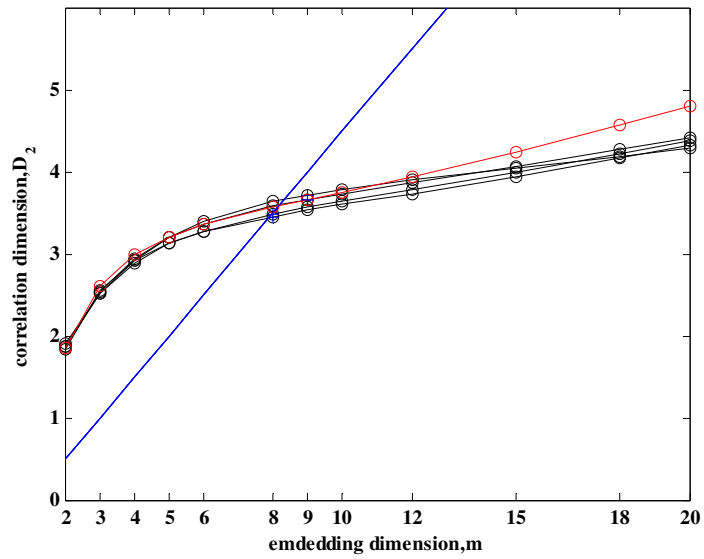


Figure 3.34. Fitted D_2 estimates of Subject 6 for varying m

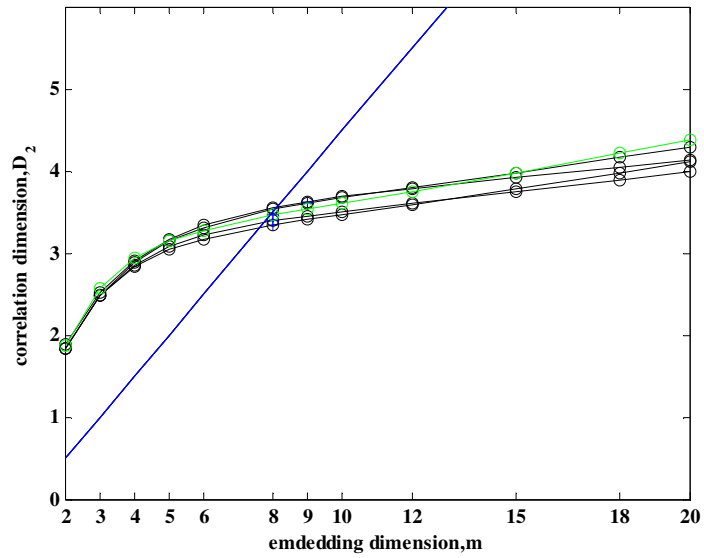


Figure 3.35. Fitted D_2 estimates of Subject 7 for varying m

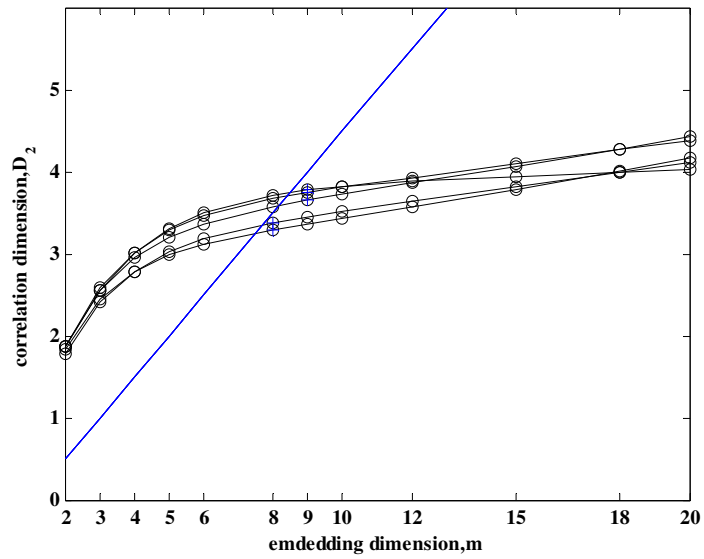


Figure 3.36. Fitted D_2 estimates of Subject 8 for varying m

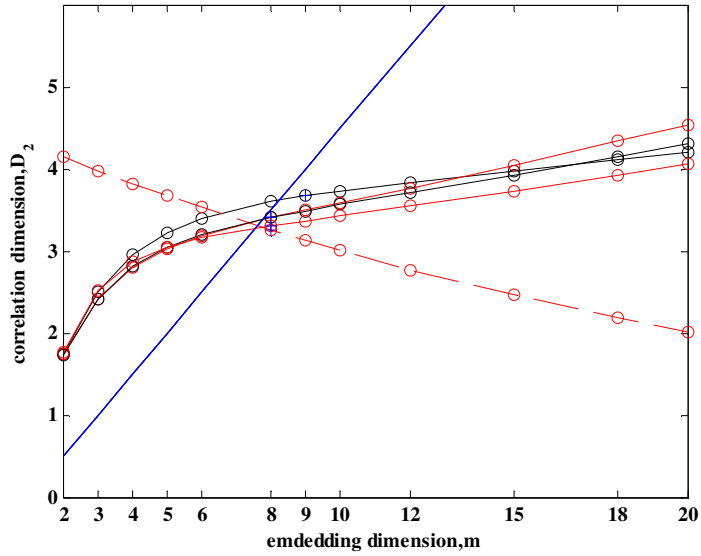


Figure 3.37 Fitted D_2 estimates of Subject 9 for varying m

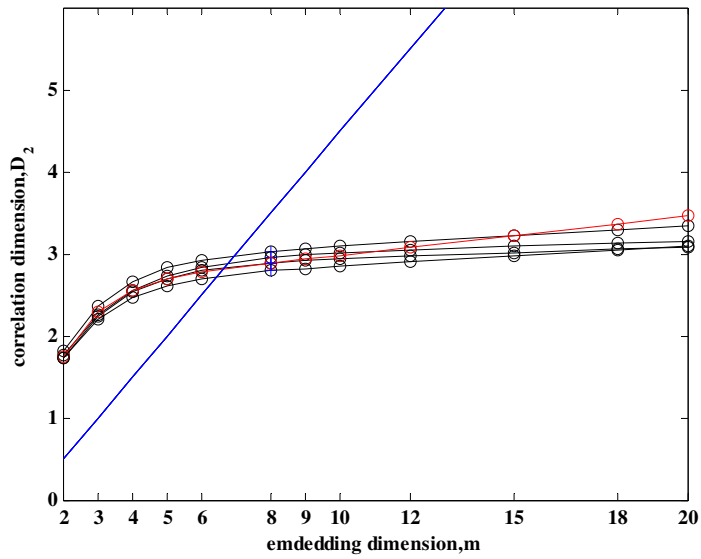


Figure 3.38. Fitted D_2 estimates of Subject 10 for varying m

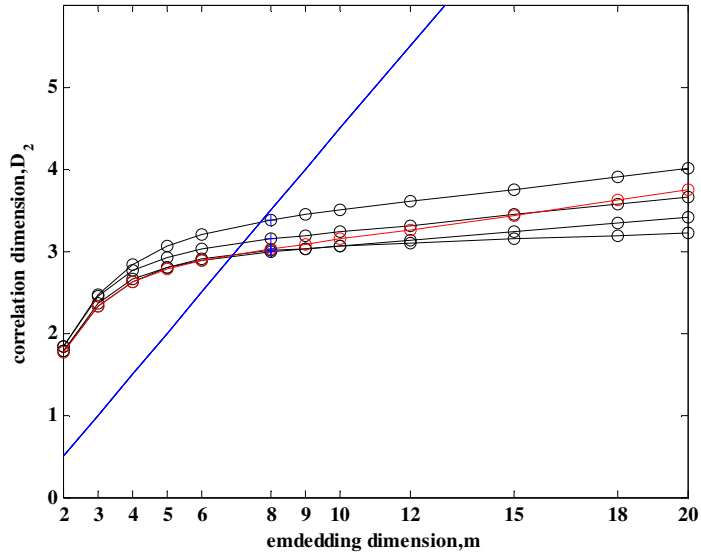


Figure 3.39. Fitted D_2 estimates of Subject 11 for varying m

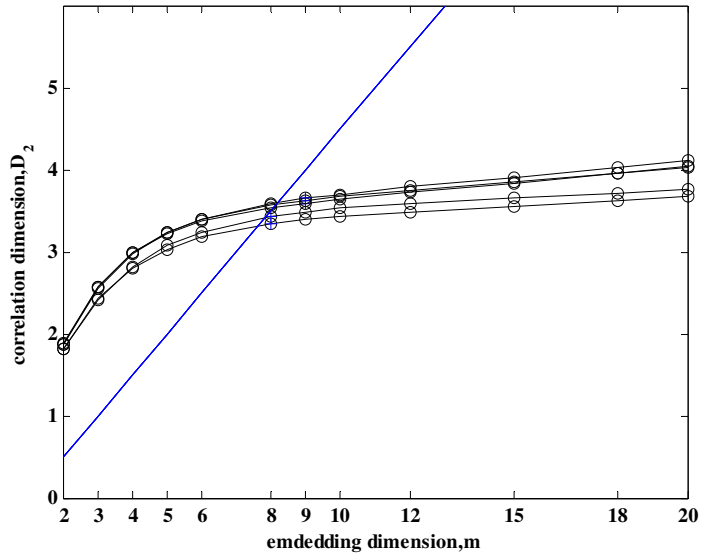


Figure 3.40. Fitted D_2 estimates of Subject 12 for varying m

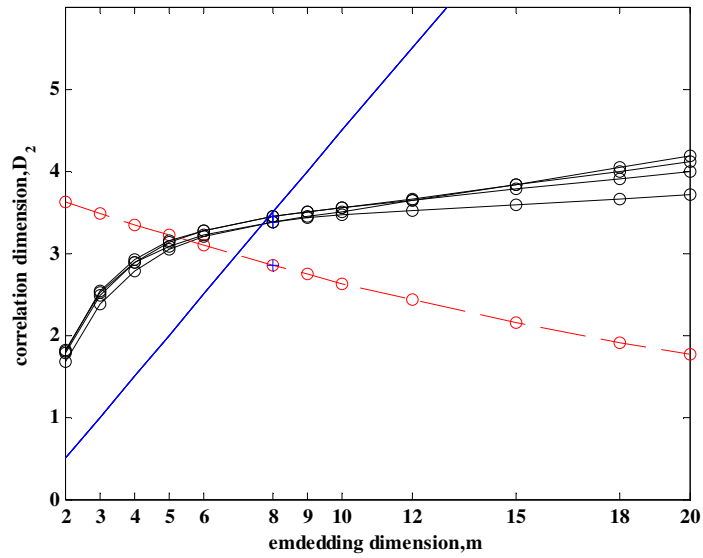


Figure 3.41. Fitted D_2 estimates of Subject 13 for varying m

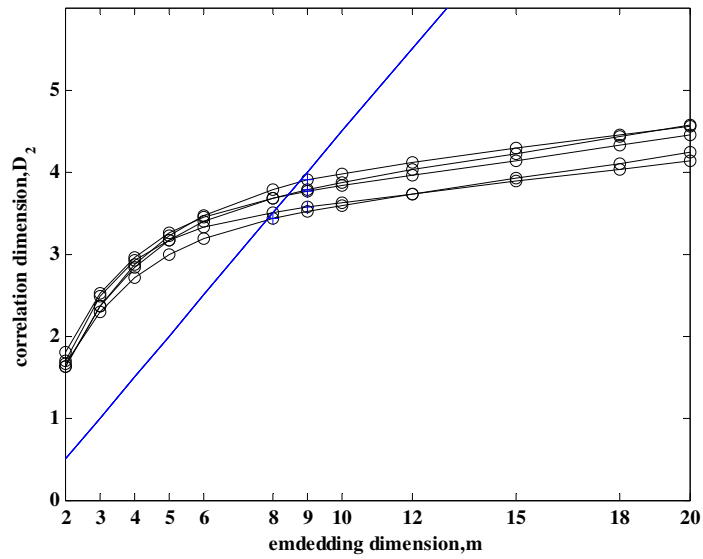


Figure 3.42. Fitted D_2 estimates of Subject 14 for varying m

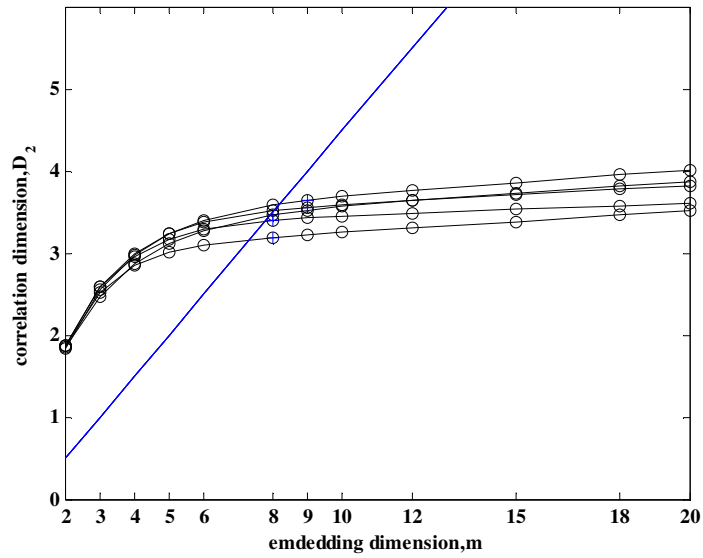


Figure 3.43. Fitted D_2 estimates of Subject 15 for varying m

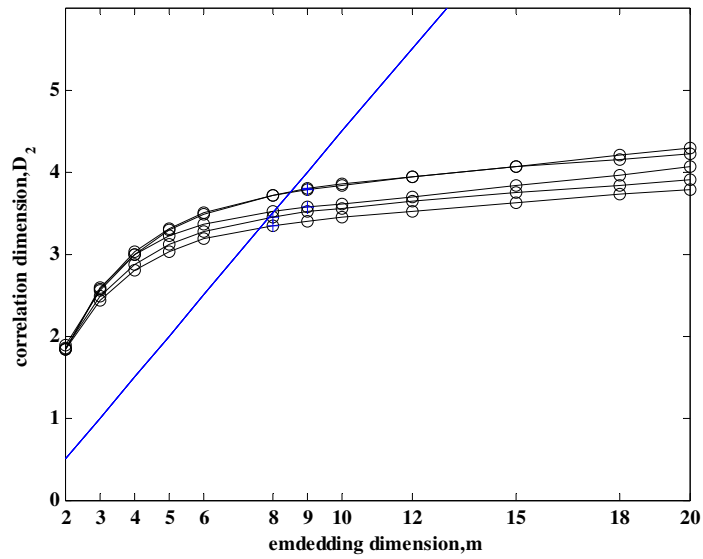


Figure 3.44. Fitted D_2 estimates of Subject 16 for varying m

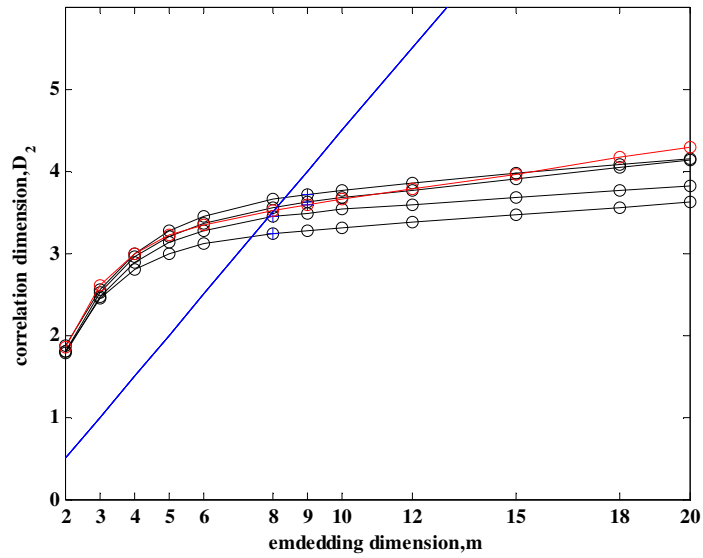


Figure 3.45. Fitted D_2 estimates of Subject 17 for varying m

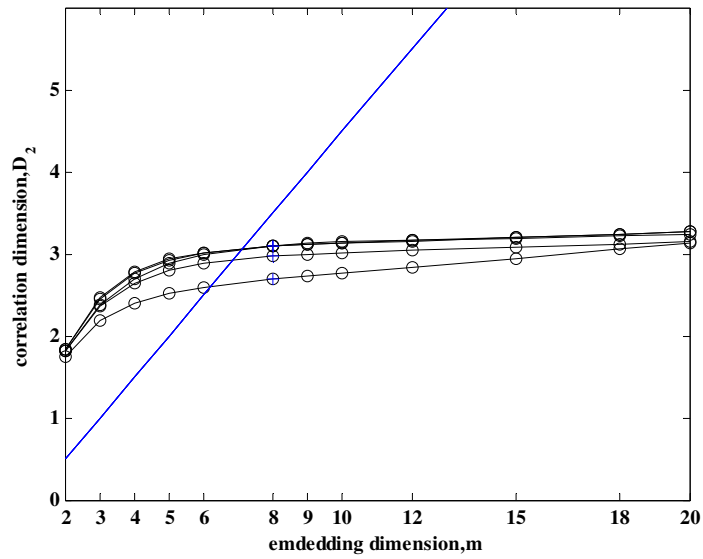


Figure 3.46. Fitted D_2 estimates of Subject 18 for varying m

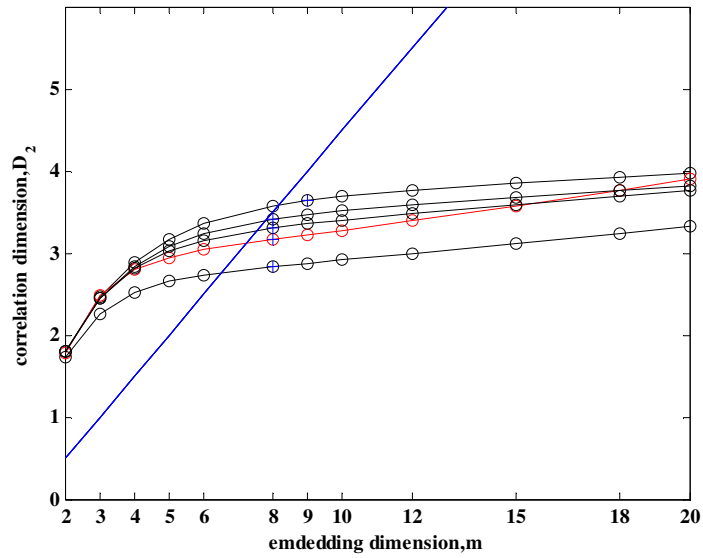


Figure 3.47. Fitted D_2 estimates of Subject 19 for varying m

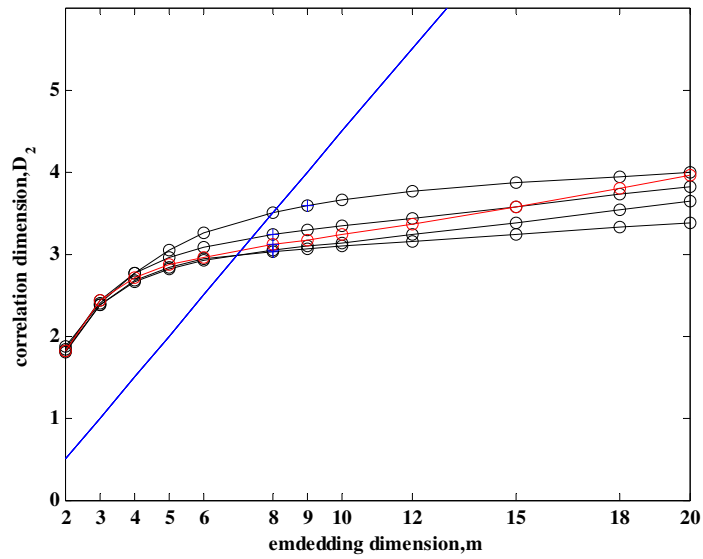


Figure 3.48. Fitted D_2 estimates of Subject 20 for varying m

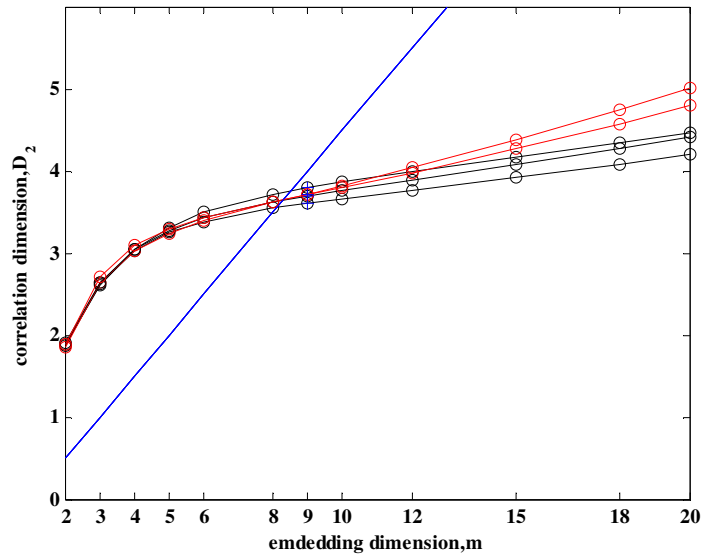


Figure 3.49. Fitted D_2 estimates of Subject 21 for varying m

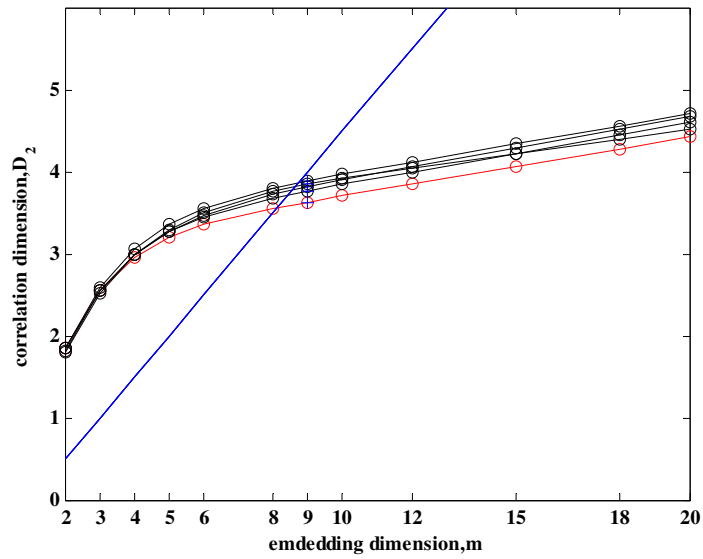


Figure 3.50 Fitted D_2 estimates of Subject 22 for varying m

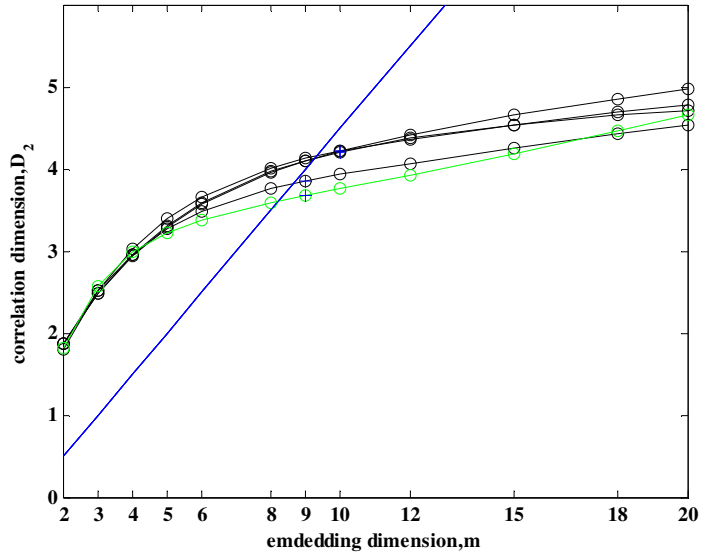


Figure 3.51. Fitted D_2 estimates of Subject 23 for varying m

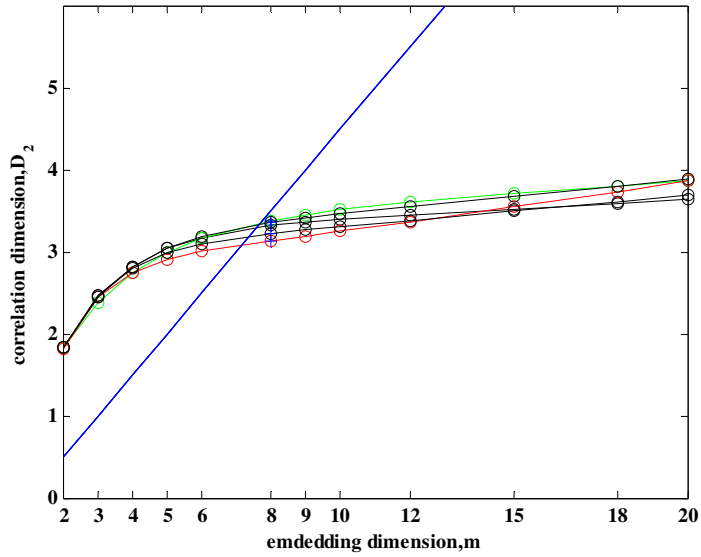


Figure 3.52. Fitted D_2 estimates of Subject 24 for varying m

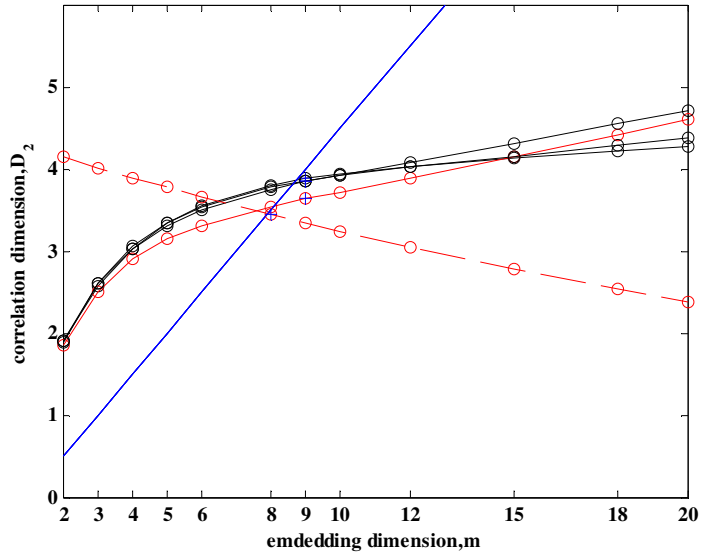


Figure 3.53. Fitted D_2 estimates of Subject 25 for varying m

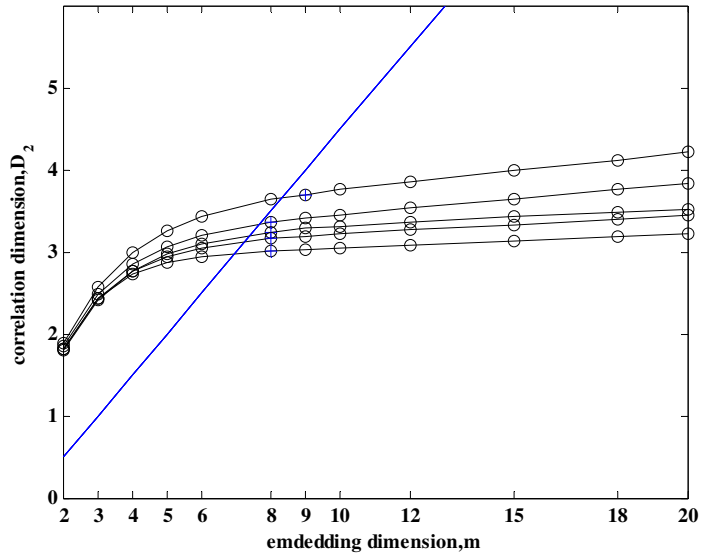


Figure 3.54. Fitted D_2 estimates of Subject 26 for varying m

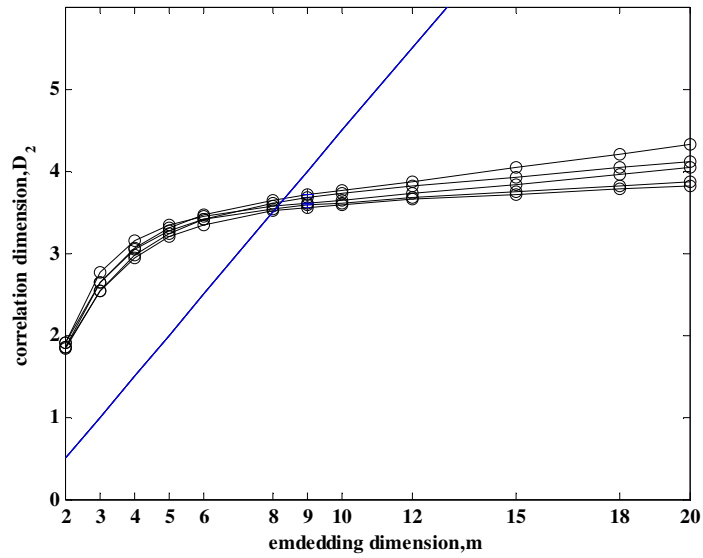


Figure 3.55. Fitted D_2 estimates of Subject 27 for varying m

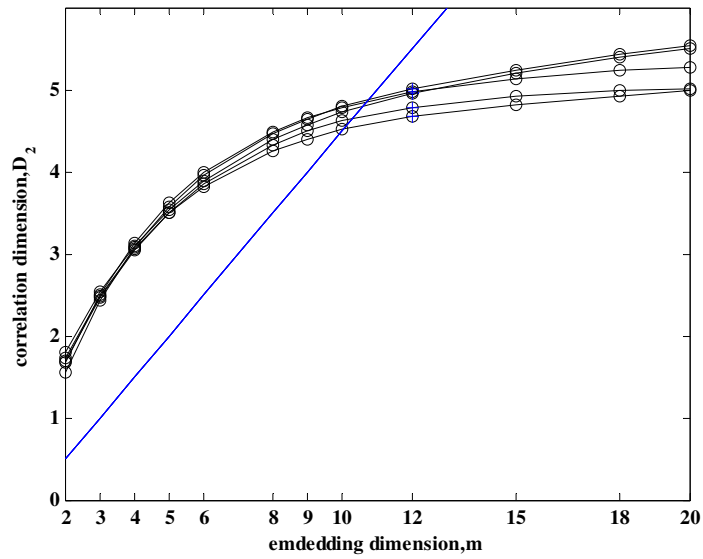


Figure 3.56. Fitted D_2 estimates of Subject 28 for varying m

CHAPTER 4

MODELING

4.1 Surrogate Data

The behavior observed in stationarity and ergodicity characteristics of the CoP_x signals has been checked against two types of linear processes by using *surrogate data* [94]. For this purpose, first a linear process was specified then the surrogate data have been generated, which were consistent with the process specified. Next, the analytical methods as *Run test* [75] and *Ensemble average* [76] (see Chapter 2 Section 2.2.1.1.2 and 2.2.1.1.3 respectively) were applied to the surrogate data created to check stationarity and ergodicity characteristics respectively. Two linear models have been used to generate the surrogate data.

4.1.1 Surrogate Data I

The first linear process was *stationary uncorrelated Gaussian noise*. In order to compare the stationary and ergodic characteristics in the CoP_x signal behavior against the first linear process, the surrogate data have been obtained by shuffling the temporal order [95] of the corresponding CoP_x signals for each experimental trial. In this process, the amplitude distribution of the experimental data is preserved (Figure 4.1).

4.1.2 Surrogate Data II

The second linear process compared to the stationary and ergodic characteristics in the CoP_x signal behavior has been chosen to be the *stationary correlated Gaussian noise*. The surrogate data which were consistent with the corresponding experimental

record and the linear process have been created for each experimental trial. The surrogate data sets (time series) for the second linear process have been created by taking the Fourier transform of the experimental CoP_x signals, randomizing the phase and then taking the inverse Fourier transform [94]. In this process Fourier power spectrum of the experimental data is preserved (Proof is given in Appendix I) (Figure 4.1).

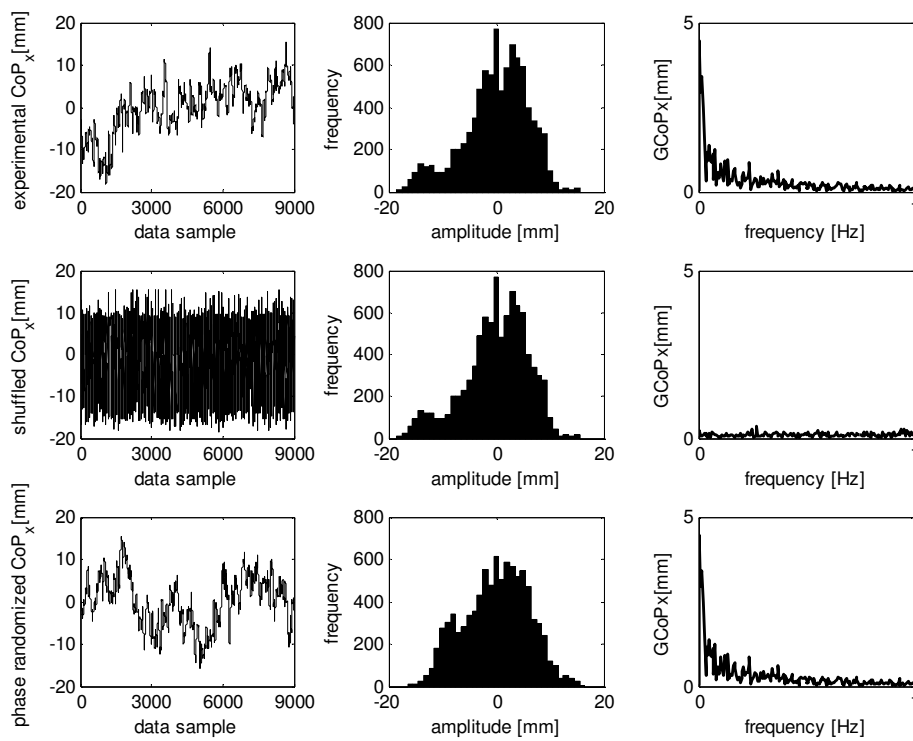


Figure 4.1. Time series (first column), amplitude distributions (second column), and Fast Fourier Transformations (third column) of the experimental, shuffled (Surrogate Data I), and phase randomized (Surrogate Data II) CoP_x signals [14th subject, F, 28]

4.2 Results

4.2.1 Results of Run Test

Run Test (Chapter 2 Section 2.2.1.1.2) has been applied to shuffled (Surrogate-1) and phase-randomized (Surrogate-2) CoP_x signals obtained from 5 successive surrogates of each of 28 subjects; i.e., a shuffled CoP_x signal and a phase randomized CoP_x signal have been generated for each experimental CoP_x signal. The results of the *Run Test* were given in *total run* (Chapter 2 Section 2.2.1.1.2) in Table 4.1. The test results for the shuffled CoP_x signal has suggested that 2 out of 140 surrogates, which belong to Subjects 5 (Male, 7 years old), were non-stationary (refer to Chapter 2 Section 2.2.1.1.2). One surrogate is non-stationary from the left-side and one is non-stationary from the right-side [84]. Hence, 138 of the shuffled CoP_x signals (98.6%) were stationary. On the other hand, phase randomized CoP_x signals' Run Test results established that 3 out of 28 subjects (Subject 12,13,23) presented non-stationarity from the left-side [84] in one of their five successive surrogates. Thus, 137 of the phase randomized CoP_x signals (97.9%) were stationary.

4.2.2 Results of Ensemble Average Analysis

The *ensemble average* analysis (Section 2.2.1.1.3) has been applied to the shuffled and phase-randomized CoP_x signals that belong to the subjects who demonstrated stationary signal characteristics in each of the five successive surrogates [94]; i.e., 27 out of 28 subjects have been evaluated for the shuffled CoP_x signal (Subject 2 excluded) and 25 out of 28 subjects have been assessed for the phase-randomized CoP_x signal (Subject 12,13,23 excluded). The results were presented in *p*-values (Table 4.2 and Table 4.3) obtained from 2-way ANOVA test (Appendix C) performed on *T* matrix (Chapter 2 Section 2.2.1.1.3, Equation (2.14)). The results for the shuffled CoP_x signal (Table 4.2) revealed that 27 subjects have *p* values more than

0.05 on both rows and columns. Thus, all 27 subjects' shuffled CoP_x signals that performed in the ensemble average analysis were ergodic.

Besides, the phase-randomized CoP_x signals of Subjects 2 and 22 have p values less than 0.05 on columns (Table 4.3). Thus, the phase-randomized CoP_x signals which belong to Subjects 2 and 22 were not ergodic. Subsequently, phase-randomized CoP_x signals of 23 subjects (Subjects 1, 3, 4, 5, 6, 7, 8, 9, 10, 11, 14, 15, 16, 17, 18, 19, 20, 21, 24, 25, 26, 27, and 28) were stationary and ergodic.

Table 4.1. Run Test Results in *total run*

Subject	Group	Shuffled CoP _x					Phase Randomized CoP _x				
		T 1	T 2	T 3	T 4	T 5	T 1	T 2	T 3	T 4	T 5
1	Group 1	9	10	10	13	9	11	12	12	8	6
2		6	10	9	15*	5*	8	14	10	9	10
3		9	13	8	12	7	9	10	9	8	7
4		6	9	7	6	10	12	10	7	8	8
5		13	10	10	12	10	8	8	8	10	6
6		10	12	10	10	8	8	11	9	6	11
7		9	10	11	7	11	8	7	9	14	6
8	Group 2	13	9	11	11	12	11	9	7	8	9
9		11	9	8	9	8	10	10	9	9	7
10		10	13	13	11	11	10	8	8	7	8
11		8	11	11	8	11	8	6	9	7	11
12		9	8	9	10	10	9	8	10	9	5*
13		11	10	9	14	10	9	10	9	5*	8
14		7	13	8	9	9	8	13	10	9	7
15	Group 3	12	9	9	12	9	12	8	10	8	8
16		8	10	10	8	8	7	7	7	7	7
17		11	10	11	11	9	10	9	7	7	6
18		7	10	8	11	10	7	9	10	11	9
19		8	14	10	12	13	10	9	7	12	7
20		8	10	7	10	10	11	10	11	10	8
21		11	6	13	8	8	8	7	9	10	9
22	Group 4	6	10	11	10	8	12	12	9	10	8
23		8	8	8	11	12	9	4*	10	6	10
24		12	9	14	13	8	10	9	7	9	10
25		13	10	9	10	8	11	8	9	9	11
26		9	7	10	6	10	9	11	9	10	9
27		12	12	11	7	10	9	9	10	11	11
28		11	6	9	9	12	10	10	10	11	8

*indicates non-stationary trials

Table 4.2. p -values obtained from the two-way ANOVA of T matrix for the shuffled CoP_x

Subject	p_{columns}	p_{rows}
1	0.95	1.00
3	0.848	1.000
4	0.186	1.000
5	0.318	1.000
6	0.930	1.000
7	0.786	1.000
8	0.654	1.000
9	0.661	1.000
10	0.077	1.000
11	0.393	1.000
12	0.221	1.000
13	0.385	1.000
14	0.106	1.000
15	0.373	1.000
16	0.963	1.000
17	0.163	1.000
18	0.716	1.000
19	0.239	1.000
20	0.881	1.000
21	0.607	1.000
22	0.270	1.000
23	0.425	1.000
24	0.841	1.000
25	0.934	1.000
26	0.130	1.000
27	0.211	1.000
28	0.376	1.000

Table 4.3. p -values obtained from the two-way ANOVA of T matrix for the phase-randomized CoP_x

Subject	p_{columns}	p_{rows}
1	0.980	1.000
2	0.003	1.000
3	0.397	1.000
4	0.522	1.000
5	0.293	1.000
6	0.608	1.000
7	0.321	1.000
8	0.101	1.000
9	0.985	1.000
10	0.059	1.000
11	0.593	1.000
14	0.508	1.000
15	0.050	1.000
16	0.897	1.000
17	0.375	1.000
18	0.190	1.000
19	0.446	1.000
20	0.765	1.000
21	0.068	1.000
22	0.039	1.000
24	0.839	1.000
25	0.078	1.000
26	0.998	1.000
27	0.866	1.000
28	0.810	1.000

4.2.3 Sign Test of the Results of Run Test and Ergodicity Analysis

In this section, a sign test has been applied to the results obtained from the stationarity and ergodicity analyses. The surrogates of a subject were named as fully-stationary if all of the 5 successive surrogates are stationary (indicated with '+' in Tables 4.4 and 4.5, Column 'Stationarity'). However, even if one of the five successive surrogates of a subject were to be found non-stationary, then the surrogates of that subject were called as not-fully-stationary (indicated with '-' in Table 4.4 and 4.5, Column 'Stationarity'). Furthermore, subjects who demonstrated ergodic trials were recorded with a '+' sign, while the subjects who had non-ergodic trials were recorded with a '-' sign in Table 4.4 and 4.5, Column 'Ergodicity'. The last columns (Sign Test) of the Table 4.4 and 4.5 have been composed in a way that has been described in Chapter 3 Section 3.1.1.4.

The results suggested that 27 out of 28 subjects' shuffled CoP_x signals have been marked with a '+' sign, which means that the shuffled signals demonstrated "fully-stationary and ergodic" characteristics for 27 subjects out of 28. On the other hand; Group 2, 3, and 4 differed significantly ($p < 0.05$) from the Group 1 in terms of demonstrating fully-stationary shuffled CoP_x signal characteristics, since the one-tailed probability of the case "fully-stationary signal characteristics own by all of seven of the subjects in Group 2 or 3 or 4" was 0.008 by reference to the binomial distribution (Appendix F).

Lastly, Group 3 differed significantly from other groups in terms of the fully-stationary characteristics of phase-randomized CoP_x , since the one-tailed probability of the case "fully-stationary signal characteristics of 7 subjects out of 7" was 0.008 by reference to the binomial distribution (Appendix F).

In Table 4.6, Sign test results of the experimental, shuffled, and phase-randomized CoP_x signals were summarized. There were 11, 27, and 23 out of 28 subjects who demonstrated fully-stationary and ergodic trials for the experimental, shuffled, and phase-randomized CoP_x signals respectively. No subject had fully-stationary but non-ergodic trials for the shuffled CoP_x signals; however, 13 and 2 subjects had fully-stationary but non-ergodic trials for experimental and phase-randomized CoP_x signals respectively. Finally, the number of subjects for the case having not-fully-stationary trials was as 13, 1, and 2 for the experimental, shuffled, and phase-randomized CoP_x signals respectively. Being fully-stationary but non-ergodic behavior of the experimental CoP_x signals was not observed for the shuffled CoP_x signals yet it exists for the phase-randomized CoP_x signals.

Table 4.4. Sign Test Table for shuffled CoP_x

Subjects	Group	Stationarity	Ergodicity	Sign
1	Group 1	+	+	+
2		-	-	0
3		+	+	+
4		+	+	+
5		+	+	+
6		+	+	+
7		+	+	+
8	Group 2	+	+	+
9		+	+	+
10		+	+	+
11		+	+	+
12		+	+	+
13		+	+	+
14		+	+	+
15	Group 3	+	+	+
16		+	+	+
17		+	+	+
18		+	+	+
19		+	+	+
20		+	+	+
21		+	+	+
22	Group 4	+	+	+
23		+	+	+
24		+	+	+
25		+	+	+
26		+	+	+
27		+	+	+
28		+	+	+

Table 4.5. Sign Test Table for phase-randomized CoP_x

Subjects	Group	Stationarity	Ergodicity	Sign
1	Group 1	+	+	+
2		+	-	-
3		+	+	+
4		+	+	+
5		+	+	+
6		+	+	+
7		+	+	+
8	Group 2	+	+	+
9		+	+	+
10		+	+	+
11		+	+	+
12		-	+	0
13		-	+	0
14		+	+	+
15	Group 3	+	+	+
16		+	+	+
17		+	+	+
18		+	+	+
19		+	+	+
20		+	+	+
21		+	+	+
22	Group 4	+	-	-
23		-	+	0
24		+	+	+
25		+	+	+
26		+	+	+
27		+	+	+
28		+	+	+

Table 4.6. Sign Test Results for experimental, shuffled, and phase-randomized CoP_x

Subjects	Group	Experimental	Shuffled	Phase-randomized
1	Group 1	+	+	+
2		-	0	-
3		-	+	+
4		+	+	+
5		0	+	+
6		+	+	+
7		0	+	+
8	Group 2	+	+	+
9		-	+	+
10		+	+	+
11		-	+	+
12		-	+	0
13		-	+	0
14		-	+	+
15	Group 3	-	+	+
16		+	+	+
17		+	+	+
18		+	+	+
19		-	+	+
20		-	+	+
21		+	+	+
22	Group 4	-	+	-
23		0	+	0
24		0	+	+
25		+	+	+
26		-	+	+
27		-	+	+
28		+	+	+

CHAPTER 5

DISCUSSION

Complex nature of the human postural sway has been investigated by analyzing the CoP signals (CoP signals covers both CoP_x and CoP_y signals) of 28 subjects from a wide range of different ages. Firstly, the variance/standard deviation [74] of the signals was computed. Standard deviation is a measure of variability or amount of postural sway. Secondly, Run test [75], which is a non-parametric statistical test, was applied to examine whether the signals are non-stationary or stationary. Thirdly, Ensemble average [76] of the CoP signal was used to check whether the signals are ergodic or not. Fourthly, to explore the frequency content of the CoP signals, FFT [77] analysis was applied. Fifthly, PSD estimates via Welch's method [78] were computed to quantify the distribution of the power of the signals in frequency spectrum. Finally, nonlinear analysis methods such as reconstruction of the dynamics of the CoP_x signals in state-space [37,38] and calculation of correlation dimension estimates (D_2) [35] were applied.

The first analysis was computing standard deviation values (Chapter 3 Section 3.1.1.1), which is a measure of amount of postural sway, for detrended CoP_x and CoP_y signals. The maximum values for the observed measure was 16.0 mm (Subject 1, F, 6 years old) and 23.3 mm (Subject 14, M, 39 years old) in sagittal (CoP_x) and coronal (CoP_y) planes respectively. This finding showed that even for the worst individual performance on this measure, Center-of-Pressure is bounded in area compatible with a matchbox. This finding has suggested that all subjects were very successful to assure their balance in quiet stance. For almost all of the subjects (26 out of 28 subjects), the sway in the sagittal plane has been more than the sway in the coronal plane (exceptions are Subject 2 and 27) when the mean values of the five

successive trials are compared (Table 3.1(a) and Table 3.1(b) Column “Means” in Chapter 3 Section 3.1.1.1). The reason for this outcome may be the anatomical structure of the human body as it allows more movement in sagittal plane. Human upright biped stance in sagittal plane can be modeled with an inverted pendulum [9,11]; still in coronal (frontal) plane, it can be modeled with a four-bar linkage [100,101]. This kind of modeling approach may shed light to the finding about the relative stability of CoP_x signal compared to CoP_y signal, where further research is warranted. The subject who swayed most was the youngest subject (Subject 1, 6 years old, Female) participated in the experiments. The best performance on this measure was performed by Subject 14 (39 years old, Male). He has done sport almost in his entire life so he may be better on controlling his muscles [10] for a good performance on this measure. The ANOVA tests suggested that subjects are different ($p < 0.000$ for both CoP_x and CoP_y) for the measure of amount of postural sway (inter-subject variability). Besides, subjects behaved similar in trials in the amount postural sway since standard deviation values of the CoP signals were not significantly different on the trials ($p < 0.195$ for CoP_x and 0.511 for CoP_y). This has been suggested as a good indicator of repeatability of this measure (standard deviation values of CoP signals) over the trials. Lastly, groups were not found to be significantly different from each other when amount of postural sway was considered ($p < 0.414$ for CoP_x and 0.112 for CoP_y). This result is not consistent with the previously reported studies about the amount of postural sway in different age groups (e.g. [71,72]). However, the subjects have been experimented in more difficult stances than quiet stance (e.g. stimulated stance or one-legged stance) at the aforementioned studies [71,72]. Provoking quiet stance may be more effective to detect changes in amount of postural sway with respect to ages when working at different age groups. In general, all groups included both good and bad performers in amount of postural sway at this particular study.

Only 4 CoP_x and 14 CoP_y trials were found to be non-stationary (Chapter 3 Section 3.1.1.2). So in the light of this finding, it can be suggested that CoP can be considered as a stationary signal, in our case where it has been observed 180 seconds long in quiet stance. Also it was interesting to observe that if a CoP signal is non-stationary then it is non-stationary from left-side [84]. In other words, none of the signals were non-stationary from the right-side [84]. In the analysis of stationarity by the Run Test [75], the total run (Chapter 2 Section 2.2.1.1.2) span is divided into three intervals (left, middle, and right, see Appendix A and B; and Equations (2.8), (2.9), (2.10) in Chapter 2 Section 2.2.1.1.2; and also Chapter 4). If the number of total run for the particular case is in the middle interval (Equation (2.8) in Chapter 2 Section 2.2.1.1.2), then the observed signal is stationary [75]. However, the left and right intervals indicate a non-stationary signal [75]. So, if a signal is non-stationary as its number of total run is in the left interval (Equation (2.9) in Chapter 2 Section 2.2.1.1.2), then it is called as “non-stationary from left-side” for the first time by Celik and Gürses (2007) [84]. Similarly, if a signal is non-stationary as its number of total run is in the right interval (Equation (2.10) in Chapter 2 Section 2.2.1.1.2), then it is called as “non-stationary from right-side” [84]. Dynamical correspondences of left and right side non-stationarity could be suggested such that non-stationary from left-side indicates consistent linear trend in time; however, non-stationary from right points to consistent oscillatory trend in time, both of which are sensitive to the data window size. Contrary to stationarity of the CoP signal observed in this study, some of the previous work on the CoP signal reported non-stationary characteristics of the CoP signal (e.g., [49,50,51]). Carroll et al. [49] used 60 seconds, Schumann et al. [50] 100 seconds and Loughlin et al. [51] used 90 seconds trials. Duarte et al. (2000 and 2001) [28,29] suggested that some previous researchers tested only small portions of a longer process. In addition, for a stationary analysis, it is a critical issue to decide on the data window size, since underestimated window sizes may give spurious results. In this study, it has been taken as 500 data samples (10 seconds), since a data window width of 500 data samples, which has been sampled with a frequency of 50 Hz would

then cover at least one full cycle of CoP dynamics reported (the CoP dynamics consists of at least two natural frequencies in the frequency band of 0.1-1 Hz [4,21]). The robustness of the selection on 500 data samples was also examined and robustness was observed (Chapter 3 Section 3.1.1.4). So, the authors (e.g., [13,14,15]) who reported that CoP is a non-stationary signal have probably observed a “small” (60-second for Carroll et al. [49], 100-second for Schumann et al. [50] and 90 seconds trials for Loughlin et al. [51]) fraction of a “longer process” (1800-second for Duarte et al. [28,29], and 180-second for this particular study). It resembles to say that the mean value of sinus signal is a positive rational number rather than zero, by observing half of it. A study on “how long the CoP signal should be observed?”, Doyle et al. (2007) [96] suggested that CoP measures reached acceptable levels of reliability with at least five 60-second trials. This criterion (at least five 60-second trials) supports the choice of time-length (180 seconds) and the number of the trials (5 trials for each subject) for this particular study. However, their measures for this outcome [96] were standard deviation, velocity, and 95% confidence ellipse area; but a stationarity analysis.

Another issue was the ergodicity of the CoP signals (Chapter 3 Section 3.1.1.3). Nearly half of the subjects had ergodic signals (11 for CoP_x and 12 for CoP_y out of 28). However, if the five successive 180-sec long trials are regarded, CoP_y signal is more likely to be ergodic compared to the CoP_x signal. As the one-tailed probability of the case “fully-stationary and ergodic” has been 0.975 (see Chapter 3 Section 3.1.1.4) for the CoP_y signal (it was 0.419 for CoP_x). Stationarity indicate trend-free behavior of a subject in a trial however ergodicity indicates behavioral consistency in the whole data collection period. Ergodicity increases the “usability” of measures of a signal as it does not continuously change on the successive trials. In other words, it makes more sense defining measures of a signal that does not change character over the trials to quantify patterns, behaviors etc. So, if an individual signature as a

dynamical pattern [103] exists for each subject in terms of human postural sway, then this pattern should be observed in all trials of a subject (be ergodic).

The results of the Modeling Chapter (Chapter 4) suggested that temporal order of CoP_x is important. Since, when the temporal order of the CoP_x signal was destroyed by shuffling the temporal order of the signal (Surrogate I), the previously revealed behavior of the CoP_x signal on stationarity and ergodicity (Chapter 3 Section 3.1.1.2-3.1.1.5) was diminished (see also Chapter 4 Section 4.2). However; that was not the case when the phase information of the CoP_x signal was randomized (Surrogate II); ie, the behavior of experimentally obtained CoP_x signal (Chapter 3 Section 3.1.1.2-3.1.1.5) and phase-randomized CoP_x signal (Chapter 4 Section 4.2) was similar on stationarity and ergodicity. This outcome might indicate that the phase relation is not the critical control variable between the mod shapes of the CoP_x signal [21] on biped upright stance.

In the frequency domain (Chapter 2 Section 3.1.2), all CoP signals showed dynamics with larger amplitudes at lower frequencies. This was a common pattern of the CoP signal. Another characteristic of the FFT pattern was that almost the whole power of the signal has settled at 0-1 Hz frequency band (the grand mean of all subjects all trials was 0.98). This broad and side-banded FFT pattern is a strong indicator of chaotic behavior as it points out bifurcations in the dynamics of the CoP signals [102]. Besides, the significant low frequency dynamics was appended with long-range correlations of the CoP signal by Duarte et al. (2000 and 2001) [28,29]. They realized the similarity between the long-range correlations revealed in the CoP signal and a dynamics like $1/f$ noise. Most probably, it is the dynamics at the low frequencies, which cause the long-range correlations in the control process of human upright posture. Collins et al. [13] proposed both open (<1 second) and closed (>1 second) loop dynamics co-existing simultaneously for the control process of human upright posture, and the long-range correlations is most likely related with the closed-

loop control scheme. Also, it could be also suggested that open loop dynamics cause low frequency drift [13]. Additionally; when the rambling-trembling [17,18] dynamics was considered, low frequency (larger in amplitude) dynamics may be related with rambling and high frequency (smaller in amplitude) dynamics can be associated with trembling. The ANOVA tests performed on the power of the signals settled on 0-0.1 Hz and 0-1 Hz bands showed that people behaved different on these PSD measures. However, PSD of the signals were not significantly different on different trials, which states that the subjects used the same frequency bands in successive experiments. For the PSD R1 of CoP_x, PSD R2 of CoP_x, and PSD R1 of CoP_y measures, groups were not significantly different; however, PSD R2 of CoP_y is the measure that differed among the groups significantly in this particular study ($p < 0.044$). However; as the p-value is greater 0.010, it does not make much sense to claim that PSD R2 of CoP_y is a key measure to differ the groups.

Another issue on posture studies is fatigue which might emerge in the experiments. Fatigue is defined for the muscles as the reduction in the force generating capacity of the muscles [109]. Motor control performance and the proprioceptive ability decreases with increasing fatigue in the muscles [110,111]. It was also shown that fatigue causes increased CoP displacements [112]. In this study; third, fourth, and twenty first subjects stated tiredness, a bit of tiredness and no tiredness during the experiments respectively. However, no significant changes in the calculated measures were observed over the trials of these subjects. Besides, the subjects were allowed 3 minutes to rest between the successive trials during the data collection. Therefore, it might be proposed that fatigue didn't appear on the conducted experiments for this particular study. However, measurements with proper instruments should be made in order to evaluate fatigue if it is a concern of the study.

Is postural sway good or bad? If not leading fall, there is no disadvantage for swaying. The basic function of postural control system is preventing fall by

maintaining static equilibrium. In addition, trying to maintain static equilibrium without swaying may be more energy-inefficient [113] compared to quasi equilibrium with swaying, since the former task is much more difficult to perform. Besides, action (swaying) supports perception [8]. In other words, postural sway may have a functional role as it provides adaptation by information transmission [8,32]. For example, when a person walks in a dark room, he/she usually “sway”s his/her arm to learn environment.

The main hypothesis of the study was that “CoP signal is stationary chaotic in nature and its measures change with aging”. To explore the possible chaotic structure of the human postural sway correlation dimension estimates (D_2) [35] were calculated for the stationary CoP_x signals (Chapter 3 Section 3.2.2). In order to compute D_2 estimates CoP_x signals were initially reconstructed in m -dimensional state-space by using proper time delays [37,38]. Generally, the time delay values (τ) (Chapter 3 Section 3.2.1) computed have decreased with increasing embedding dimension (m) and also tended to get saturated after a critical embedding dimension, m -value. Conversely, the reconstruction window values (τ_w) [88] (Chapter 3 Section 3.2.1) continuously increased with increasing m , which makes suspectable to define a reconstruction window (τ_w) for the CoP_x signal. So, the suggested phenomenon by Martinerie et al. (1992) [89] and Rosenstein et al. (1994) [88]: the correlation integral is sensitive to τ_w but not to τ and m individually seemed not to be valid for the dynamics re-constructed from the CoP_x signals. Low frequency drift dynamics [13] might have caused some problems to apply τ_w to the dynamics re-constructed from the CoP_x signal.

The correlation dimension (D_2) estimate computed through a signal is related with the dimension (degrees-of-freedom) of the inherent dynamics of the system from which a signal has been collected. The correlation dimension of limit cycle is 1; D_2 of a torus is 2 [33]. A limit cycle and a torus correspond to uniformly distributed points that

constitute a line and a plane in the state space respectively. When a sphere of radius r (Chapter 2 Section 2.2.6.3) is constructed and expanded gradually to look for D_2 , the points in the sphere will be proportional to r^1 and r^2 for a limit cycle and a torus respectively [87]. So, the D_2 of limit cycle is 1 and D_2 of a torus is 2. The results of correlation dimension analysis suggested that 112 trials out of 140 converged and the remaining 28 not. The correlation dimension estimate value that was computed for 112 converged trials was fractional dimensions rather than being an integer. Convergence indicated determinism since a signal composed of noise does not converge to a value for D_2 with increasing m [87]. This was showed by the Surrogate-I analysis of the CoP_x signals, since shuffled CoP_x signals (modeled as uncorrelated Gaussian noise) did not converge to a value with increasing m [13]. Also, fractional correlation dimension values pointed a strange attractor rather than a limit cycle or torus. So, both the convergence of D_2 estimates and the fractal structure revealed from the 112 CoP_x signals suggested a chaotic behavior for the postural sway. Followed by, it could be claimed that at the remaining 28 trials, i.e., the human postural sway observed at 28 not-converged CoP_x signals, stochastic characteristics were predominating the deterministic characteristics of the signal. Then comes the question: What caused this main difference on the dynamical structure of the postural sway (112 deterministic chaos versus 28 stochastic (e.g., random walk) sway) obtained from the experimentally recorded 180-sec long CoP data collected at identical laboratory conditions from 28 different subjects? Nevertheless, switching in between deterministic chaos and stochastic sway has also been diagnosed during the five successive trials of the same subject. Perception of the subjects who have been instructed as “stand still as quiet as possible with an upright posture” might be different over subjects [8]. Also the perception of “standing still” might have changed continuously during and over the trials since some of the subjects had both converged and not-converged trials (refer to the Table 3.17 in Chapter 3). In the experiments, subjects were not instructed to look at a target but have been instructed as to look forward. Some of the subjects stated orally (in the conversation part after the

experiments) that they selected an imaginary point on the wall, which is in front of them and might have fixed their gaze to that point look at that point (may result in less eye movements), while the other subjects have not orally expressed such a behavior; i.e., their eyes might have “swayed” in stance (may result in considerable eye movements). The latter case might lead changes in self perception of their motion in space for those subjects (e.g., [8,98]). This may be a reason for both having deterministic and stochastic results from the same quiet stance experiment for different subjects, and even for different trials of a subject. However, as the eye movements was not measured while the experiments, it is not possible to claim proposed relationship between eye movements and dynamics of human postural sway quantitatively (i.e., it need to be further studied with suitable instruments).

Human is not a machine out of a mass-production with constant system parameters or a dynamical system that can be described definitely (in the sense of Newtonian mechanics) with a set of differential equations. It is a living organism that changes at every time it is sampled and also in time it is evolving. Different people have different bodies and minds. However, in spite of these inherent differences, common patterns are also used by the subjects, which suit most of the people’s behavior observed in many of the scientific research performed. For example, in this particular study, the pattern of FFTs were quiet similar for different subjects. This indicates that most of the people use a common frequency band (0-1 Hz) for their postural body dynamics. Another common pattern was the behavior of the correlation integral curves i.e., the curves $\ln r$ vs. $C(r)$ (e.g., Figure 3.19 in Chapter 3 Section 3.2.2). The pattern for all trials could be described with a sigmoid rather than a knee [97]. A knee pattern offers two significant linear scaling regions, so two non-interacting subsystems with different number of degrees-of freedom [97] for the observed dynamics. However that is not the case for the CoP_x signal, the sigmoid pattern offers one significant linear scaling region, so one unified system for the dynamics of human postural system. Nevertheless, D_2 values obtained by correlation integral

curves were significantly different on subjects. Moreover, we found that groups were also significantly different for the measure D_2 values.

In this part, the method for computing the correlation dimension in this particular study are discussed against the other previous studies. Previously Collins et al. [13] have shown that computing D_2 estimates gives erroneous results since there is no significant linear scaling region. They used 90-second long experimental records and varying embedding dimension from $m=2$ to $m=20$. However, Yamada [32] computed D_2 estimates from reconstructed CoP_x dynamics in 3-dimensional state space for 5 subjects and found a D_2 estimate between 2.1 and 2.5 using 200-second long trials. Recently, Pascolo et al. [46] reported correlation dimension estimates between 1.312 and 1.514 computed from 60-sec long CoP_x signals embedded in 3-dimensional state space for 4 healthy subjects. However, Pascolo et al. [46] and Yamada [32] have not shown that their estimates of correlation dimension were robust against variation in embedding dimension, m [42]. In our research, we were also able to compute correlation dimension estimates between 2.88 and 5.28 and observed that D_2 values converged when the embedding dimension, m is larger than 8 up to 12. However, Yamada [32] and Pascolo et al. [46] used embedding dimension, m up to 3 for reconstructing the CoP_x dynamics, where the correlation dimension estimate curves (e.g., Figure 3.29-3.56 in Chapter 3 Section 3.2.2) have not saturated yet. This might lead them to underestimate the correlation dimension values of the reconstructed CoP_x dynamics. Contrary to Collins et al. [13], we have shown that there existed a significant linear scaling region to quantify an estimate for the correlation dimension and further this estimate was robust to varying embedding dimension, m .

Finally, the physiological reason behind the quantified topological dimension of the postural dynamics is discussed. Postural dynamics during quiet stance has been shown to consist of two simultaneously co-existing excitable modes each with a separate eigen-frequency [21]. Two simultaneously co-existing modes point to a

postural dynamics with an order of four. Nevertheless, the nonlinear features of the human postural sway during quiet stance have been extensively reported in the literature (e.g. [5,19,51,91,104,105]). The integer dimension of the human postural sway is expected to become a non-integer value due to the nonlinear features of the oscillations. This may be one of the reasons for the observed fractal correlation dimension values up to 4. In contrast, the correlation dimension estimate values higher than 4 may be pointing to higher order dynamics which are due to the sensory feedbacks in the closed-loop postural dynamics or other modal frequencies involved in human quiet stance posture [23,99].

In conclusion, when the main hypothesis of the study: “CoP_x signal is stationary and chaotic in nature and its measures change due to aging” is considered; it has been suggested that human postural sway is a stationary process when 180-second long biped quiet stance data is considered. Additionally, it demonstrates variable dynamical structure (112 deterministic chaos versus 28 stochastic postural sway (e.g., random walk)) for different subjects and different trials of the same subjects. Finally, we observed significant change for the D_2 values computed from the CoP_x signal in this particular study due to aging. We conclude that, it is possible to suggest human postural sway reflecting a mixture of deterministic (chaotic) and stochastic components [5], such that determinism is more dominant to stochasticity for some individuals while stochasticity predominating for some of the others.

Further Studies: To solidify the chaotic structure of the converged CoP_x signal, Lyapunov exponents [36], which quantifies the initial condition sensitivity of the trajectories, should be computed. Also to find the physical/physiological correspondence of the degrees-of-freedom pointed by the correlation dimension estimates, kinematic and EMG data during quiet stance should be collected and the postural control system should be identified by using a dynamical biomechanical model.

REFERENCES

- [1] J. T. Inglis, F. B. Horak, C.L. Shupert, C. Jones-Rycewicz, “The importance of somatosensory information in triggering and scaling automatic postural responses in humans”, **Experimental Brain Research**, Vol. 101, 1994, pp.159-164.
- [2] F. B. Horak, C.L. Shupert, V. Dietz, G. Horstmann “Vestibular and somatosensory contributions to responses to head and body displacements in stance”, **Experimental Brain Research**, Vol. 100, 1994, pp.93-106.
- [3] J. Dichgans, K. H. Mauritz, J. H. Allum, T. Brandt, “Postural sway in normals and atactic patients: Analysis of the stabilizing and destabilizing effects of vision”, **Agressologie**, Vol. 17, 1976, pp.15-24.
- [4] R. J. Peterka, “Sensorimotor Integration in Human Postural Control”, **Journal of Neurophysiology**, Vol. 88, No.3, 2002, pp.1097-1118.
- [5] T. Kiemel, K.S. Oie, J.J. Jeka, “Multisensory Fusion and the Stochastic Structure of Postural Sway”, **Biological Cybernetics**, Vol.87, No.4, 2002, pp.262-277.
- [6] K.S. Oie, T. Kiemel, J.J. Jeka, “Multisensory Fusion: Simultaneous Re-weighting of Vision and Touch for the Control of Human Posture”, **Cognitive Brain Research**, Vol.14, No.1, 2002, pp.164-176.
- [7] A. D. Kuo, R. A. Speers, R. J. Peterka, F. B. Horak, “Effect of altered sensory conditions on multivariate descriptors of human postural sway”, **Experimental Brain Research**, Vol.122, No.2, 1998, pp.185-195.
- [8] G. E. Riccio, “Information in movement variability about the qualitative dynamics of posture and orientation”, In K. E. Newell, D. M. Corcos (Eds), **Variability and Motor Control**, Champaign, IL: Human Kinetics, 1993, pp.317-357.
- [9] R. Johansson, M. Magnusson, M. Akesson, “Identification of human postural dynamics”, **IEEE Transactions on Biomedical Engineering**, Vol.35, No.10, 1988, pp.858-869.
- [10] I. D. Loram, C. N. Maganaris, M. Lakie, “Human postural sway results from frequent, ballistic bias impulses by soleus and gastrocnemius”, **The Journal of Physiology**, Vol.564, No.1, 2005, pp.295-311.
- [11] R. J. Peterka, “Postural control model interpretation of stabilogram diffusion analysis”, **Biological Cybernetics**, Vol. 83, 2000, pp.335-343.

- [12] S. Park, F. B. Horak, A. D. Kuo, "Postural feedback responses scale with biomechanical constraints in human standing", **Experimental Brain Research** Vol.154, No.4, 2004, pp.417-427.
- [13] J.J. Collins and C. J. De Luca, "Random Walking during Quiet Standing", **Physical Review Letters**, Vol.73, No.5, 1994, pp.764-767.
- [14] J. J. Collins and C. J. De Luca, "Upright, correlated random walks: A statistical-biomechanics approach to the human postural control system", **Chaos**, Vol.5, No.1, 1995, pp.57-63.
- [15] A. Bottaro, M. Casadio, P. G. Morasso, V. Sanguineti, "Body sway during quiet standing: Is it the residual chattering of an intermittent stabilization process?", **Human Movement Science**, Vol.24, 2005, pp.588-615.
- [16] C. Edwards and S.K. Spurgeon, **Sliding Mode control: Theory and Applications**, London: Taylor & Francis, 1998.
- [17] V. M. Zatsiorsky and M. Duarte, "Instant equilibrium point and its migration in standing tasks: rambling and trembling components of the stabilogram", **Motor Control**, Vol.3, No.1, 1999, pp.28-38.
- [18] V. M. Zatsiorsky and M. Duarte, "Rambling and trembling in quiet standing", **Motor Control**, Vol. 4, No. 2, 2000, pp.185-200.
- [19] S. Gürses, **Postural Dynamics and Stability**, Ph.D. Dissertation Ankara, Turkey: Middle East Technical University, 2002.
- [20] S. Gürses, Y. Dhaher, T. C. Hain, E. A. Keshner, Nonlinear response of the head to small amplitude perturbations, **Chaos**, Vol.15, No.2, 2005.
- [21] R. Creath, T. Kiemel, F. Horak, R. Peterka, J. Jeka, "A Unified View of Quiet and Perturbed Stance: Simultaneous Co-Existing Excitable Modes", **Neuroscience Letters**, Vol.377, No.2, 2005, pp.75-80.
- [22] B. Colobert, A. Créteil, P. Allard, P. Delamarche, "Force-plate based computation of ankle and hip strategies from double-inverted pendulum model", **Clinical Biomechanics** , Vol.21 , No.4 , 2006, pp.427 – 434.
- [23] A.V. Alexandrov, A.A. Frolov, F.B. Horak, P. Carlson-Kuhta, S. Park, "Feedback Equilibrium Control During Human Standing", **Biological Cybernetics**, Vol.93, No.5, 2005, pp.309-322.

- [24] E.V. Gurfinkel, “Physical Foundations of Oscillography”, **Agressologie C**, Vol.14, 1973, pp.9-13.
- [25] D.A. Winter, **Biomechanics and Motor Control of Human Movement**, New York: John Wiley & Sons, Inc., 1990.
- [26] K. E. Newell and D. M. Corcos, “Issues in Variability and Motor Control”, In K. E. Newell, D. M. Corcos (Eds), **Variability and Motor Control**, Champaign, IL: Human Kinetics, 1993, pp.1-13.
- [27] T. Schreiber and A. Schmitz, “Surrogate Time Series”, **Physica D**, Vol.142, 2000, pp.346-382.
- [28] M. Duarte and V.M. Zatsiorsky, “On the Fractal Properties of Natural Human Standing”, **Neuroscience Letters**, Vol.283, No.3, 2000, pp.173-176
- [29] M. Duarte and V.M. Zatsiorsky, “Long-range Correlations in Human Standing”, **Physics Letters A**, Vol.283, No.1-2, 2001, pp.124-128.
- [30] K. M. Newell, S. M. Slobounov, E. S. Slobounova, P. C. M. Molenaar, “Stochastic processes in postural center-of-pressure profiles”, **Experimental Brain Research**, Vol. 113, No.1, 1997, pp.158-164.
- [31] M. Roerdink, M. De Haart, A. Daffertshofer¹, S. F. Donker, A. C. H. Geurts, P. J. Beek, Dynamical structure of center-of-pressure trajectories in patients recovering from stroke, **Experimental Brain Research**, Vol.174, No.2, 2006, pp.256-269.
- [32] N. Yamada, “Chaotic Swaying of the Upright Posture”, **Human Movement Science**, Vol.14, No.6, 1995, pp.711-726.
- [33] S. H. Strogatz, **Nonlinear Dynamics and Chaos: With Applications to Physics, Biology, Chemistry, and Engineering**, Perseus Books Group, 2000.
- [34] B. B. Mandelbrot, **Fractals: form, chance, and dimension**, San Francisco: Freeman, 1977.
- [35] P. Grassberger and I. Procaccia, “Characterization of Strange Attractors”, **Physical Review Letters**, Vol.50, No.5, 1983, pp.346-349.
- [36] A. Wolf, J. B. Swift, H. L. Swinney, J. A. Vastano, “Determining Lyapunov exponents from a time series”, **Physica D**, Vol.16, 1985, pp.285-317.

- [37] N. H. Packard, J.P. Crutchfield, J.D. Farmer, R.S. Shaw, “Geometry from a Time Series”, **Physical Review Letters**, Vol.45, No.9, 1980, pp.712-716.
- [38] F. Takens, in **Dynamical Systems and Turbulence**, edited by D.A. Rand and L.-S. Young, Berlin: Springer-Verlag, 1981.
- [39] J. Theiler, S. Eubank, A. Longtin, B. Galdrikian, J. Farmer, “Testing for Nonlinearity in Time Series: The Method of Surrogate Data”, **Physica D**, Vol.58, 1992, pp.77-94.
- [40] L. Glass, M. C. Mackey, **From Clocks to Chaos**, Princeton: Princeton University Press, 1988.
- [41] P. Faure and H. Korn, “Is there chaos in the brain? I. Concepts of nonlinear dynamics and methods of investigation”, **Comptes Rendus de l’Académie des Sciences - Series III - Sciences de la Vie**, Vol.324, No.9, 2001, pp.773-793.
- [42] P.E. Rapp, A.M. Albano, T.I. Schmah, L.A. Farwell, “Filtered Noise can Mimic Low-dimensional Chaotic Attractors”, **Physical Review E**, Vol.47, No.4, 1993, pp.2289-2297.
- [43] J. Feder, **Fractals**, New York: Plenum, 1988.
- [44] J. A. Scheinkman and B. LeBaron, “Nonlinear Dynamics and Stock Returns”, **The Journal of Business**, Vol.62, No.3, 1989, pp.311-337.
- [45] E. Nelson, **Dynamical Theories of Brownian Motion**, Princeton: Princeton University Press, 2001.
- [46] P.B. Pascolo, A. Marini, R. Carniel, F. Barazza, “Posture as a Chaotic System and an Application to the Parkinson’s Disease”, **Chaos, Solitons and Fractals**, Vol.24, No.5, 2005, pp.1343-1346.
- [47] J. S. Richman, J. R. Moorman, Physiological time-series analysis using approximate entropy and sample entropy, **American Journal of Physiology – Heart and Circulatory Physiology**, Vol.278, 2000, pp.2039–2049.
- [48] C. C. Chow, M. Lauk, J. J. Collins, “The dynamics of quasi-static posture control”, **Human Movement Science** Vol.18, No. 5, 1999, pp.725-740.
- [49] J. P. Carroll and W. Freedman, “Nonstationary properties of postural sway”, **Journal of Biomechanics**, Vol. 26, No. 4-5, 1993, pp.409-416.

- [50] T. Schumann, M. S. Redfern, J. M. Furman, A. El-Jaroudi, L. F. Chaparro, "Time-frequency analysis of postural sway", **Journal of Biomechanics**, Vol.28, No.5, 1995, pp.603-607.
- [51] P.J. Loughlin, M.S. Redfern, J.M. Furman, "Time-varying Characteristics of Visually Induced Postural Sway", **IEEE Transactions on Rehabilitation Engineering**, Vol.4, No.4, 1996, pp.416-424.
- [52] P.M. Conn, **Handbook of models for human aging**, Amsterdam: Elsevier Academic Press, 2006.
- [53] N.W. Shock, "Aging of physiological systems", **Journal of Chronic Diseases**, Vol.36, No.1, 1983, pp.137-142.
- [54] S.K. Whitbourne, "Physiological Aspects of Aging: Relation to Identity and Clinical Implications", **Comprehensive Clinical Psychology**, Vol.7, 2000, pp.1-24.
- [55] D.E. Vaillancourt, K.M. Newella, "Changing complexity in human behavior and physiology through aging and disease", **Neurobiology of Aging**, Vol.23, 2002, pp.1-11.
- [56] B.A. McClenaghan, H.G. Williams, J. Dickerson, M. Dowda, L. Thombs, P. Eleazer, "Spectral characteristics of ageing postural control", **Gait & Posture**, Vol.3, No.3, 1995, pp.123-131.
- [57] J.W. Blaszczyk, D.L. Lowe, P.D. Hansen, "Ranges of postural stability and their changes in the elderly", **Gait & Posture**, Vol.2, No.1, 1994, pp.11-17.
- [58] K.E. Forth, E.J. Metter, W.H. Paloski, "Age associated differences in postural equilibrium control: A comparison between EQscore and minimum time to contact (TTC_{min})", **Gait & Posture**, Vol.25, No.1, 2007, pp.56-62.
- [59] F.B. Horak, C.L. Shupert, A. Mirka, "Components of postural dyscontrol in the elderly: A review", **Neurobiology of Aging**, Vol.10, No.6, 1989, pp.727-738.
- [60] D.L. Gallahue, J.C. Ozmun, **Understanding motor development: Infants, children, adolescents, adults**, Boston: McGraw-Hill, 2006.
- [61] K. M. DeGoede, J.A. Ashton-Miller, A.B. Schultz, "Fall-related upper body injuries in the older adult: a review of the biomechanical issues", **Journal of Biomechanics**, Vol.36, No.7, 2003, pp.1043-1053.
- [62] J.H. van Dieën, M. Pijnappels, "Falls in older people", **Journal of Electromyography and Kinesiology**, Vol.18, No.2, 2008, pp.169-171.

- [63] J.A. Stevens, Falls among older adults-risk factors and prevention strategies, **Journal of Safety Research**, Vol.36, No.4, 2005, pp.409-411.
- [64] P.F. Adams, A.N. Dey, J.L. Vickerie, "Summary health statistics for the U.S. population: National Health Interview Survey, 2005", **Vital Health Statistics**, Vol.233, 2007, pp.1-104.
- [65] T. Allison, A.L. Hume, C.C. Wood, W. R. Goff, "Developmental and aging changes in somatosensory, auditory and visual evoked potentials", **Electroencephalography and Clinical Neurophysiology**, Vol.58, No.1, 1984, pp.14-24.
- [66] R.A. Speers, A.D. Kuo, F.B. Horak, "Contributions of altered sensation and feedback responses to changes in coordination of postural control due to aging", **Gait & Posture**, Vol.16, No.1, 2002, pp.20-30.
- [67] G. Serratrice, H. Roux, R. Aquaron, "Proximal muscular weakness in elderly subjects Report of 12 cases", **Journal of the Neurological Sciences**, Vol.7, No.2, 1968, pp.275-299.
- [68] C.A. Laughton, M. Slavin, K. Katdare, L. Nolan, J.F. Bean, D.C. Kerrigan, et al., "Aging, muscle activity, and balance control: physiologic changes associated with balance impairment", **Gait & Posture**, Vol.18, No.2, pp.101-108.
- [69] M. Bosek, B. Grzegorzewski, A. Kowalczyk, I. Lubiński, "Degradation of postural control system as a consequence of Parkinson's disease and ageing", **Neuroscience Letters**, Vol. 376, 2005, pp.215-220.
- [70] P. Boucher, M. Descarreaux, M.C. Normand, "Postural Control in People with Osteoarthritis of the Cervical Spine," **Journal of Manipulative and Physiological Therapeutics**, Vol.31, 2008, pp.184-190.
- [71] M. H. Woollacott, A. Shumway-Cook, "Changes in posture control across the life span - a systems approach", **Physical Therapy**, Vol.70, No.12, 1990, pp.799-807.
- [72] I. G. Amiridis, V. Hatzitaki, F. Arabatzi, "Age-induced modifications of static postural control in humans", **Neuroscience Letters**, Vol.350, No.3, 2003, pp.137-140.
- [73] A. Hedberg, C. Schmitz, H. Forssberg, M. Hadders-Algra, "Early development of postural adjustments in standing with and without support", **Experimental Brain Research**, Vol.178, No.4, 2007, pp.439-449.

- [74] E. Kreyszig, **Advanced Engineering Mathematics**, New York: John Wiley & Sons, Inc., 1999.
- [75] J.S. Bendat and A.G. Piersol, **Random Data: Analysis and Measurement Procedures**, New York: John Wiley & Sons, Inc., 1971.
- [76] A.H. Nayfeh and B. Balachandran, **Applied Nonlinear Dynamics: Analytical, Computational, and Experimental Methods**, New York: John Wiley & Sons, Inc., 1995.
- [77] W. Cochran et al., “What is the Fast Fourier Transform?”, **IEEE Transactions on Audio and Electroacoustics**, Vol.15, No.2, 1967, pp.45-55.
- [78] P. D. Welch, “The Use of Fast Fourier Transforms for the Estimation of Power Spectra: A method Based on Time Averaging over Short Modified Periodogram”, **IEEE Transactions on Audio and Electroacoustics**, Vol. 15, 1967, pp. 70-73.
- [79] H.C. Güler, S.T. Tümer, **Yürüyüş Analizi: Temel Kavramlar ve Uygulama**, Makina Mühendisliği Bölümü, Orta Doğu Teknik Üniversitesi, Ankara, 1996.
- [80] F.J. Gravetter and L.B. Wallnau, **Statistics for the Behavioral Sciences**, Belmont, CA: Wadsworth Publishing, 2004.
- [81] H. Kantz and T. Schreiber, **Nonlinear Time Series Analysis**, Cambridge: Cambridge University Press, 2003.
- [82] D.E. Newland, **An Introduction to Random Vibrations, Spectral & Wavelet Analysis**, New York: Longman Scientific & Technical, 1993.
- [83] J. W. Cooley and J. W. Tukey, "An Algorithm for the Machine Computation of the Complex Fourier Series", **Mathematics of Computation**, Vol. 19, 1965, pp.297-301.
- [84] H. Celik, S. Gurses, “Statistical Analysis and Simulation of Experimentally Obtained CoP_x Signal”, in *Proceedings of Biyomut 2007*, edited by Y. Ulgen, A. Akin, 2007, pp.25-28.
- [85] J.D. Farmer, E. Ott, J. Yorke, “The Dimension of Chaotic Attractors”, **Physica D**, Vol.7, 1983, pp.153-180.
- [86] H.S. Greenside, A. Wolf, J. Swift, T. Pignataro, “Impracticality of a Box-counting Algorithm for Calculating the Dimensionality of Strange Attractors”, **Physical Review A**, Vol.25, No.6, 1982, pp.3453-3456.

- [87] J. Argyris, G. Faust, M. Haase, **An Exploration of Chaos**, Amsterdam: Elsevier Science, 1994.
- [88] M.T. Rosenstein, J.J. Collins, C. J. De Luca, “Reconstruction Expansion as a Geometry-based Framework for Choosing Proper Delay Times”, **Physica D**, Vol.73, 1994, pp.82-98.
- [89] J.M. Martinerie, A.M. Albano, A.I. Mees, P.E. Rapp, “Mutual Information, Strange Attractors, and the Optimal Estimation of Dimension”, **Physical Review A**, Vol.45, No.10, 1992, pp.7058-7064.
- [90] J.L. Kelley, **General Topology**, New York: Springer-Verlag, 1955.
- [91] S. Gurses, B.E. Platin, S.T. Tumer, N. Akkas, in **Proceedings of Sixth IFAC Symposium**, edited by D.D. Feng, O. Dubois, J. Zaytoon, E. Carson, 2006, pp.225-230.
- [92] S. Siegel and N.J. Cast, **Nonparametric Statistics for the Behavioral Sciences**, New York: McGraw-Hill Book Company, 1988.
- [93] B. W. Lindgren, **Statistical theory**, New York: Macmillan, 1976.
- [94] J. Theiler, S. Eubank, A. Longtin, B. Galdrikian, J. Farmer, “Testing for Nonlinearity in Time Series: The Method of Surrogate Data”, **Physica D**, Vol.58, 1992, pp.77-94.
- [95] J. A. Scheinkman and B. LeBaron, “Nonlinear Dynamics and Stock Returns”, **The Journal of Business**, Vol.62, No.3, 1989, pp.311-337.
- [96] R. Doyle, E. Hsiao-Wecksler, B. Ragan, K. Rosengren, “Generalizability of center of pressure measures of quiet standing”, **Gait & Posture**, Vol.25, No.2, 2007, pp.166 – 171.
- [97] J. P. Eckmann, D. Ruelle, “Ergodic theory of chaos and strange attractors”, **Reviews of Modern Physics**, Vol.57, 1985, pp.617 – 656.
- [98] T. Mergner and W. Becker, “A Modeling Approach to the Human Spatial Orientation System”, **Annals of the New York Academy of Sciences**, Vol.1004, 2003, pp.303-315.
- [99] T. Mergner, “The Matryoshka Dolls Principle in Human Dynamic Behavior in Space: A Theory of Linked References for Multisensory Perception and Control of Action”, **Cahiers de Psychologie Cognitive/Current Psychology of Cognition**, Vol.21, No.2-3, 2002, pp.129-212.

- [100] H. Hemami, B.F. Wyman, "Modeling and Control of Constrained Dynamic Systems with Application to Biped Locomotion in the Frontal Plane", **IEEE Transactions on Automatic Control**, Vol.24, No.4, 1979, pp.526-535.
- [101] J.J. Abbas, H.J. Chizeck, "Feedback Control of Coronal Plane Hip Angle in Paraplegic Subjects Using Functional Neuromuscular Stimulation", **IEEE Transactions on Biomedical Engineering**, Vol.38, No.7, 1991, pp.687-698.
- [102] F.C. Moon, **Chaotic and Fractal Dynamics: An Introduction for Applied Scientists and Engineers**, New York: John Wiley, 1992.
- [103] M.C. Cross, P.C. Hohenberg, "Pattern formation outside of equilibrium", *Reviews of Modern Physics*, Vol.65, 1993, pp.851-1112.
- [104] P.J. Loughlin, M.S. Redfern, "Spectral Characteristics of Visually Induced Postural Sway in Healthy Elderly and Healthy Young Subjects", **IEEE Transactions on Neural Systems and**
- [105] K.S. Oie, T. Kiemel, J.J. Jeka, "Human Multisensory Fusion of Vision and Touch: Detecting Non-Linearity with Small Changes in the Sensory Environment", **Neuroscience Letters**, Vol.315, No.3, 2001, pp.113-116.
- [106] D.C. Montgomery and G.C. Runger, **Applied Statistics and Probability for Engineers**, New York: John Wiley & Sons, Inc., 1995.
- [107] S. C. Chapra and R. P. Canale, **Numerical Methods for Engineers**, New York: McGraw Hill, 2002.
- [108] A.M. Zoubir, D.R. Iskander, **Bootstrap Techniques for Signal Processing**, Cambridge, 2004.
- [109] B. Bigland-Ritchie, J.J. Woods, "Changes in muscle contractile properties and neural control during human muscular fatigue", **Muscle & Nerve**, Vol.7, No.9, 1984, pp.691-699.
- [110] R.B. Johnston, M.E. Howard, P.W. Cawley, G.M. Losse, "Effect of lower extremity muscular fatigue on motor control performance", **Medicine & Science in Sports & Exercise**, Vol.30, No.12, 1996, pp. 1703-1707.
- [111] M.L. Voight, J.A. Hardin, T.A. Blackburn, S. Tippett, G.C. Canner, "The effects of muscle fatigue on and the relationship of arm dominance to shoulder proprioception", **Journal of Orthopaedic & Sports Physical Therapy**, Vol.23, No. 6, 1996, pp.348-352.

[112] N. Vuillerme, N. Forestier, V. Nougier, “Attentional demands and postural sway: the effect of the calf muscles fatigue”, **Medicine & Science in Sports & Exercise**, Vol.34, No.12, 2002, pp.1907-1912.

[113] J. Tarantola, A. Nardonea, E. Tacchinia, M. Schieppatib, “Human stance stability improves with the repetition of the task: effect of foot position and visual condition”, **Neuroscience Letters**, Vol.228, 1997, pp.75–78.

[114] H. Whitney, “Differentiable manifolds”, **The Annals of Mathematics**, Vol.37, No.3, 1936, pp. 645-680.

APPENDIX A

RUN TEST DEMONSTRATION

In this Appendix, a demonstration of Run Test [75] (described in Chapter 2 Section 2.2.1.1.2) is presented. .

Step 1. 180-second (9000 data samples) CoP_x time series of the Subject 11 (first trial, F, 28) was presented in Figure 1.

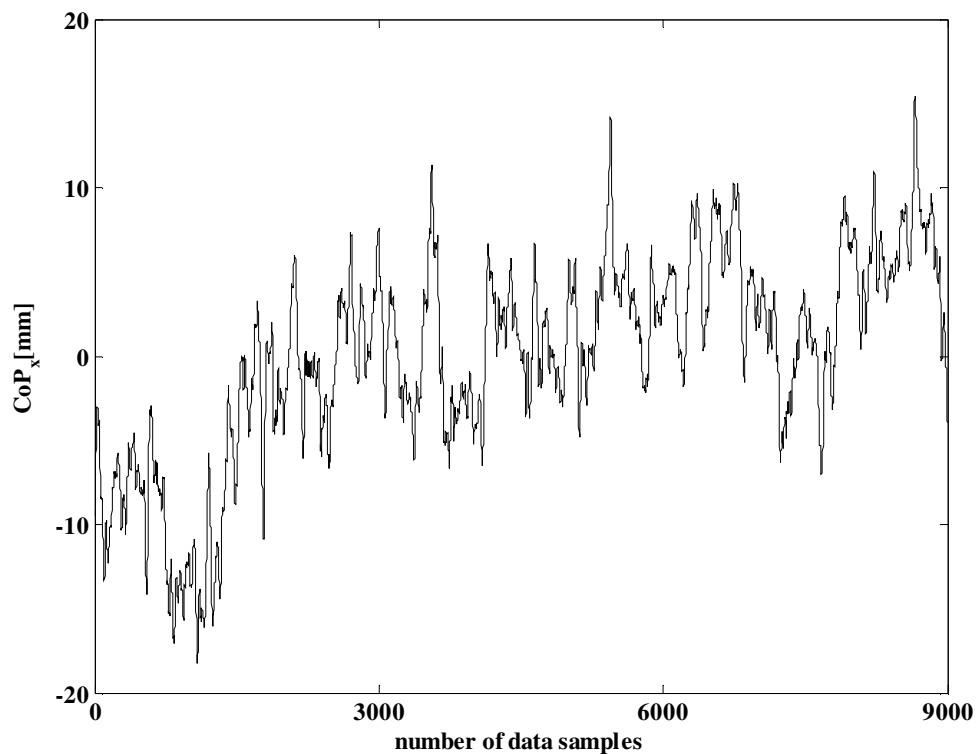


Figure 1. The CoP_x time series used in this Appendix.

Step 2. CoP_x signal was divided into 18 equal segments (Figure 2) each containing 10 second-long (500 data samples) data. The mean square of each segment (Ψ^2) was computed (Equation 1). Thus a series of 18 elements each being an estimate of the segmental mean square was computed (Equation (2)).

$$\Psi_r^2, r = 1 \dots 18 \quad (1)$$

$$\Psi_r^2 = \frac{1}{500} \sum_i^w X_i^2$$

where $i = (r-1) \cdot 500 + 1$, $w = r \cdot 500$, $r = 1 \dots 18$ (2)

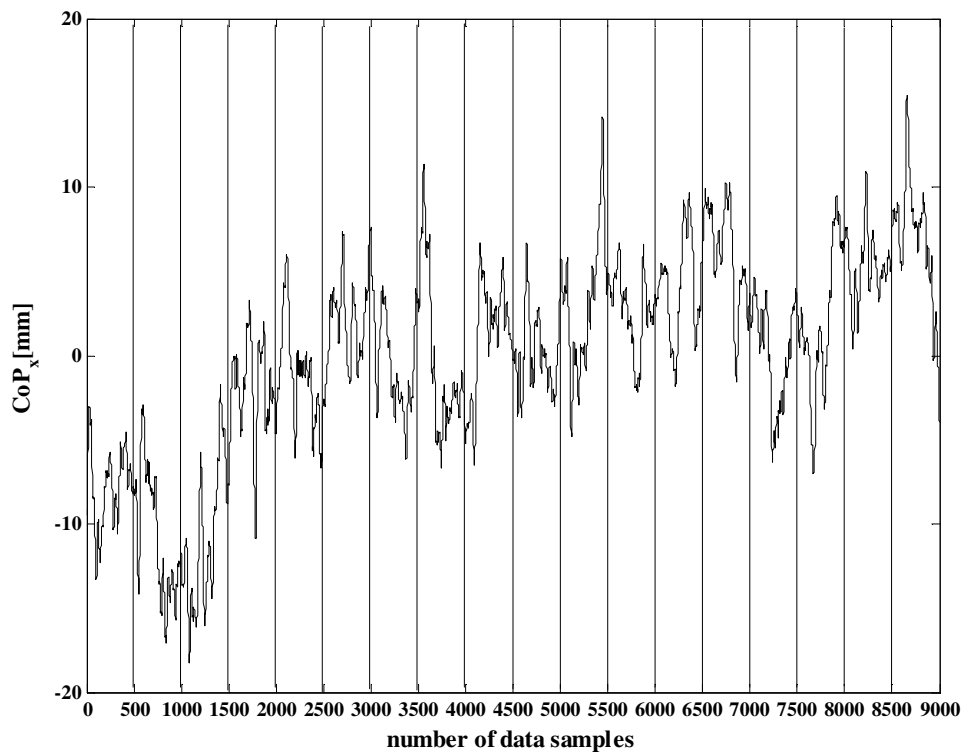


Figure 2. The segmented (18 segments) CoP_x time series

Step 3. The median of the series (Equation (1)) was calculated (Equation (3)). Then, for applying the non-parametric statistical Run Test, the elements of the series (Equation (1)), which are larger than the median of the series (Equation (3)) were marked with the symbol '+'; while the elements of the series, which are less than the median of the series were marked with the symbol '-' (Figure 3).

$$\text{median}(\Psi_r^2, r = 1 \dots 18) \tag{3}$$

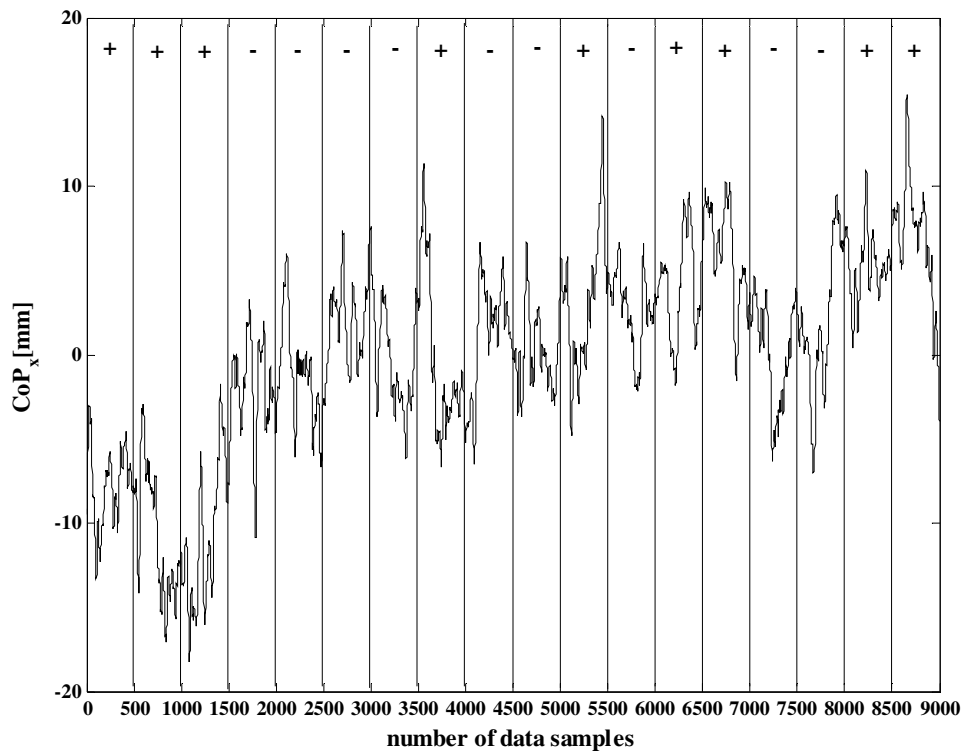


Figure 3. The marked (with the symbol '+' or '-') CoP_x time series

Step 4. Sequences of '+'s and '-'s were grouped separately and each group was counted as a *run*. By this way, the value of the *total run* was found. In this particular case the value of total run was 9 (Figure 4). So; by the Equation (2.8) (in Chapter 2 Section 2.2.1.1.2, for the explanation of the Equation refer to same Section as well), this particular CoP_x signal is stationary.

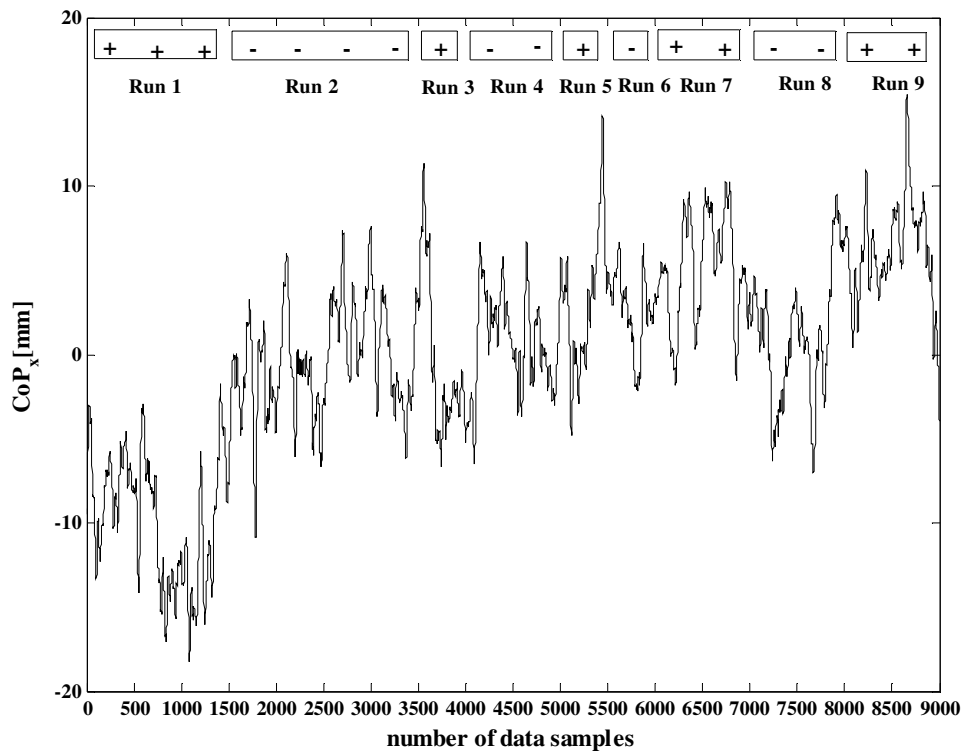


Figure 4. The grouped (by sequences of '+'s and '-'s) CoP_x time series

APPENDIX B

THE RUN DISTRIBUTION TABLE

The Run Distribution Table [75] is given in this Appendix.

Percentage Points of Run Distribution
 Values of $r_{n; \alpha}$ such that $\text{Prob} [r_n > r_{n; \alpha}] = \alpha$, where $n = N_1 = N_2 = N/2$

$n = N/2$	α					
	0.99	0.975	0.95	0.05	0.025	0.01
5	2	2	3	8	9	9
6	2	3	3	10	10	11
7	3	3	4	11	12	12
8	4	4	5	12	13	13
9	4	5	6	13	14	15
10	5	6	6	15	15	16
11	6	7	7	16	16	17
12	7	7	8	17	18	18
13	7	8	9	18	19	20
14	8	9	10	19	20	21
15	9	10	11	20	21	22
16	10	11	11	22	22	23
18	11	12	13	24	25	26
20	13	14	15	26	27	28
25	17	18	19	32	33	34
30	21	22	24	37	39	40
35	25	27	28	43	44	46
40	30	31	33	48	50	51
45	34	36	37	54	55	57
50	38	40	42	59	61	63
55	43	45	46	65	66	68
60	47	49	51	70	72	74
65	52	54	56	75	77	79
70	56	58	60	81	83	85
75	61	63	65	86	88	90
80	65	68	70	91	93	96
85	70	72	74	97	99	101
90	74	77	79	102	104	107
95	79	82	84	107	109	112
100	84	86	88	113	115	117

Source: Bendat and Piersol (1985), pp.532 [75]

APPENDIX C

ANOVA TEST

Analysis of variance (ANOVA) test was used in Chapter 3 Section 3.1. Here is presented the formal description of the test [106].

To compare several means, the analysis of variance (ANOVA) is a commonly used tool. The method can be described with a simple case – single factor experiment with replicates (repeated measures). The statistical linear model for a single effect (treatment) experiment is described in the Equation (1).

$$Y_{ij} = \mu + \tau_i + \varepsilon_{ij} \begin{cases} i = 1, 2, \dots, a \\ j = 1, 2, \dots, n \end{cases} \quad (1)$$

Y_{ij} is a random variable denoting the $(ij)^{\text{th}}$ observation, μ is the overall mean, τ_i is the i^{th} treatment effect, and ε_{ij} is the random error component. Also a and n indicate the number of levels of effect and replicates respectively.

The terms of μ and τ_i could be combined to define the mean of the i^{th} treatment (Equation (2)).

$$\mu_i = \mu + \tau_i \quad (2)$$

The treatment effect, τ_i is defined as deviation from the overall mean μ . So, it is apparent that sum of deviations from the overall mean μ is zero (Equation (3)).

$$\sum_{i=1}^a \tau_i = 0 \tag{3}$$

The main point of the analysis is testing the equality of the treatment means $\mu_1, \mu_2, \dots, \mu_a$. To search it, the null hypothesis can be stated by using Equations (2) and (3) such that; the treatment effect (τ_i) is equal to zero (Equation (4)).

$$H_0 = \tau_1 = \tau_2 = \dots = \tau_a = 0 \tag{4}$$

Data composed of N ($a \cdot n$) many observations should be arranged as in the Table 1 for the ANOVA test.

Table 1. The data layout for the ANOVA test

Treatment	Observations					Totals	Averages	
1	y_{11}	y_{12}	.	.	.	y_{1n}	$y_{1.}$	$\overline{y_{1.}}$
2	y_{21}	y_{22}	.	.	.	y_{2n}	$y_{2.}$	$\overline{y_{2.}}$
.
.
.
a	y_{a1}	y_{a1}	.	.	.	y_{an}	$y_{a.}$	$\overline{y_{a.}}$
							$y_{..}$	$\overline{y_{..}}$

3 sum of squares (SS) are computed for the test (Equation 5).

$$\begin{aligned}
SS_{total} &= \sum_{i=1}^a \sum_{j=1}^n y_{ij}^2 - \frac{y_{..}^2}{N} \\
SS_{treatments} &= \sum_{i=1}^a \frac{y_{i.}^2}{n} - \frac{y_{..}^2}{N} \\
SS_{error} &= SS_{total} - SS_{treatments}
\end{aligned} \tag{5}$$

Then the f_0 value is:

$$f_0 = \frac{SS_{treatments} / (a-1)}{SS_{error} / [a(n-1)]} \tag{6}$$

The null hypothesis is accepted if each observation consists of the overall mean μ and a realization of the random error ε_{ij} . The hypothesis is tested by the f_0 (Equation (6)) value (the measure of variability of the treatment) which is computed in the analysis and the F value comes from the F -distribution (a statistical distribution used for checking equality of variances) with proper level of significance (α) and degree of freedoms (related with the number of levels of treatment). Null hypothesis is rejected if the condition defined in Equation (7) satisfied.

$$f_0 > F \tag{7}$$

Also, p -value of the f_0 which is defined in Equation (6) must be less than a level of significance for rejection.

$$p = P(F_{a-1, a(n-1)} > f_0) < \alpha \tag{8}$$

The rejection of null hypothesis corresponds to that treatment means $\mu_1, \mu_2, \dots, \mu_a$ are significantly different.

The methodology can be extended the case: two main effects. The statistical linear model for two main effect (treatments) experiment is described in the Equation (9).

$$Y_{ij} = \mu + \tau_i + \beta_j + \varepsilon_{ij} \begin{cases} i = 1, 2, \dots, a \\ j = 1, 2, \dots, b \end{cases} \quad (9)$$

Y_{ij} is a random variable denoting the $(ij)^{\text{th}}$ observation, μ is the overall mean, τ_i is the i^{th} first treatment effect, β_j is the j^{th} second treatment effect, and ε_{ij} is the random error component. Also a and b indicate the number of levels of first and second treatments respectively. There are two null hypotheses (Equations (10) and (11)) and should be checked independently described above (Equation (7) and (8)).

$$H_0 = \tau_1 = \tau_2 = \dots = \tau_a = 0 \quad (10)$$

$$H_0 = \beta_1 = \beta_2 = \dots = \beta_b = 0 \quad (11)$$

The level of significance (α) was used as 0.05 in all ANOVA analysis in this study.

APPENDIX D

TRAPEZOID RULE

Trapezoid rule was used to compute the integrals in Equation (2.16) and (2.17) in Chapter 2 Section 2.2.1.2.2 by numerically. Here is presented the formal description of the rule [107].

Let $f(x)$ (Equation (1)) be the function considered. The definite integral in Equation (2) is to be approximated (grey area in Figure 1) by the trapezoid rule.

$$y = f(x) \tag{1}$$

$$I = \int_a^b f(x)dx \tag{2}$$

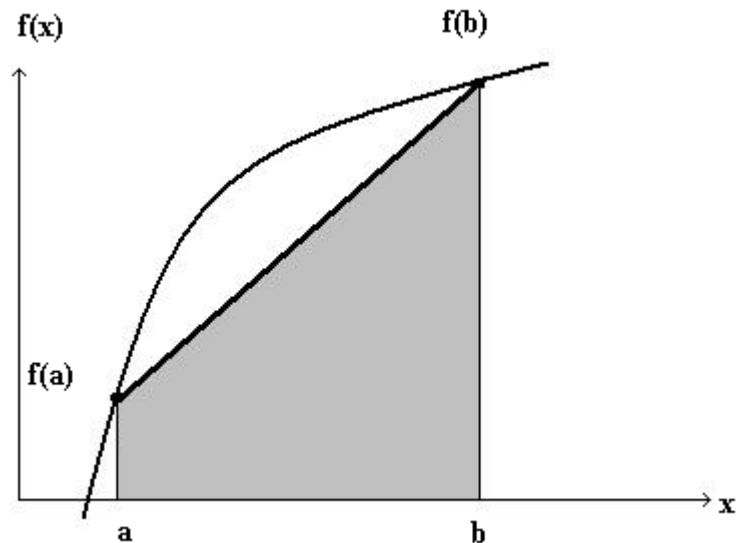


Figure 1. Graphical presentation of the trapezoidal rule

Then the estimate of the integral in Equation (2) is:

$$I \approx \frac{1}{2} \frac{f(a) + f(b)}{(b-a)} \quad (3)$$

In order to improve the estimate of the integral in Equation (2), the interval between a to b (Figure 1) should be divided into n pieces. Then the width of the each piece, h is:

$$h = \frac{b-a}{n} \quad (4)$$

Finally, the improved estimate for the integral defined in Equation (2) is:

$$I \approx \frac{h}{2} (f(a) + 2f(a+h) + 2f(a+2h) + \dots + 2f(a+(n-1)h) + f(b)) \quad (5)$$

APPENDIX E

DERIVATION OF THE SPECTRAL ESTIMATE

In order to evaluate Power Spectral Density estimates, the Welch's method was used in Chapter 2 Section 2.2.1.2.2. Here, the derivation of the spectral estimate ($\hat{P}(f)$), in Equation 2.16 and 2.17 in Chapter 2 Section 2.2.1.2.2) is given [78].

Step 1. Let $X(j)$, $j=0, \dots, N-1$ be a time series. The mean estimate of the series was assumed as zero and the spectral density was $P(f)$, $|f| \leq 1/2$. The overlapping length was L with the starting point D units apart for successive segments (K many segments).

$$\begin{aligned} X_1(j) &= X(j) & j &= 0, \dots, L-1 \\ X_2(j) &= X(j+D) & j &= 0, \dots, L-1 \\ X_K(j) &= X(j+(K-1)D) & j &= 0, \dots, L-1 \quad \text{and} \quad (K-1)D + L = N \end{aligned} \quad (1)$$

Step 2. For each segment, a modified periodogram was calculated (e.g., with a data window $W(j)$, $j=0, \dots, N-1$; the sequences was $X_1(j)W(j), \dots, X_K(j)W(j)$). Then the finite Fourier transforms of the sequences was taken (Equation (2)).

$$A_k(n) = \frac{1}{L} \sum_{j=0}^{L-1} X_k(j)W(j)e^{-2kijn/L} \quad \text{where} \quad i = \sqrt{-1} \quad (2)$$

Step 3. K modified periodograms were obtained (Equation (3)).

$$I_k(f_n) = \frac{L}{U} |A_k(n)|^2 \quad k = 1, 2, \dots, K$$

where $f_n = \frac{n}{L} \quad n = 0, \dots, L/2$ (3)

and $U = \frac{1}{L} \sum_{j=0}^{L-1} W^2(j)$

Step 4. Finally, the spectral estimate was the average of these periodograms.

$$\hat{P}(f_n) = \frac{1}{K} \sum_{k=1}^K I_k(f_n) \quad (4)$$

APPENDIX F

SIGN TEST

Sign test was used in Chapter 3 Section 3.1.1.4. Here is presented the formal description of the test [92].

The sign test is used to determine the difference between two conditions when only available information is the direction on differences. The null hypothesis of the test is given in Equation (1).

$$P[X_i > X_j] = P[X_i < X_j] = 1/2 \quad (1)$$

X_i (in Equation (1)) is the judgment (or score) under one condition and Y_i (in Equation (1)) is the judgment (or score) under the other condition. The direction of the differences was coded by the sign '+' or '-' for every X_i and Y_i . In order to be accepted the null hypothesis, the number of pairs $X_i > Y_i$ should be equal to the number of pairs $X_i < Y_i$. The probability of a condition on a particular number of '+'s and/or '-'s can be determined with the binomial distribution with $p=q=1/2$ (given in Table 1, next page).

Table 1. Binomial distribution for $p=q=1/2$

Table of probabilities associated with values as small as (or smaller than) observed values of k in the binomial test
 Given in the body of the table are one-tailed probabilities under H_0 for the binomial test when $p = q = 1/2$.

Entries are $P[Y \leq k]$. Note that entries may also be read as $P[Y \geq N - k]$

N	k																	
	0	1	2	3	4	5	6	7	8	9	10	11	12	13	14	15	16	17
4	0.62	312	688	938	1.0													
5	0.31	188	500	812	969	1.0												
6	0.16	109	344	656	891	984	1.0											
7	0.08	62	227	500	773	938	992	1.0										
8	0.04	35	145	363	637	855	965	996	1.0									
9	0.02	20	90	254	500	746	910	980	998	1.0								
10	0.01	11	55	172	377	623	828	945	989	999	1.0							
11		0.6	0.33	113	274	500	726	887	967	994	999+	1.0						
12		0.03	0.19	0.73	194	387	613	806	927	981	997	999+	1.0					
13		0.02	0.11	0.46	133	291	500	709	867	954	989	998	999+	1.0				
14		0.01	0.06	0.29	0.90	212	395	605	788	910	971	994	999	999+	1.0			
15			0.04	0.18	0.59	151	304	500	696	849	941	982	996	999+	999+	1.0		
16			0.02	0.11	0.38	105	227	402	598	773	895	962	989	998	999+	999+	1.0	
17			0.01	0.06	0.25	0.72	166	315	500	685	834	928	975	994	999	999+	999+	1.0
18			0.01	0.04	0.15	0.48	119	240	407	593	760	881	952	985	996	999	999+	999+
19				0.02	0.10	0.32	0.84	180	324	500	676	820	916	968	990	998	999+	999+
20				0.01	0.06	0.21	0.58	132	252	412	588	748	868	942	979	994	999	999+

Note: Decimal points omitted, and values less than .0005 are omitted.

Source: Siegel and Castellan (1988), pp.324-325 [92]

APPENDIX G

CONFIDENCE INTERVAL ESTIMATION BY BOOTSTRAPPING TECHNIQUE

Confidence interval estimation by bootstrapping technique was used in the study. Here is presented the formal description of the analysis [108].

Let X (Equation 1) be a random variable with n number of elements.

$$X = \{X_1, \dots, X_n\} \quad (1)$$

The confidence interval can be estimated by the principle of bootstrap by following steps:

- 1) Resample N number of bootstrap resample, X^* by replacement.
- 2) Calculate the mean, μ^* of each bootstrap resample, X^* .
- 3) Sort the means, μ^* s in ascending order.
- 4) The $100(1-\alpha)\%$ bootstrap confidence interval is $(\mu^*_{q_1}, \mu^*_{q_2})$ where $q_1=N\alpha/2$ and $q_2=N-q_1+1$. For example; for 95% confidence interval, $q_1=25$ and $q_2=976$; so the confidence interval is $(\mu^*_{25}, \mu^*_{976})$.

APPENDIX H

KRUSKAL-WALLIS TEST

Kruskal-Wallis test was used in Chapter 3 Section 3.2.2. Here is presented the formal description of the test [92].

Kruskal-Wallis is a one-way analysis of variance by using ranks but not the scores (in a parametric Analysis of Variance (ANOVA)) of k many independent groups from different populations. The test is used for searching significance difference between groups.

Data should be arranged as Table 1 for the analysis.

Table 1. The data layout for the Kruskal-Wallis test

Group				
1	2	3	...	k
X_{11}	X_{21}	...		X_{k1}
X_{21}	X_{22}	...		X_{k1}
\vdots				
X_{n_11}	...			\vdots
		...		X_{n_k1}
	X_{n_21}			

X_{ij} (Table 1) is the score for the i th observation in the j th group and the n_j is the number of the observations in the j th group. Each value in Table 1 should be replaced by ranks in this manner: smallest score is replaced by rank 1, the next smallest score

is replaced by rank 2, ... ,and largest score is replaced by rank N (total number of observations in the analysis).

The null hypothesis of the test is: $H_0 : \theta_1 = \theta_2 = \dots = \theta_k$ where θ_j is the median of the j th group. The null hypothesis is evaluated by computing Kruskal-Wallis statistics (Equation 1).

$$KW = \left[\frac{12}{N(N+1)} \sum_{j=1}^k n_j \bar{R}_j^2 \right] - 3(N+1) \quad (1)$$

where

k = number of groups

n_j = number of observation in the j th group

N = total number of observation in the analysis

R_j = sum of the ranks in the j th group

\bar{R}_j = average of the ranks in the j th group

\bar{R} = average of the ranks in the analysis (the grand mean)

If the number of the groups is equal or less than 3, then Table 2; if the number of the groups is larger than 3, then Table 3 is used to obtain critical value of KW to compare with the Kruskal-Wallis statistics computed by the Equation (1). If the critical value of KW (obtained from Table 2 or 3 for predefined n_j s and level of significance (α)) is equal or larger than the Kruskal-Wallis statistics computed by the Equation (1), then the null hypothesis cannot be rejected; if not the null hypothesis should be rejected.

Table 2. The critical values for KW

Critical values for the Kruskal-Wallis one-way analysis of variance by ranks statistic, KW

Sample sizes			α				
n_1	n_2	n_3	.10	.05	.01	.005	.001
2	2	2	4.25				
3	2	1	4.29				
3	2	2	4.71	4.71			
3	3	1	4.57	5.14			
3	3	2	4.56	5.36			
3	3	3	4.62	5.60	7.20	7.20	
4	2	1	4.50				
4	2	2	4.46	5.33			
4	3	1	4.06	5.21			
4	3	2	4.51	5.44	6.44	7.00	
4	3	3	4.71	5.73	6.75	7.32	8.00
4	4	1	4.17	4.97	6.67		
4	4	2	4.55	5.45	7.04	7.28	
4	4	3	4.55	5.60	7.14	7.59	8.30
4	4	4	4.65	5.69	7.66	8.00	8.65
5	2	1	4.20	5.00			
5	2	2	4.36	5.16	6.53		
5	3	1	4.02	4.96			
5	3	2	4.65	5.25	6.82	7.18	
5	3	3	4.53	5.65	7.08	7.51	8.24
5	4	1	3.99	4.99	6.95	7.36	
5	4	2	4.54	5.27	7.12	7.57	8.11
5	4	3	4.55	5.63	7.44	7.91	8.50
5	4	4	4.62	5.62	7.76	8.14	9.00
5	5	1	4.11	5.13	7.31	7.75	
5	5	2	4.62	5.34	7.27	8.13	8.68
5	5	3	4.54	5.71	7.54	8.24	9.06
5	5	4	4.53	5.64	7.77	8.37	9.32
5	5	5	4.56	5.78	7.98	8.72	9.68
Large samples			4.61	5.99	9.21	10.60	13.82

Note: The absence of an entry in the extreme tails indicates that the distribution may not take on the necessary extremes values.

Adapted from Table F in Kraft, C. H., and van Eeden, C., (1968). *A nonparametric introduction to statistics*. New York: Macmillan, with the permission of the publisher.

Source: Siegel and Castellan (1988), pp.356 [92]

Table 3. The critical values for KW by chi-square distribution

Critical values of the chi-square distribution*

df	Probability under H_0 that $\chi^2 \geq X^2$													
	.99	.98	.95	.90	.80	.70	.50	.30	.20	.10	.05	.02	.01	.001
1	.00016	.00063	.0039	.016	.064	.15	.46	1.07	1.64	2.71	3.84	5.41	6.64	10.83
2	.02	.04	.10	.21	.45	.71	1.39	2.41	3.22	4.60	5.99	7.82	9.21	13.82
3	.12	.18	.35	.58	1.00	1.42	2.37	3.66	4.64	6.25	7.82	9.84	11.34	16.27
4	.30	.43	.71	1.06	1.65	2.20	3.36	4.88	5.99	7.78	9.49	11.67	13.28	18.46
5	.55	.75	1.14	1.61	2.34	3.00	4.35	6.06	7.29	9.24	11.07	13.39	15.09	20.52
6	.87	1.13	1.64	2.20	3.07	3.83	5.35	7.23	8.56	10.64	12.59	15.03	16.81	22.46
7	1.24	1.56	2.17	2.83	3.82	4.67	6.35	8.38	9.80	12.02	14.07	16.62	18.48	24.32
8	1.65	2.03	2.73	3.49	4.59	5.53	7.34	9.52	11.03	13.36	15.51	18.17	20.09	26.12
9	2.09	2.53	3.32	4.17	5.38	6.39	8.34	10.66	12.24	14.68	16.92	19.68	21.67	27.88
10	2.56	3.06	3.94	4.86	6.18	7.27	9.34	11.78	13.44	15.99	18.31	21.16	23.21	29.59
11	3.05	3.61	4.58	5.58	6.99	8.15	10.34	12.90	14.63	17.28	19.68	22.62	24.72	31.26
12	3.57	4.18	5.23	6.30	7.81	9.03	11.34	14.01	15.81	18.55	21.03	24.05	26.22	32.91
13	4.11	4.76	5.89	7.04	8.63	9.93	12.34	15.12	16.98	19.81	22.36	25.47	27.69	34.53
14	4.66	5.37	6.57	7.79	9.47	10.82	13.34	16.22	18.15	21.06	23.68	26.87	29.14	36.12
15	5.23	5.98	7.26	8.55	10.31	11.72	14.34	17.32	19.31	22.31	25.00	28.26	30.58	37.70
16	5.81	6.61	7.96	9.31	11.15	12.62	15.34	18.42	20.46	23.54	26.30	29.63	32.00	39.29
17	6.41	7.26	8.67	10.08	12.00	13.53	16.34	19.51	21.62	24.77	27.59	31.00	33.41	40.75
18	7.02	7.91	9.39	10.86	12.86	14.44	17.34	20.60	22.76	25.99	28.87	32.35	34.80	42.31
19	7.63	8.57	10.12	11.65	13.72	15.35	18.34	21.69	23.90	27.20	30.14	33.69	36.19	43.82
20	8.26	9.24	10.85	12.44	14.58	16.27	19.34	22.78	25.04	28.41	31.41	35.02	37.57	45.32
21	8.90	9.92	11.59	13.24	15.44	17.18	20.34	23.86	26.17	29.62	32.67	36.34	38.93	46.80
22	9.54	10.60	12.34	14.04	16.31	18.10	21.24	24.94	27.30	30.81	33.92	37.66	40.29	48.27
23	10.20	11.29	13.09	14.85	17.19	19.02	22.34	26.02	28.43	32.01	35.17	38.97	41.64	49.73
24	10.86	11.99	13.85	15.66	18.06	19.94	23.34	27.10	29.55	33.20	36.42	40.27	42.98	51.18
25	11.52	12.70	14.61	16.47	18.94	20.87	24.34	28.17	30.68	34.38	37.65	41.57	44.31	52.62
26	12.20	13.41	15.38	17.29	19.82	21.79	25.34	29.25	31.80	35.56	38.88	42.86	45.64	54.05
27	12.88	14.12	16.15	18.11	20.70	22.72	26.34	30.32	32.91	36.74	40.11	44.14	46.96	55.48
28	13.56	14.85	16.93	18.94	21.59	23.65	27.34	31.39	34.03	37.92	41.34	45.42	48.28	56.89
29	14.26	15.57	17.71	19.77	22.48	24.58	28.34	32.46	35.14	39.09	42.56	46.69	49.59	58.30
30	14.95	16.31	18.49	20.60	23.36	25.51	29.34	33.53	36.25	40.26	43.77	47.96	50.89	59.70

* Table C is abridged from Table IV of Fisher and Yates: *Statistical tables for biological, agricultural, and medical research*, published by Longman Group UK Ltd., London (previously published by Oliver and Boyd Ltd., Edinburgh) and by permission of the authors and publishers.

Source: Siegel and Castellan (1988), pp.323 [92]

APPENDIX I

DERIVATION OF SURROGATE DATA WITH PHASE RANDOMIZATION

The author's version for the proof of the derivation of surrogate data with phase randomization is presented in this Appendix.

A periodic function $x(t)$ with period T could be represented by trigonometric series:

$$x(t) = a_0 + 2 \cdot \sum_{k=1}^{\infty} \left(a_k \cos \frac{2\pi kt}{T} + b_k \sin \frac{2\pi kt}{T} \right) \quad (1)$$

where a_0 and a_k and b_k are constant Fourier coefficients given by:

$$\begin{aligned} a_0 &= \frac{1}{T} \int_0^T x(t) dt \\ a_k &= \frac{1}{T} \int_0^T x(t) \cos \frac{2\pi kt}{T} dt \\ b_k &= \frac{1}{T} \int_0^T x(t) \sin \frac{2\pi kt}{T} dt \end{aligned} \quad (2)$$

If the mean value of $x(t)$ is zero then a_0 will be zero. Equation (2) can be combined into a single equation by defining:

$$X_k = a_k - ib_k \quad (3)$$

And putting:

$$e^{-i(2\pi kt/T)} = \cos \frac{2\pi kt}{T} - i \sin \frac{2\pi kt}{T} \quad (4)$$

to give:

$$X_k = \frac{1}{T} \int_0^T x(t) e^{-i(2\pi kt/T)} dt \quad (5)$$

If $x(t)$ is not known and only equally spaced samples are available as in an experimental time series which was represented by the discrete series $\{x_r\}$, $r = 0, 1, 2, \dots, (N-1)$, where $t = r\Delta$ and $\Delta = T/N$.

Then the integral in the equation (5) may be replaced approximately by the summation:

$$X_k = \frac{1}{T} \sum_{r=0}^{N-1} x_r e^{-i(2\pi k/T)(r\Delta)} \Delta \quad (6)$$

Substituting $T = N\Delta$ into the equation (6) gives:

$$X_k = \frac{1}{N} \sum_{r=0}^{N-1} x_r e^{-i(2\pi kr/N)} \quad (7)$$

To obtain phase randomized surrogate data described by Theiler et al (1992) which was used in Modeling Chapter, each X_k multiplied by $e^{i\phi_k}$ where ϕ_k is independently chosen from the interval $[0, 2\pi]$.

$$X_{k,r} = \frac{1}{N} \sum_{r=0}^{N-1} x_r e^{-i(2\pi kr/N)} e^{i\phi_k} \quad (8)$$

By applying substitutions $T = N\Delta$, $t = r\Delta$ and $\Delta = T/N$ inversely equation (8) can be written in the integral form as:

$$X_{k,r} = \frac{1}{T} \int_0^T x(t) e^{-i(2\pi kt/T - \phi_k)} dt \quad (9)$$

Also equation (9) can be written in open form as follows:

$$\begin{aligned} a_{k,r} &= \frac{1}{T} \int_0^T x(t) \cos\left(\frac{2\pi kt}{T} - \phi_k\right) dt \\ b_{k,r} &= \frac{1}{T} \int_0^T x(t) \sin\left(\frac{2\pi kt}{T} - \phi_k\right) dt \end{aligned} \quad (10)$$

Using trigonometric identities:

$$\begin{aligned} \cos(\alpha - \beta) &= \cos \alpha \cdot \cos \beta + \sin \alpha \cdot \sin \beta \\ \sin(\alpha - \beta) &= \sin \alpha \cdot \cos \beta - \sin \beta \cdot \cos \alpha \end{aligned} \quad (11)$$

Equation (10) could be expanded in a form

$$\begin{aligned} a_{k,r} &= \frac{1}{T} \int_0^T x(t) \left[\cos \frac{2\pi kt}{T} \cdot \cos \phi_k + \sin \frac{2\pi kt}{T} \cdot \sin \phi_k \right] dt \\ b_{k,r} &= \frac{1}{T} \int_0^T x(t) \left[\sin \frac{2\pi kt}{T} \cdot \cos \phi_k - \cos \frac{2\pi kt}{T} \cdot \sin \phi_k \right] dt \end{aligned} \quad (12)$$

Equation (12) could be further manipulated as ϕ_k is independent of “t”.

$$\begin{aligned}
a_{k,r} &= \cos \phi_k \cdot \frac{1}{T} \int_0^T x(t) \cos \frac{2\pi kt}{T} dt + \sin \phi_k \cdot \frac{1}{T} \int_0^T x(t) \sin \frac{2\pi kt}{T} dt \\
b_{k,r} &= \cos \phi_k \cdot \frac{1}{T} \int_0^T x(t) \sin \frac{2\pi kt}{T} dt - \sin \phi_k \cdot \frac{1}{T} \int_0^T x(t) \cos \frac{2\pi kt}{T} dt
\end{aligned} \tag{13}$$

Using equation (2), one can write equation (13) as:

$$\begin{aligned}
a_{k,r} &= \cos \phi_k \cdot a_k + \sin \phi_k \cdot b_k \\
b_{k,r} &= \cos \phi_k \cdot b_k - \sin \phi_k \cdot a_k
\end{aligned} \tag{14}$$

Then, periodic function $x(t)$ with period T could be written with new coefficients:

$$x(t) = a_0 + 2 \cdot \sum_{k=1}^{\infty} \left(\begin{aligned} &(\cos \phi_k \cdot a_k + \sin \phi_k \cdot b_k) \cdot \cos \frac{2\pi kt}{T} + \\ &(\cos \phi_k \cdot b_k - \sin \phi_k \cdot a_k) \cdot \sin \frac{2\pi kt}{T} \end{aligned} \right) \tag{15}$$

Equation (15) expanded and manipulated as:

$$x(t) = a_0 + 2 \cdot \sum_{k=1}^{\infty} \left[\begin{aligned} &a_k \left(\cos \frac{2\pi kt}{T} \cdot \cos \phi_k - \sin \frac{2\pi kt}{T} \cdot \sin \phi_k \right) + \\ &b_k \left(\sin \frac{2\pi kt}{T} \cdot \cos \phi_k + \cos \frac{2\pi kt}{T} \cdot \sin \phi_k \right) \end{aligned} \right] \tag{16}$$

Using trigonometric identities

$$\begin{aligned}
\cos \alpha \cdot \cos \beta - \sin \alpha \cdot \sin \beta &= \cos(\alpha + \beta) \\
\sin \alpha \cdot \cos \beta + \cos \alpha \cdot \sin \beta &= \sin(\alpha + \beta)
\end{aligned} \tag{17}$$

Equation (16) take its final form:

$$x(t) = a_0 + 2 \cdot \sum_{k=1}^{\infty} \left[a_k \cos\left(\frac{2\pi kt}{T} + \phi_k\right) + b_k \sin\left(\frac{2\pi kt}{T} + \phi_k\right) \right] \quad (18)$$

It concludes derivation of surrogate data with phase randomization.

APPENDIX J

THE KNOWLEDGE ABOUT THE SUBJECTS

Subject 1: 6 years old. Female. Experimented at 27.07.2007. No evidence of a motor disorder. She was attending the sport and art summer school for children organized by METU in 2007. After the experiments, she said “I got tired. I didn’t feel comfortable. I held my attention on not stepping and not making head movement.”

Subject 2: 7 years old. Male. Experimented at 09.08.2007. No evidence of a motor disorder. He was attending the sport and art summer school for children organized by METU in 2007. He has just finished first grade of primary school. After the experiments, he said “I didn’t get tired. I felt itching due to sweating.”

Subject 3: 9 years old. Male. Experimented at 27.07.2007. No evidence of a motor disorder. He was attending the sport and art summer school for children organized by METU in 2007. After the experiments, he said “I didn’t get tired. I paid my attention on the pattern at the wall.”

Subject 4: 10 years old. Male. Experimented at 06.08.2007. No evidence of a motor disorder. He was attending the tennis club in METU for 3 years. After the experiments, he said “I got a bit tired. I paid attention to my arm. I got bored.”

Subject 5: 11 years old. Female. Experimented at 27.07.2007. No evidence of a motor disorder. She was attending the sport and art summer school for children organized by METU in 2007. After the experiments, she said “I didn’t get tired. I didn’t think so much during the experiments. I looked at a point on the wall. I felt comfortable while standing.”

Subject 6: 14 years old. Male. Experimented at 27.07.2007. No evidence of a motor disorder. He was attending the sport and art summer school for children organized by METU in 2007. After the experiments, he said “I didn’t get tired. I looked at a pattern on the wall.”

Subject 7: 14 years old. Female. Experimented at 17.08.2007. No evidence of a motor disorder. She was attending the sport and art summer school for children organized by METU in 2007. After the experiments, she said “I didn’t get tired. I sang in my mind during the third trial. I thought about different things in my mind during the other trials.”

Subject 8: 21 years old. Male. Experimented at 01.08.2007. No evidence of a motor disorder. He was an undergraduate student at METU in 2007. He was not doing sport in a regular base. After the experiments, he said “I got tired. I tried not to move too much.”

Subject 9: 25 years old. Female. Experimented at 25.07.2007. No evidence of a motor disorder. She was an academic personnel at METU in 2007. She was not doing sport in a regular base. After the experiments, she said “I didn’t get tired. I tried not to move too much. I looked forward. I tried to focus.”

Subject 10: 27 years old. Female. Experimented at 02.08.2007. No evidence of a motor disorder. She was an academic personnel at METU in 2007. She was not doing sport in a regular base. After the experiments, she said “I got a bit tired. I got bored. I counted numbers in my mind. I paid attention to the pattern on the wall.”

Subject 11: 28 years old. Female. Experimented at 24.07.2007. No evidence of a motor disorder. She was academic personnel of METU in 2007. She was an athlete.

After the experiments, she said “I got tired. I got bored. I paid attention on my breathing.”

Subject 12: 31 years old. Male. Experimented at 31.07.2007. No evidence of a motor disorder. He was an academic personnel at METU in 2007. He was not doing sport in a regular base. After the experiments, he said “I got a bit tired. I had my attention on standing upright without moving. I tried to look at the same point on the wall.”

Subject 13: 35 years old. Female. Experimented at 02.07.2007. No evidence of a motor disorder. She was an academic personnel at METU in 2007. She was not doing sport in a regular base. After the experiments, she said “I didn’t get tired. I got attention to the pattern on the wall. I didn’t feel very comfortable.”

Subject 14: 39 years old. Male. Experimented at 21.08.2007. No evidence of a motor disorder. He was an academic personnel at METU in 2007. He was an athlete. After the experiments, he said “I didn’t get tired. I have always tried to stand upright and look forward straightly.”

Subject 15: 41 years old. Female. Experimented at 01.04.2008. No evidence of a motor disorder. She was an administrative personnel at METU in 2007. She was not doing sport in a regular base. After the experiments, she said “I didn’t get tired. I got attention to the pattern on the wall.”

Subject 16: 42 years old. Male. Experimented at 02.04.2008. No evidence of a motor disorder. He was an academic personnel at METU in 2007. He was an athlete. After the experiments, he said “I didn’t get tired. I tried to look at the same point on the wall.”

Subject 17: 43 years old. Female. Experimented at 16.08.2007. No evidence of a motor disorder. She was not doing sport in a regular base. After the experiments, she said “I didn’t get tired. I looked at the same point on the wall.”

Subject 18: 54 years old. Female. Experimented at 11.08.2007. No evidence of a motor disorder. She was not doing sport in a regular base. After the experiments, she said “I didn’t get tired. I felt like a pendulum.”

Subject 19: 48 years old. Male. Experimented at 19.07.2007. No evidence of a motor disorder. He was an academic personnel at METU in 2007. He was walking in a regular base. After the experiments, he said “I didn’t get tired. I had my attention on the eye movements, breathing, swallowing, and hand movements.”

Subject 20: 50 years old. Male. Experimented at 20.08.2007. No evidence of a motor disorder. He was not doing sport in a regular base. After the experiments, he said “I got a bit tired. I got attention to the pattern on the wall. I sang in my mind and also counted numbers.”

Subject 21: 55 years old. Female. Experimented at 02.04.2008. No evidence of a motor disorder. She was not doing sport in a regular base. After the experiments, she said “I didn’t get tired. I got attention to look forward.”

Subject 22: 65 years old. Female. Experimented at 04.04.2008. No evidence of a motor disorder. She was not doing sport in a regular base. She didn’t have a chronic illness. After the experiments, she said “I didn’t get tired. I looked the same point in the wall.”

Subject 23: 65 years old. Male. Experimented at 03.04.2008. No evidence of a motor disorder. He was an academic personnel at METU in 2008. He was not doing sport in

a regular base. He didn't have a chronic illness. After the experiments, he said "I didn't get tired. I had attention on oscillations."

Subject 24: 68 years old. Male. Experimented at 03.04.2008. No evidence of a motor disorder. He was not doing sport in a regular base. He didn't have a chronic illness. He was using anti-depressant drugs. After the experiments, he said "I didn't get tired. I looked at the wall."

Subject 25: 73 years old. Male. Experimented at 04.04.2008. No evidence of a motor disorder. He was not doing sport in a regular base. He didn't have a chronic illness. After the experiments, he said "I didn't get tired. I had attention on standing upright."

Subject 26: 78 years old. Male. Experimented at 20.08.2007. No evidence of a motor disorder. He was not doing sport in a regular base. He didn't have a chronic illness. He was using anti-hypertension drugs. After the experiments, he said "I didn't get tired. I looked the same point in the wall."

Subject 27: 83 years old. Female. Experimented at 20.08.2007. No evidence of a motor disorder. She was not doing sport in a regular base. She didn't have a chronic illness. She had had a lung surgery ten years ago. She was using drugs for ulcerative colitis. After the experiments, she said "I didn't get tired. I got attention on my balance. I counted numbers in my mind."

Subject 28: 84 years old. Female. Experimented at 11.08.2007. No evidence of a motor disorder. She was not doing sport in a regular base. She had an anxiety disorder which is under control. She was using anti-hypertension drugs. After the experiments, she said "I didn't get tired. I always looked forward. I felt that the platform is moving."

APPENDIX K

ALTERNATIVE ALGORITHM FOR CONVERGENCE

In order to define a criterion for convergence of the D_2 estimate curves (Figure 1), the following alternative algorithm has also been developed in the study:

Step 1. The slope of D_2 estimate curves (Figure 2) were calculated on 11 intervals as being $m=2-m=3$, $m=3-m=4$, $m=4-m=5$, $m=5-m=6$, $m=6-m=8$, $m=8-m=9$, $m=9-m=10$, $m=10-m=12$, $m=12-m=15$, $m=15-m=18$, $m=18-m=20$ for 140 trials. The intervals were called as “ m index”; such as m index of the interval $m=2-m=3$ is 1, m index of the interval $m=3-m=4$ is 2, and goes on.

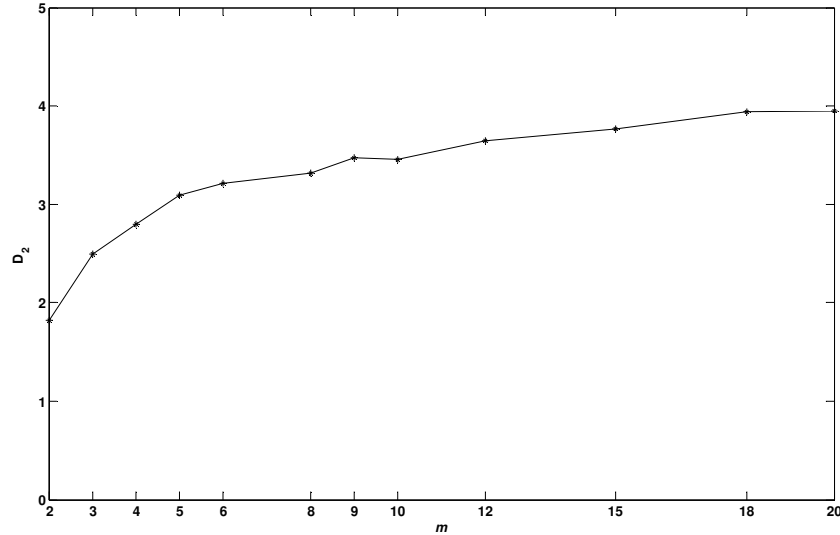


Figure 1. D_2 estimate curve of the Subject 11, trial 1

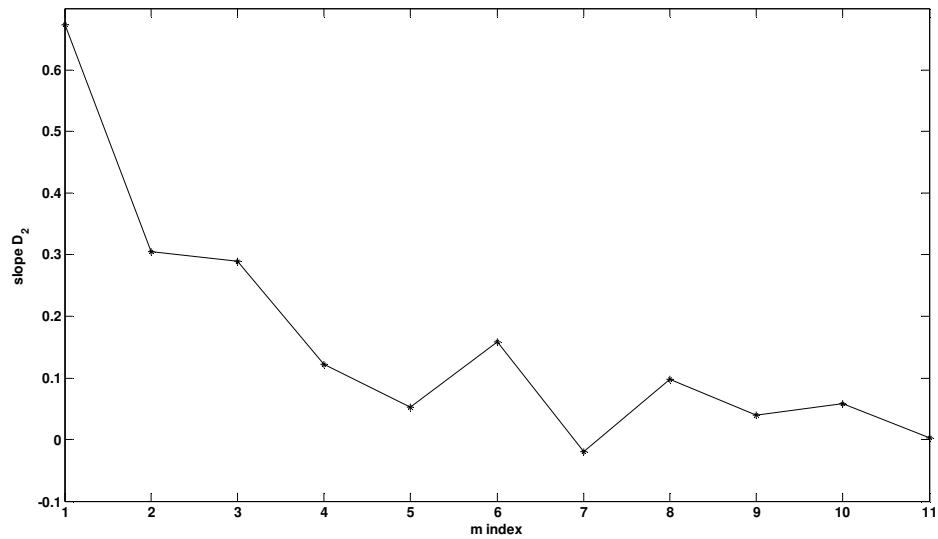


Figure 2. Slope of D_2 estimate curve of the Subject 11, trial 1

Step 2. The slope values of D_2 estimate curves were normalized with respect to the initial value of the slope of the D_2 estimate curve of corresponding trial at m index = 1 (Figure 3(a)).

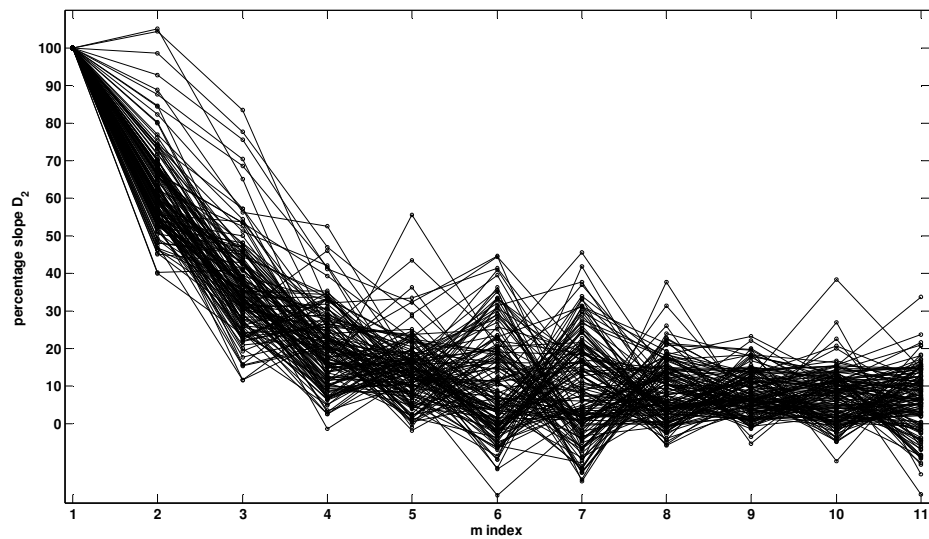


Figure 3(a). The percentage slope values of D_2 estimate curves

Step 3. The percentage slope values of D_2 estimate curves of each trial of each subject were fitted to the exponential model (Equation (1)), where a and b are the two constants of the model. The reason of modeling with an exponential model was to smooth the percentage slope values of D_2 estimate curves. The constants were calculated by using the built-in function, “fit” of the software Matlab[®].

$$\text{percentage slope values of } D_2 \text{ estimate curves} = a \cdot e^{b \cdot m \text{ index}} \quad (1)$$

Step 4. Interpolated values of modeled percentage slopes of D_2 estimate curves were computed at each m index and (Figure 3(b)) by using Equation (1). Then, mean (μ), standard deviation (σ), and coefficient of variation (CoV) values (Equation (2)) of interpolated slopes at each m index were calculated (Table 1(a)).

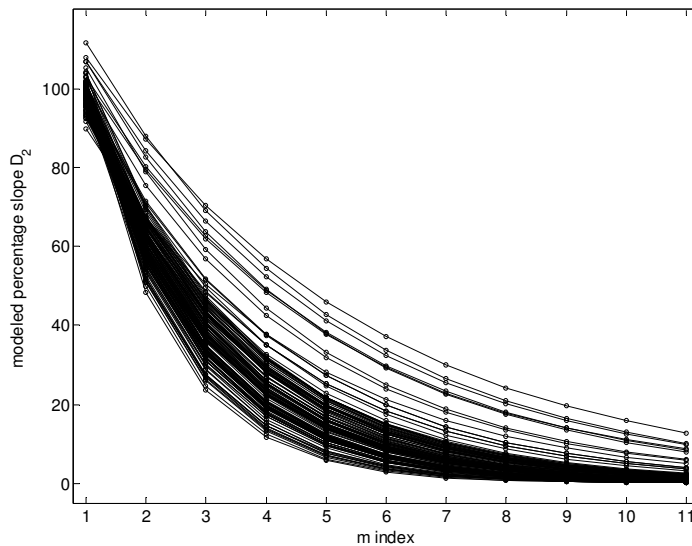


Figure 3(b). The modeled percentage slopes of D_2 estimate curves

$$\text{CoV} = \sigma / \mu * 100 \quad (2)$$

As seen from Table 1(a), coefficient of variation values of modeled percentage slope of D_2 estimate curves became larger than 50% starting from m index = 6, which indicates that standard deviation and mean values are compatible in terms of magnitude [93]. It is then proposed that the saturation point for D_2 estimate curves start from m index = 6 (interval within $m=8$ and $m=9$).

Table 1(a). Mean (μ), standard deviation (σ), and coefficient of variation (CoV) values of modeled percentage slopes of D_2 estimate curves for varying m index.

m index	μ	σ	CoV
1	98.8	3.2	3.2
2	62	7	11.3
3	39.3	8.6	21.9
4	25.2	8.4	33.3
5	16.3	7.4	45.4
6	10.7	6.2	57.9
7	7.1	5.1	71.8
8	4.7	4.1	87.2
9	3.2	3.3	103.1
10	2.2	2.6	118.2
11	1.5	2.1	140.0

Step 5. 95% confidence interval (CI) of the interpolated values of modeled percentage slopes of D_2 estimate curves at each m index was computed by the method of bootstrapping (Appendix G) (Table 1(b)).

Table 1(b). The 95% confidence intervals of the interpolated values of modeled percentage slopes of D_2 estimate curves for varying m index

	95% CI	
<i>m</i> index	Lower Band	Upper Band
1	98.20	99.28
2	60.80	63.21
3	37.88	40.88
4	23.81	26.56
5	15.12	17.57
6	9.67	11.90
7	6.26	8.05
8	4.11	5.51
9	2.72	3.86
10	1.82	2.68
11	1.20	1.94

Then the saturation criterion can be defined as: D_2 estimate curves has been accepted as “saturated” if the interpolated values of modeled percentage slopes of D_2 estimate curves at m index=6 is less than 11.90% (the upper band value of 95% confidence interval of the interpolated values of modeled percentage slopes of D_2 estimate curves at m index=6, refer to Step 3,4,5). Results of the saturation test are presented in Table 2. 93 out of 136 trials passed the saturation test and named as saturated trials.

Table 2. Results of the Saturation Test

Subjects	T1	t2	t3	t4	t5
1	1	1	0	1	1
2	1	1	1	1	1
3	1	0	1	1	1
4	0	0	1	1	0
5	1	n	1	1	1
6	1	1	1	0	1
7	0	1	0	1	n
8	0	0	0	0	1
9	0	0	0	0	1
10	1	1	1	1	1
11	1	1	1	1	1
12	1	1	1	1	1
13	0	0	1	1	1
14	0	0	0	0	0
15	1	1	1	1	1
16	0	1	1	1	1
17	1	1	1	1	1
18	1	1	1	1	1
19	0	1	1	1	1
20	0	1	1	1	1
21	1	1	1	1	1
22	1	0	0	0	0
23	0	0	0	0	n
24	1	n	1	1	1
25	0	0	1	0	1
26	1	1	0	1	1
27	1	1	1	1	1
28	0	0	0	0	0

‘1’ indicates the trials which saturated, ‘0’ indicates the trials which did not saturate, ‘n’ indicates non-stationary trials

Step 6. The D_2 estimate curves were fitted to the double exponential model (due to poor fit of one exponential model, Figure 4(a)) defined in Equation (3) for each of 93 saturated trials (Figure 4(b)). The constants (a, b, c, d) were calculated by using the built-in function, “fit” of the software Matlab[®].

$$D_2 = a \cdot e^{b \cdot m} + c \cdot e^{d \cdot m} \quad (3)$$

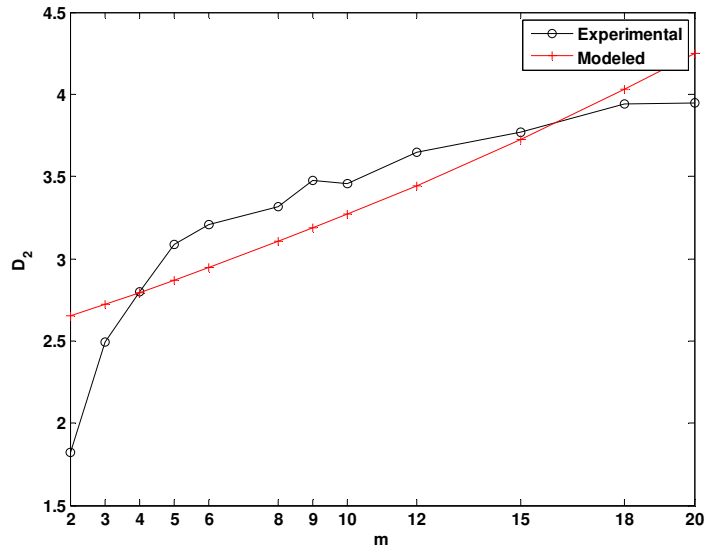


Figure 4(a). D_2 estimate curve (poor fit of one exponential model) of the Subject 11, trial 1

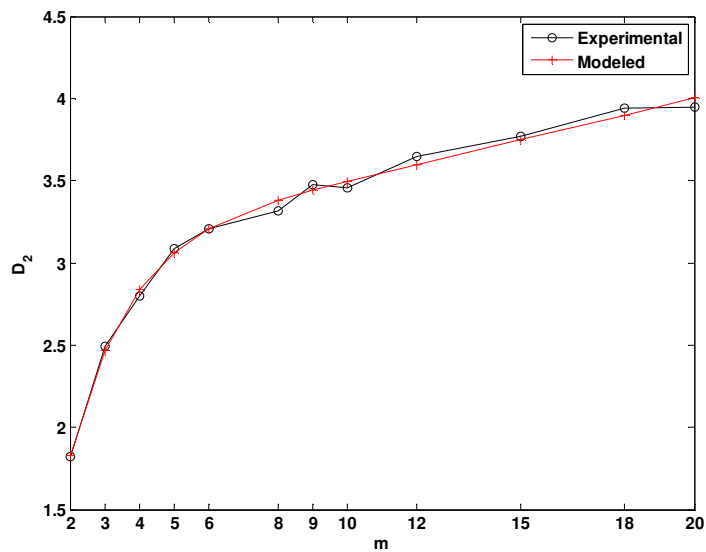


Figure 4(b). D_2 estimate curve (experimental and modeled by Equation (3)) of the Subject 11, trial 1

Step 7. The values of D_2 estimate from $m=9$ to $m=20$ (as the D_2 estimate converged starting from $m=9$) was fitted to a line (linear regression, Figure 5) to look for a linear trend by convergence criterion (next paragraph). The equation of line is defined in

Equation (4). Similarly, the constants a and b were calculated by using the built-in function, “fit” of the software Matlab[®].

$$D_2 = a \cdot m + b \tag{4}$$

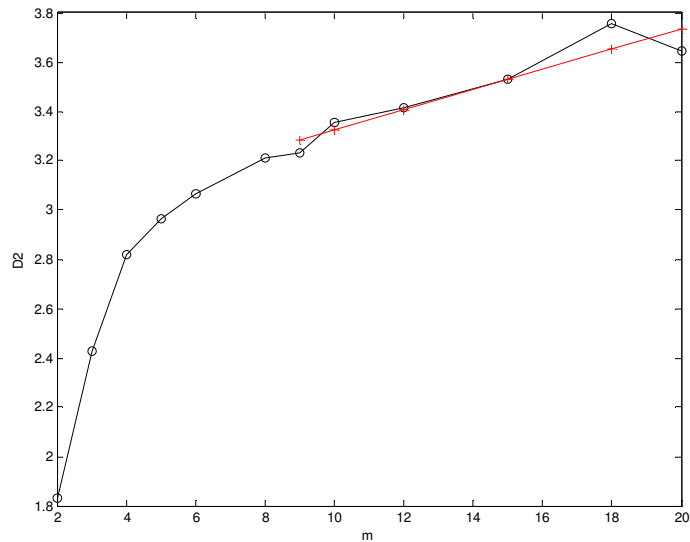


Figure 5. D_2 estimate curve of 1st trial of 1st subject (black line), fitted line (red line)

The convergence criterion is then defined as: D_2 estimate curves are accepted as “converged” if the slope of the fitted line to D_2 estimates from $m=9$ to $m=20$ (a in Equation (4)) is less than slope of the double exponentially modeled D_2 estimates at m index=6 ($m=8-m=9$). The convergence test has been applied to only the trials that possess stationary CoP_x signal characteristics and passed the saturation test. By this method, 70 out of 140 trials passed the convergence test. Mapping of the trials according to the algorithm was given in Table 3.

Table 3. Mapping of the convergence algorithm for trials

Subjects	t1	t2	t3	t4	t5
1	c	c	ns	c	c
2	c	c	nc	nc	c
3	c	ns	nc	c	c
4	ns	ns	nc	c	ns
5	nc	n	nc	nc	nc
6	c	nc	c	ns	nc
7	ns	c	ns	c	n
8	ns	ns	ns	ns	c
9	ns	ns	ns	ns	nc
10	c	c	c	nc	c
11	c	c	c	c	nc
12	c	c	c	c	c
13	ns	ns	nc	nc	c
14	ns	ns	ns	ns	ns
15	c	c	c	c	c
16	ns	c	c	c	c
17	c	c	c	c	c
18	c	c	c	c	c
19	ns	nc	nc	c	c
20	ns	c	c	c	nc
21	c	c	nc	c	nc
22	c	ns	ns	ns	ns
23	ns	ns	ns	ns	n
24	c	n	nc	c	c
25	ns	ns	c	ns	nc
26	c	c	ns	c	c
27	c	c	c	c	nc
28	ns	ns	ns	ns	ns

‘n’ indicates non-stationary trials, ‘ns’ indicates stationary but not-saturated trials, ‘nc’ indicates stationary, saturated but not converged trials, ‘c’ indicates stationary, saturated and converged trials

Figures 6 – 33 show computed D_2 estimates for varying embedding dimensions, m of each subjects’ first, second, third, fourth, and fifth trials. The non-stationary trials showed red in color and circular markers; the stationary but not-saturated trials were green in color with plus markers; the stationary, saturated but not converged trials were blue in color with square markers; and the stationary, saturated and converged trials were black in color with diamond markers for the Figures 6 – 33.

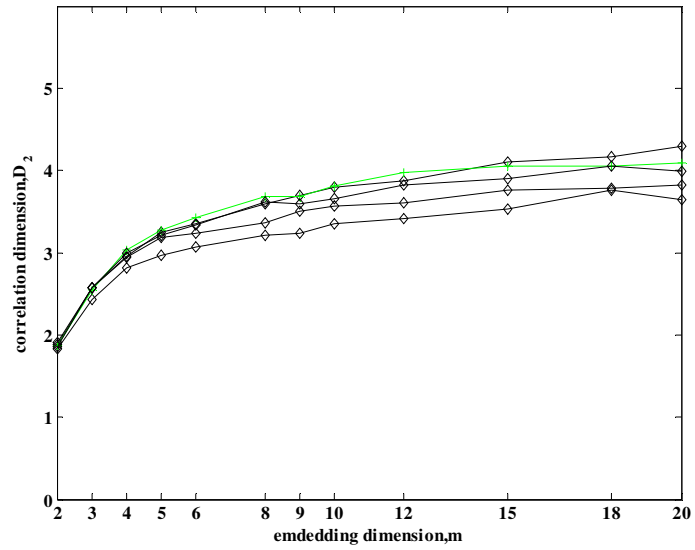


Figure 6. Computed D_2 estimates of Subject 1 for varying m

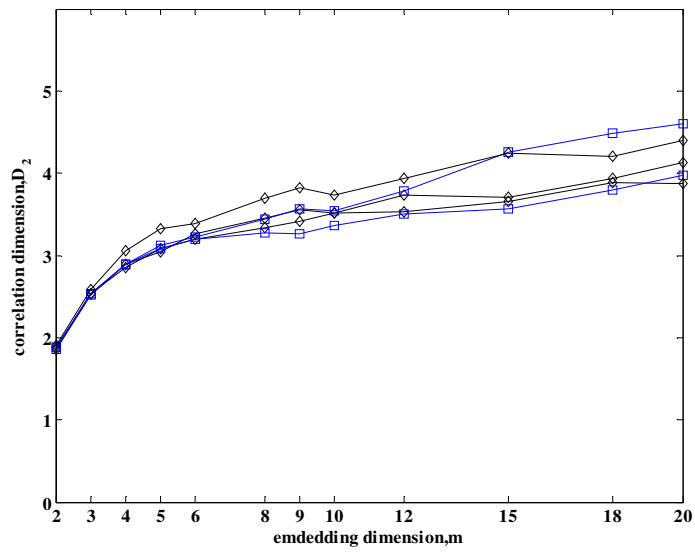


Figure 7. Computed D_2 estimates of Subject 2 for varying m

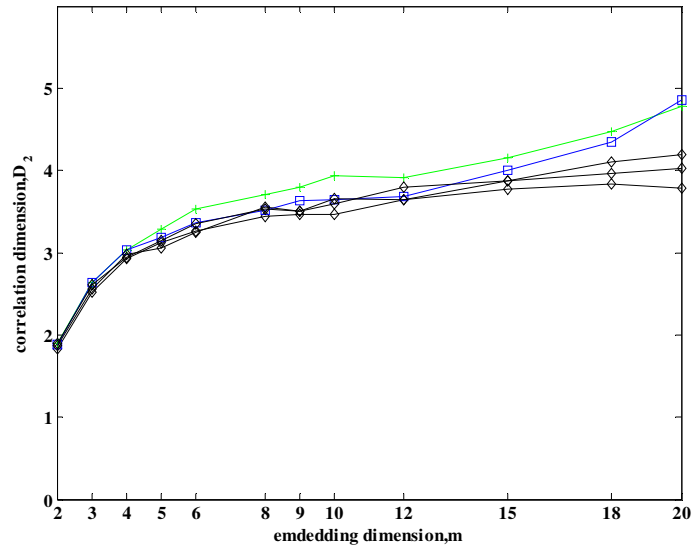


Figure 8. Computed D_2 estimates of Subject 3 for varying m

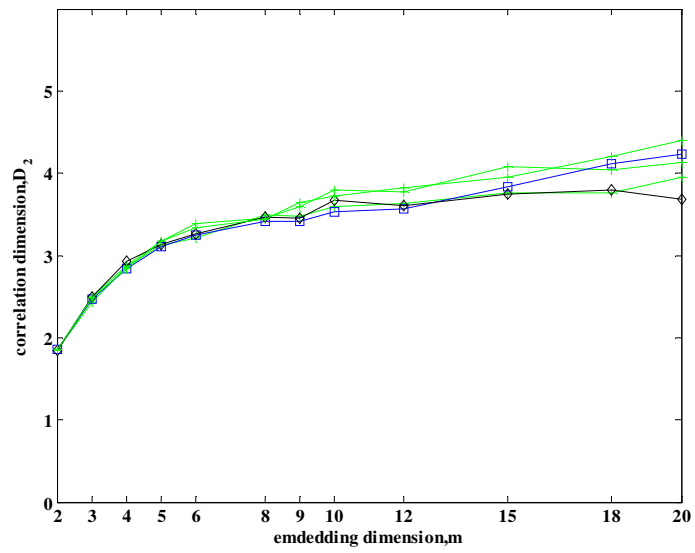


Figure 9. Computed D_2 estimates of Subject 4 for varying m

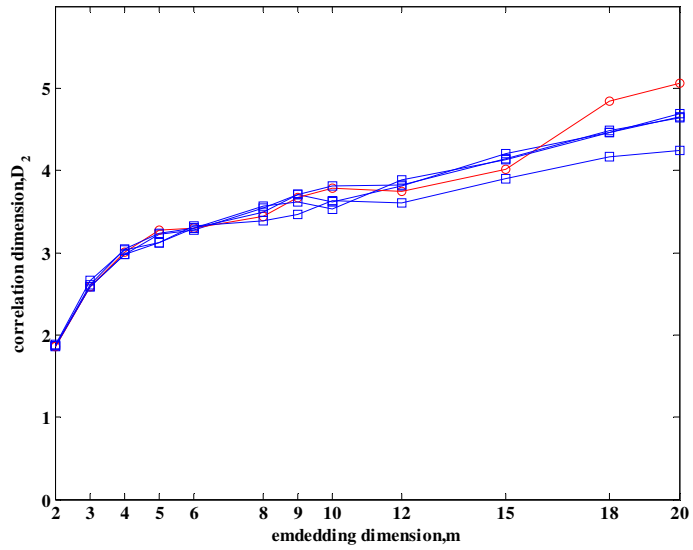


Figure 10. Computed D_2 estimates of Subject 5 for varying m

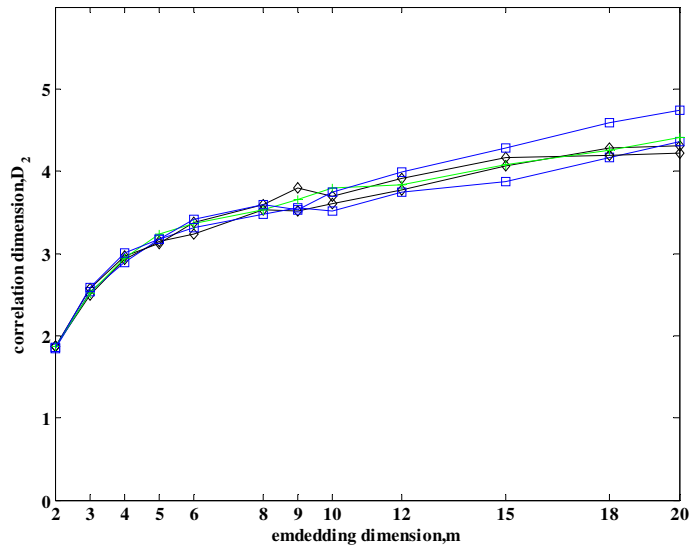


Figure 11. Computed D_2 estimates of Subject 6 for varying m

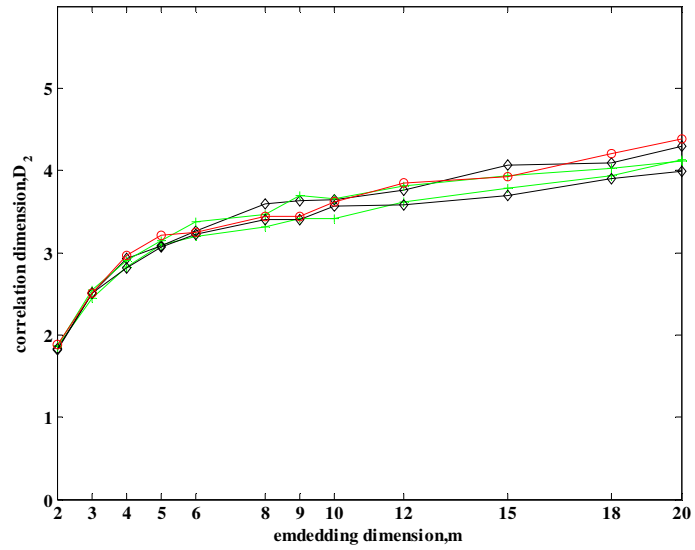


Figure 12. Computed D_2 estimates of Subject 7 for varying m

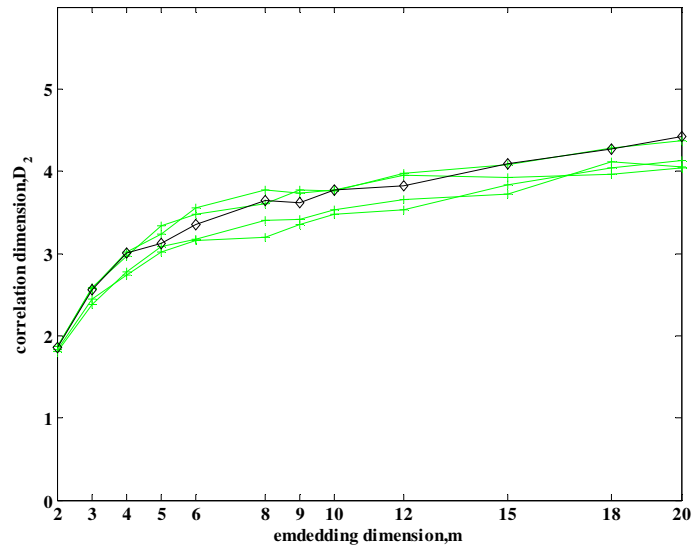


Figure 13. Computed D_2 estimates of Subject 8 for varying m

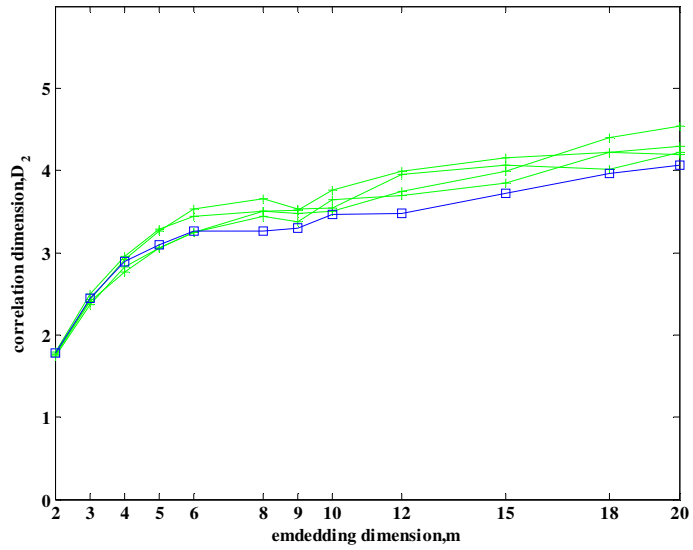


Figure 14. Computed D_2 estimates of Subject 9 for varying m

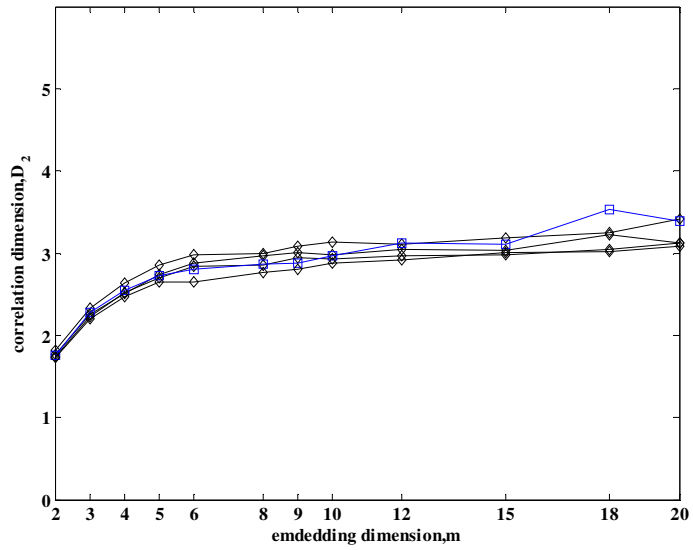


Figure 15. Computed D_2 estimates of Subject 10 for varying m

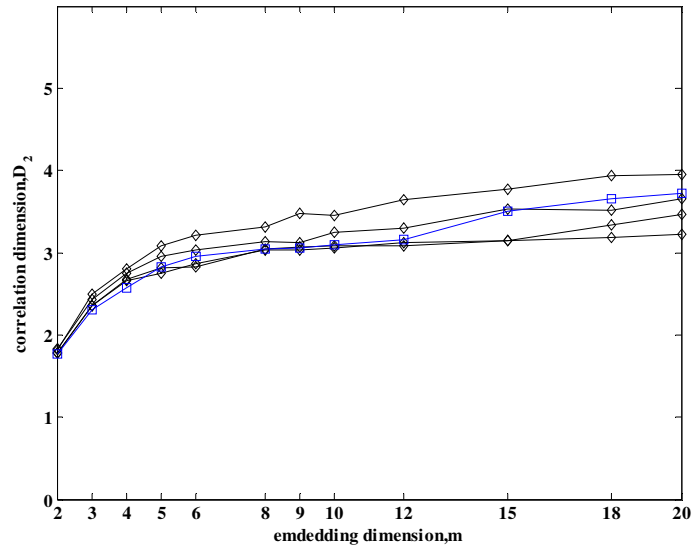


Figure 16. Computed D_2 estimates of Subject 11 for varying m

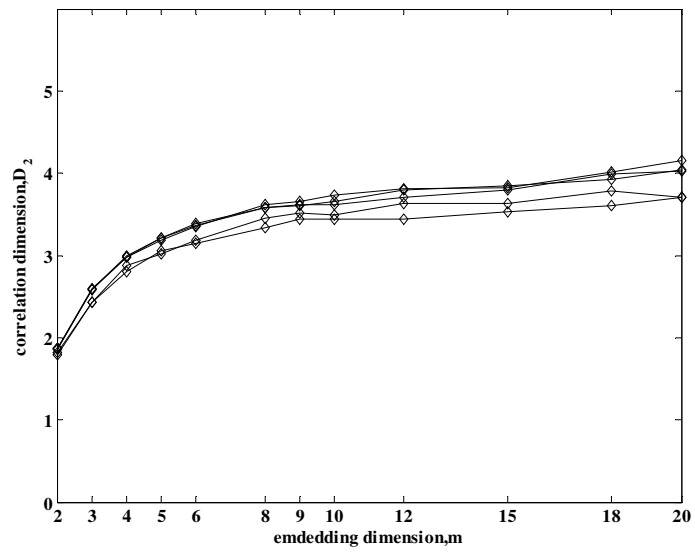


Figure 17. Computed D_2 estimates of Subject 12 for varying m

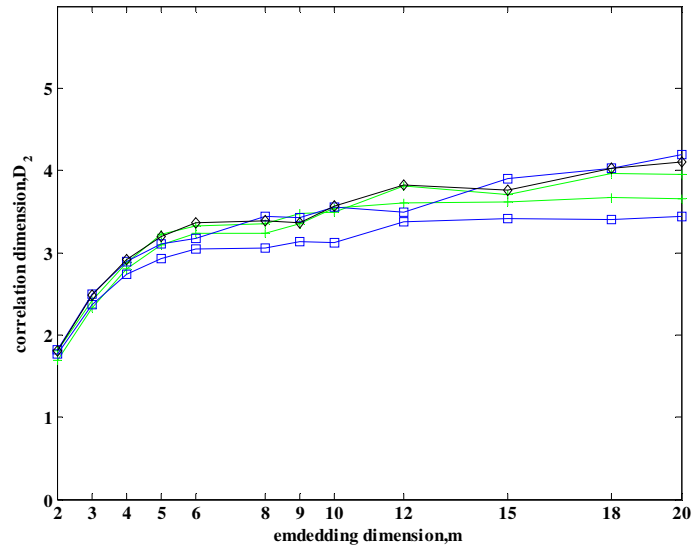


Figure 18. Computed D_2 estimates of Subject 13 for varying m

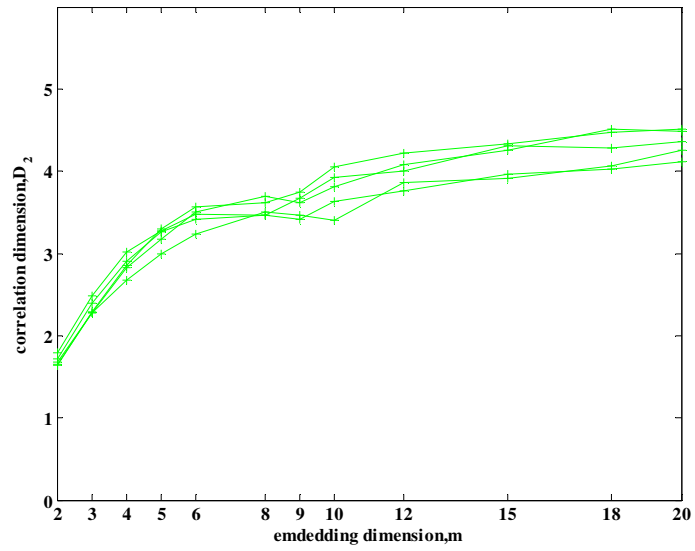


Figure 19. Computed D_2 estimates of Subject 14 for varying m

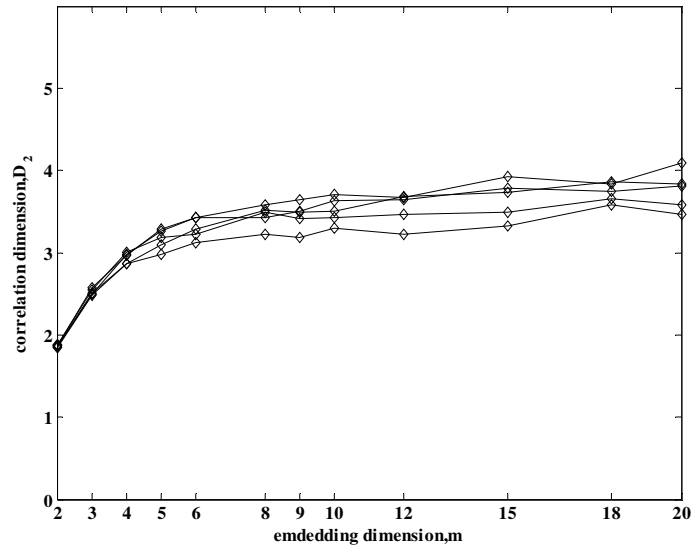


Figure 20. Computed D_2 estimates of Subject 15 for varying m

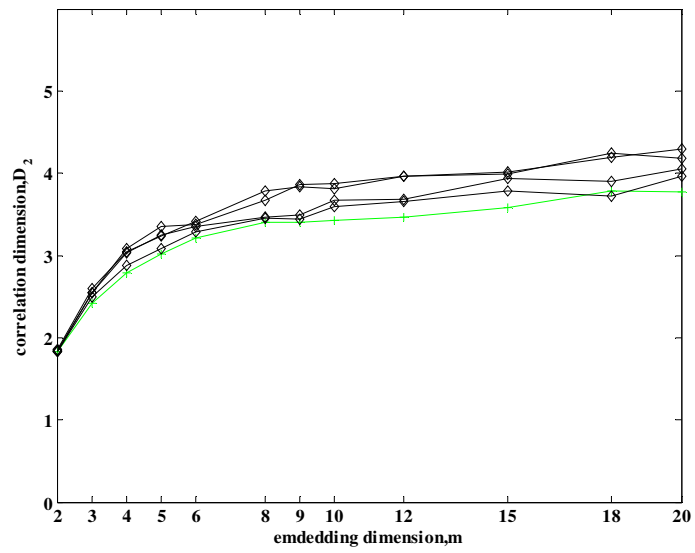


Figure 21. Computed D_2 estimates of Subject 16 for varying m

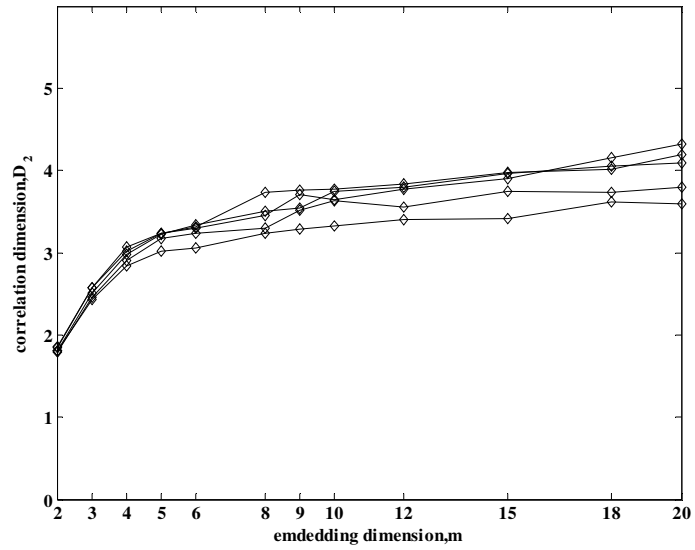


Figure 22. Computed D_2 estimates of Subject 17 for varying m

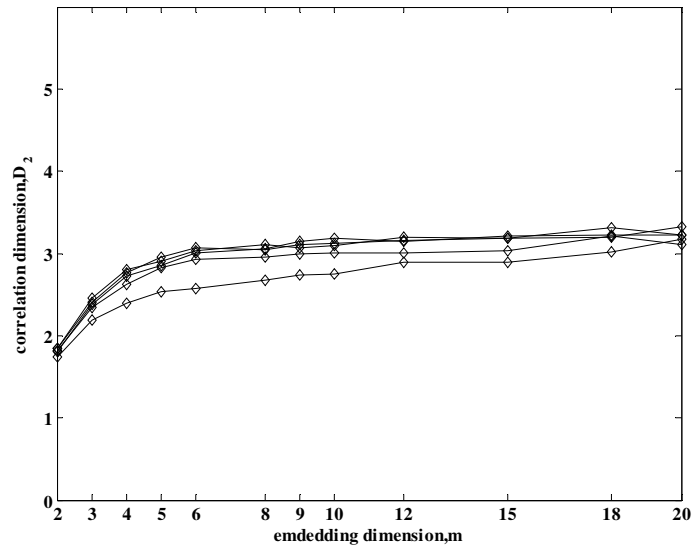


Figure 23. Computed D_2 estimates of Subject 18 for varying m

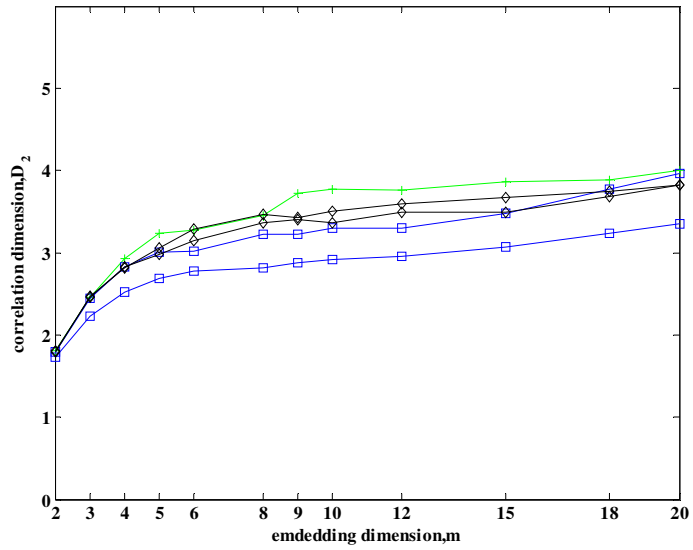


Figure 24. Computed D_2 estimates of Subject 19 for varying m

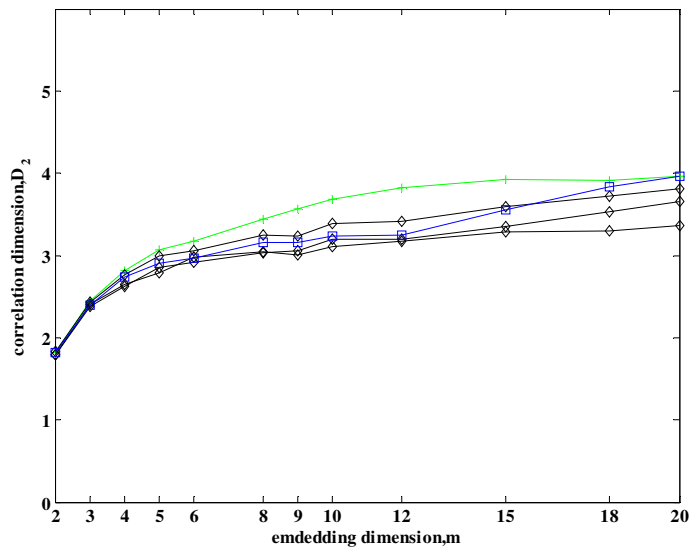


Figure 25. Computed D_2 estimates of Subject 20 for varying m

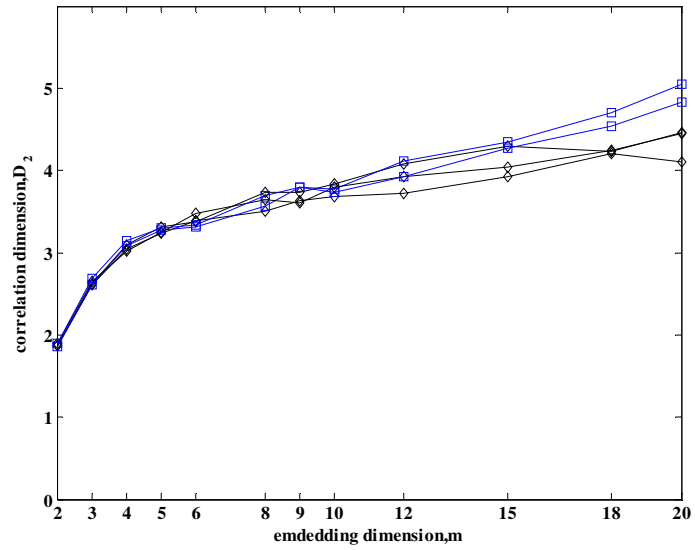


Figure 26. Computed D_2 estimates of Subject 21 for varying m

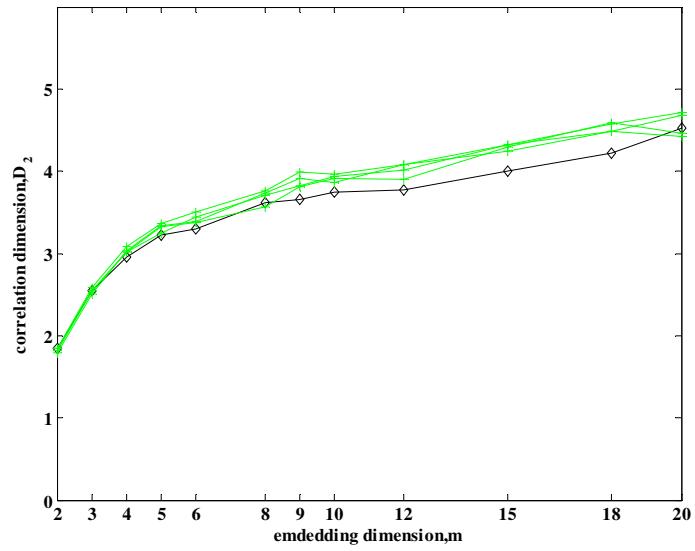


Figure 27. Computed D_2 estimates of Subject 22 for varying m

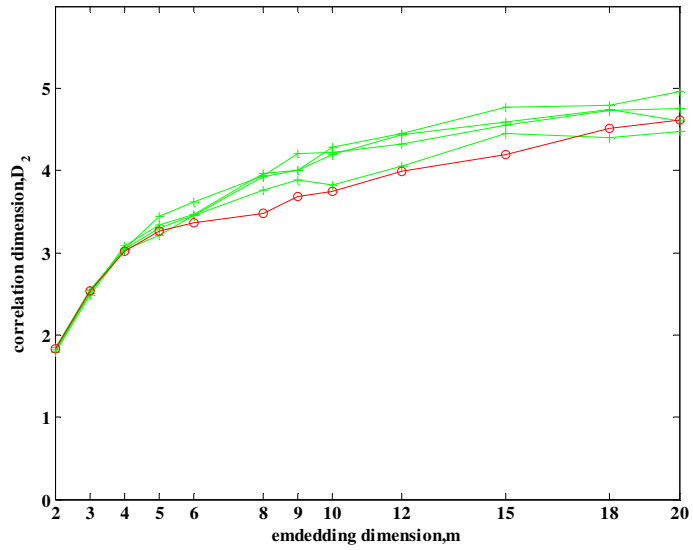


Figure 28. Computed D_2 estimates of Subject 23 for varying m

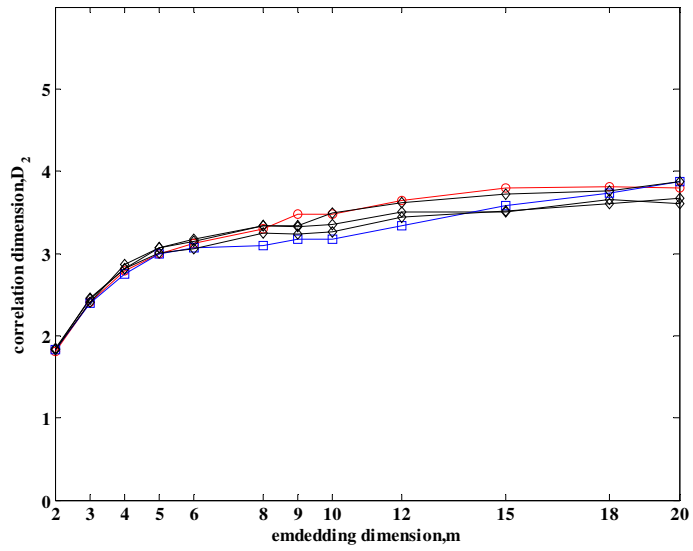


Figure 29. Computed D_2 estimates of Subject 24 for varying m

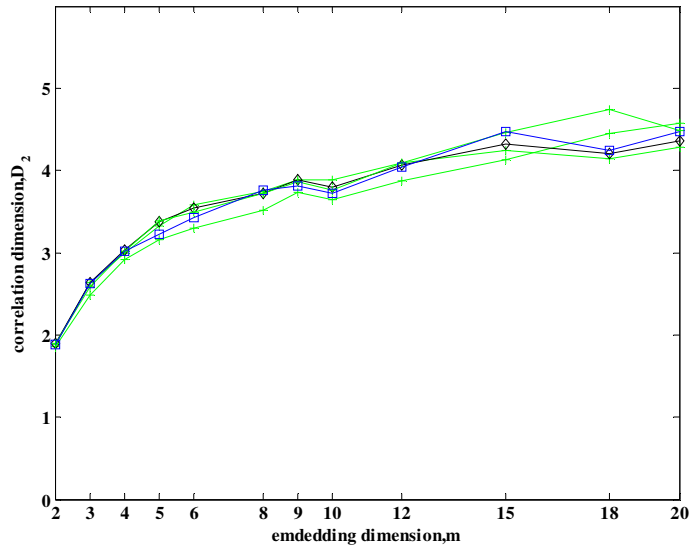


Figure 30. Computed D_2 estimates of Subject 25 for varying m

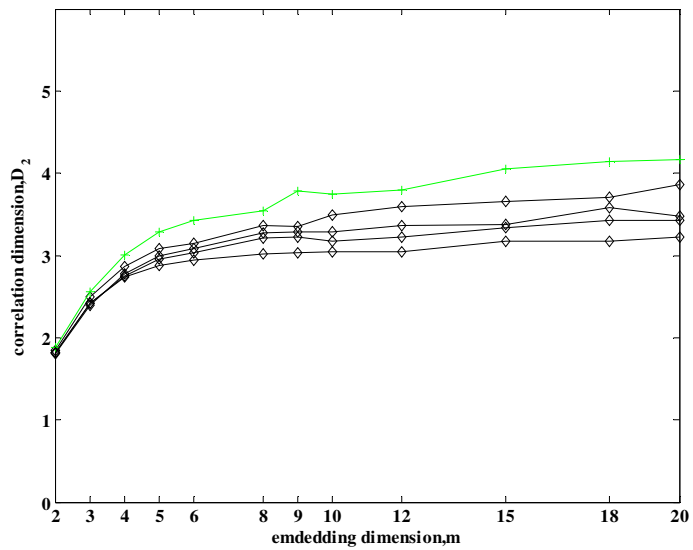


Figure 31. Computed D_2 estimates of Subject 26 for varying m

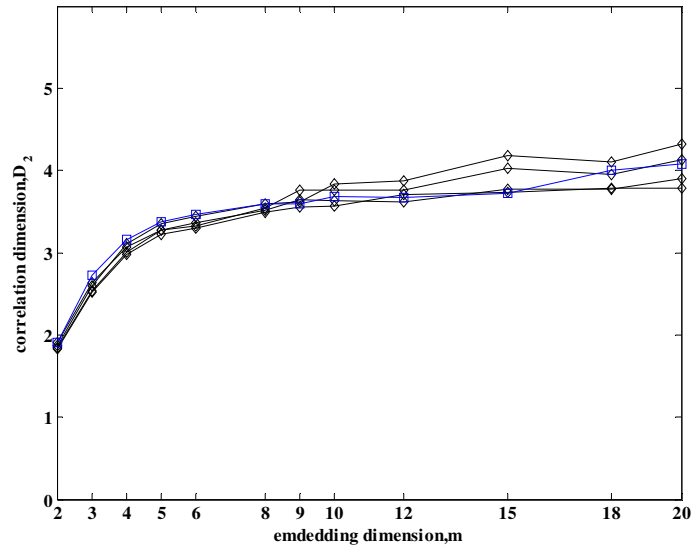


Figure 32. Computed D_2 estimates of Subject 27 for varying m

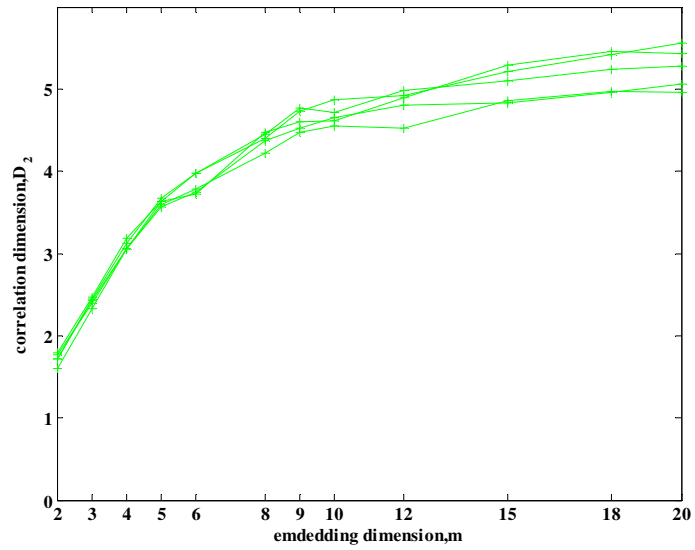


Figure 33. Computed D_2 estimates of Subject 28 for varying m

